Data-driven modeling applications in wastewater pathogen issues: Microbial safety management and epidemic interpretation

博 士 学 位 論 文

Doctoral Dissertation

Data-driven modeling applications in wastewater pathogen issues: Microbial safety management and epidemic interpretation (下水中病原体に関わる諸問題に対するデータ駆動型モデリングの適用:微生物リスク管理と感染流行検知)

東北大学大学院環境科学研究科

Graduate School of Environmental Studies, Tohoku University

先端環境創成学専攻 文化環境学コース	専攻 major／ コース course

氏　名 Name	ZHU YIFAN

指　導　教　員 Supervisor at Tohoku Univ.	佐野　大輔　教授	
研 究 指 導 教 員 Research Advisor at Tohoku Univ.		
審　査　委　員 （○印は主査） Dissertation Committee Members Name marked with “○” is the Chief Examiner	○　佐野　大輔　教授	
	1　中谷　友樹　教授	2　齊藤　繭子　准教授 (医学系研究科)
	3	4
	5	6

Table of contents

1. Introduction

1.1 Water reuse and associated microbial risk

For millennia, access to sufficient and safe water resources plays a central role in the prosperity and development of human civilization as freshwater is essential to not just the basic functions of the human body, but also agricultural and industrial production. As the world population and economy continually grow, so does the freshwater demand. It was estimated that the global water demand will increase by nearly one-third by 2050 [1]. But because the total available freshwater resource and nature's capability of regenerating it are limited, the conflict between demand and supply is more intense than ever. Keeping up with the rapidly growing demand cost-effectively and sustainably is considered one of the biggest challenges faced by water authorities around the globe. Converting wastewater into water that can be reused for certain purposes, often referred to as water reclamation and reuse, is a well-established approach that mitigates the tension between limited resources and ever-growing demand while also providing a stable water supply under unfavorable weather conditions [2–4]. The act of sewage treatment and reuse can be traced back to the very early stages of human history due to its environmental and ecological significance, an early practice of prehistoric civilizations is directly applying untreated domestic wastewater to irrigation [5,6]. Since then, the development of related technologies and the establishment of regulations have continued unabated. As new advancements in the treatment process and materials emerge, the cost efficiency, treatment capability, and effluent quality of modern wastewater treatment plants (WWTPs) have all been steadily increasing in recent decades. Diemer (2007) estimated that the usage of recycled wastewater in the U.S. will grow by 15% per year in terms of volume [7].

One solution to addressing the freshwater shortage is water reclamation, which can be defined as the process of converting wastewater into water that can be reused. As society

gradually heads toward urbanization, centralized wastewater collection and treatment systems have become increasingly accessible globally. However, despite the long history of water reclamation, only with the rapid development of modern science in recent centuries, particularly in epidemiology and microbiology, have the latent health risks and the importance of proper sanitation strategy in this practice been discussed and investigated [6,8], leading to the increasing concern from the public and authorities [9,10]. As a result, beginning in the mid-nineteenth century, the construction of modern sewage systems aimed at the effective separation and proper treatment of wastewater to protect the public from being infected by waterborne pathogens and provide efficient waste disposal [11]. Owing to the influence of human activity, both municipal and industrial wastewater may contain a variety of pathogenic microbes and other substances, including metals, pharmaceuticals, and personal care products, that could directly harm human health or lead to acute and chronic illness if not reduced to safe levels via treatment and distribution processes [12–17].

Waterborne enteric viruses in reclaimed wastewater with fecal-oral transmission route are considered a primary health concern globally since they can cause several acute illnesses, such as gastroenteritis and hepatitis [18,19]. In municipal wastewater, the primary origin of enteric viruses is the shedding from infected individuals. The shedding rate of norovirus particles has been demonstrated to reach up to 10^{10} per gram of feces [20]. Also, compared to other pathogens such as protozoa and bacteria, waterborne enteric viruses are more resistant to environmental factors and treatment processes due to their unique physical and biological characteristics despite being not able to reproduce in the environment without a host [21–23]. In an investigation of virus removal of three conventional activated sludge process wastewater treatment plants (WWTPs), the recorded log reduction value (LRV) ranged from 0.37 to 2.36 without tertiary treatment methods, leading to a high occurrence of human enteric viruses in receiving water [24]. Furthermore, the low infectious

dose of enteric viruses means that only a small amount of intake can lead to infection [25,26]. Several potential human exposure pathways have been proposed: consumption of shellfish grown in the contaminated aquatic environment and food crops irrigated by wastewater or fertilized by sludge, the ingestion of contaminated drinking water and recreational water, and farmworker exposure, including aerosol inhalation and direct intake of reclaimed irrigation water [27,28].

A dilemma is therefore faced by the stakeholders, including academicians, municipal authorities, and environmental agencies: there is an urgent need to utilize and manage water resources more efficiently and sustainably via water reclamation, yet the progress has been hindered by various factors, including the inefficient virus removal of conventional WWTPs, the inability to effectively control the treatment and distribution process, the lack of understanding of the underlying health risks, and the rising concerns about public health [18,29].

Historically, the safety of reclaimed water had been managed by setting restrictions on its use based on the intensity of human exposure to certain activities and the quality levels of treated wastewater. Commonly monitored parameters include biological oxygen demand (BOD), total suspended solids (TSS), and bacterial indicators [30,31]. However, in terms of the virological quality, these conventionally monitored chemical and bacterial parameters fail as reliable indicators [32–35]. Thus, direct virus detection is the preferred solution. Molecular techniques, notably quantitative polymerase chain reaction (qPCR), are gaining popularity in recent years largely due to not only the high sensitivity, specificity, and shortened detection time (typically within hours) compared to the culture-based methods, but also the capability of detecting viruses that are currently non-culturable *in vitro* [22,26,36–38]. However, the requirements for laboratory apparatus and trained personnel make a routinely performed detection infeasible for many WWTPs [39], especially those in less developed regions.

The uncertainty surrounding the virological quality of reclaimed water has resulted in

considerable hindrance to certain wastewater reuse practices. One of the most strictly regulated use is food crop irrigation. In the U.S., regulations regarding the use of reclaimed water on food crops vary among different states. Some states prohibit this act indiscriminately whereas others allow reclaimed water to be used only if some requirements are met. For instance, the states of Florida, Nevada, and Virginia require that the reclaimed water must not directly contact the edible parts of the crop unless the crop will be peeled or thermally processed before being consumed [30]. In California, although the practice of spraying reclaimed water onto edible parts of salad crops and strawberries has been successfully performed for over 40 years with no reports of human illness as a result [40], the Title 22 regulations specify that the highest quality standards apply to the reclaimed water that would contact the edible parts of the crop [41].

Introducing advanced treatment methods to further reduce the pathogen content in effluent is an indispensable step in promoting the use of reclaimed water. Historically, due to the inefficient virus removal of conventional WWTPs, tertiary treatments have commonly been employed for disinfection, usually in the form of the addition of chemical disinfectants such as chlorine and ozone or the use of UV [42]. Although these methods are capable of effectively bringing down pathogen concentration in the effluent and preventing the transmission of waterborne diseases, they are subject to certain derivative issues, e.g., the generation of disinfection by-products (DBPs) that possess genotoxicity and carcinogenicity [43,44], high operating costs [45], and the concern over the potential increase in antibiotic resistance [46,47].

In the last fifty years, powered by the rapid development of materials science and engineering, the use of membrane in the realm of water treatment has become increasingly popular with one successful example being the membrane bioreactor (MBR) which comes in two forms: aerobic membrane bioreactor (AeMBR) and anaerobic membrane bioreactor (AnMBR) [48]. Firstly commercialized in the early 1970s, the application of MBR technology in municipal and industrial

wastewater treatment has rapidly expanded with an average global market growth of over 10% since the turn of Millennium [49], as the result of more stringent environmental regulations as well as the various advantages MBR provides compared to conventional treatment processes, including high effluent quality, reduced environmental footprint, and nutrient recovery in the case of AnMBR. Readers interested in more information on the MBR technology are referred to the extensive reviews previously published [50–55].

The core feature of MBR is the utilization of a membrane that enables highly efficient sludge separation which, in the perspective of water safety, can also serve as a barrier against waterborne pathogens [56,57]. In addition to size exclusion which effectively rejects pathogens larger than the membrane pore size, notably pathogenic bacteria and protozoa, and aggregated virus particles [52,58–60], the presence of biosolids also enables effective virus removal.

From the standpoint of water resource management, the high effluent quality and pathogen removal capability of MBR systems can open new possibilities by expanding the scale of existing reclaimed wastewater use [61]. Better pathogen removal efficiency means the disinfectant dose required to meet the microbiological quality standard can be reduced, leading to lower health and ecosystem concerns resulted from disinfection by-products [58,62,63]. Together with the advantage of stable operation [54,56], once the MBR systems are proven to be capable of continuously delivering decent virus removal performance, the effluent can be used for purposes currently restricted for reclaimed water [64]. The usability would surpass that of most current wastewater reclamation systems while being economically viable, significantly relieving the stress on the natural freshwater supply [12,65].

1.2 Wastewater-based epidemiology

Although the hazardous materials in wastewater pose a threat to the public health, they also bring opportunities. The concept of wastewater-based epidemiology (WBE) centers around

a simple principle: certain chemical or biological agents (also referred to as 'biomarkers') excreted by human bodies can be collected by the sewage network and end up entering the wastewater, making it a rich source of these substances. Via physicochemical methods, biomarkers can be recovered from wastewater and the measured concentration can then be used to infer the size of the shedding population and provide community-level health information [66]. Following its successful early applications of tracking illicit drug usage and lifestyle factors, WBE is gradually gaining popularity among researchers in the water-related field. Blessed with its community-wide coverage, ability to "see" the underreported and asymptomatic patients, and low-cost nature, WBE has been proposed to be a promising tool in infectious diseases surveillance, and unsurprisingly, high hopes are placed for its capability of helping combat the recent COVID-19 pandemic as well [67–69].

Since the beginning of the pandemic, multiple research teams have detected SARS-CoV-2 RNA in sewage networks around the globe and many COVID-19 wastewater surveillance projects ranging from institution- to nation-wide have been initiated [70–76]. To date, more than 100 dashboards either dedicated to or containing COVID-19 wastewater surveillance results have been set up, according to data aggregation site "COVIDPoops19" (https://www.covid19wbec.org/covidpoops19). These dashboards cover a great variety of scale and data disclosure strategies (quantification results only, quantification results and trend, variant detection results, or with other epidemic metrics such as reported cases and testing rate). To date, most dashboards are from high-income countries. For example, U.S. is in the absolute lead with more than 50 dashboards established. It is worth noting that some countries and regions have established COVID-19 wastewater surveillance sites, even networks, yet the results are only for academic uses and not publicly accessible. In addition to the experimental data, the site

"COVIDPoops19" also acts as a platform on which researchers can share the latest scientific advancements as well as relevant resources such as data visualization tools.

While the technical challenges associated with this concept are gradually being solved, one key question remains unanswered: how to communicate the result efficiently and unambiguously with the public and authority so that it serves the COVID-19 response in the coming new era? After the proof-of-concept phase, the focus of research is now gradually shifting onto the next: interpretation and utilization of the results. Wastewater surveillance had expanded to multiple application scenarios including vaccination efficacy evaluation and variants of concern (VOC) tracking [77], it also served as a virus indicator for identifying asymptomatic infections and guiding clinical screening [78,79]. One simulation study stated that clinical screening enhanced by wastewater surveillance can reduce infections by 95% [80]. However, as these attempts are still at an early stage, they tend to be highly site-specific and discrete on time scale. As a result, the perception of the benefits offered by wastewater surveillance, particularly as a routine yet forward-looking tool, remains relatively restricted.

With the advancement of wastewater surveillance comes a solid need to reconsider its position in COVID-19 and future epidemic response. In addition to retrospective analysis, it is also important to realize the potential of wastewater surveillance as a forward-looking tool that supports public health practices. Information disclosure strategy may maximize its social benefits, yet related efforts are still largely inadequate. Result interpretation, data integration, and public/authority awareness are identified as the key issues to be addressed. More recognition of the potential and significance of wastewater pathogen surveillance, but this will require a concerted effort of all three sides — researchers, the public, and the authority.

1.3 Goal of this study

Seeing the research gap and the merits of data-driven modeling, the main objective of

this dissertation is to verify the feasibility of data-driven modeling techniques in addressing some of the emerging virus-related issues faced by the water sector that is now focusing on extracting the residual value in wastewater in various forms. The main reason of choosing this direction, as stated earlier, is a lack of tested and proven workflow and available models in this field. Specifically, from a forward-looking perspective, real-time monitoring of the microbial risk of novel water reuse solutions and data interpretation of wastewater pathogen surveillance are two topics that worth additional research interests for the social value they provide.

Chapter 3 discusses the development and verification of a soft sensor for real-time virus removal monitoring. Consistent with modern process control theories and sanitation guidelines, the microbial safety of the water reuse process is better put under constant monitoring. However, online virus quantification poses a huge challenge because conventional experimental methods need at least several hours to conduct, not to mention the staff and equipment requirements. Considering it is the removal performance rather than absolute virus concentration in the effluent that is in the interest of plant operators, this may be achieved by establishing a soft sensor to predict the virus removal performance, as opposed to using a hardware sensor. Soft sensor is a general term for models that take secondary variables, typically easier to measure, to predict the desired variable that due to some reasons, is difficult to be monitored in real-time. Conventionally, wastewater treatment engineers prefer mechanistic models as they provide a physical understanding of the system. However, virus removal involves processes running on different principles and is hence difficult to be integrated into one consistent and comprehensive model. By using data-driven modeling techniques, the connection between the secondary variables and desired output can be directly established without an understanding of the underlying mechanisms.

Chapter 4 focuses on designing and verifying a model that uses wastewater SARS-CoV-

2 surveillance data for public health information support. Since the reports of SARS-CoV-2's presence in municipal wastewater, many entities have built their own wastewater SARS-CoV-2 projects on various scales. There are also plans to expand to other pathogens and biomarkers found in wastewater, but they will be affected by how much value the SARS-CoV-2 surveillance projects can provide. One primary bottleneck is data interpretation and utilization, for which a consensus has yet to be reached. Particularly, rather than simply reporting the presence and concentration of viruses in the wastewater, a quantitative perspective of what the result indicates and how should the public health policy react to it is much-needed. Therefore, in this chapter, the detection result is further analyzed to explore the possibilities of data-driven model application.

In addition to the two main research topics, in Chapter 2, literature review was conducted for each topic to provide a knowledge base as well as to identify the research needs. Finally, in Chapter 5, a summary is made to discuss the lessons learned from the studies, the limitations and challenges lying ahead, and the perspective of where this research field should go in the future.

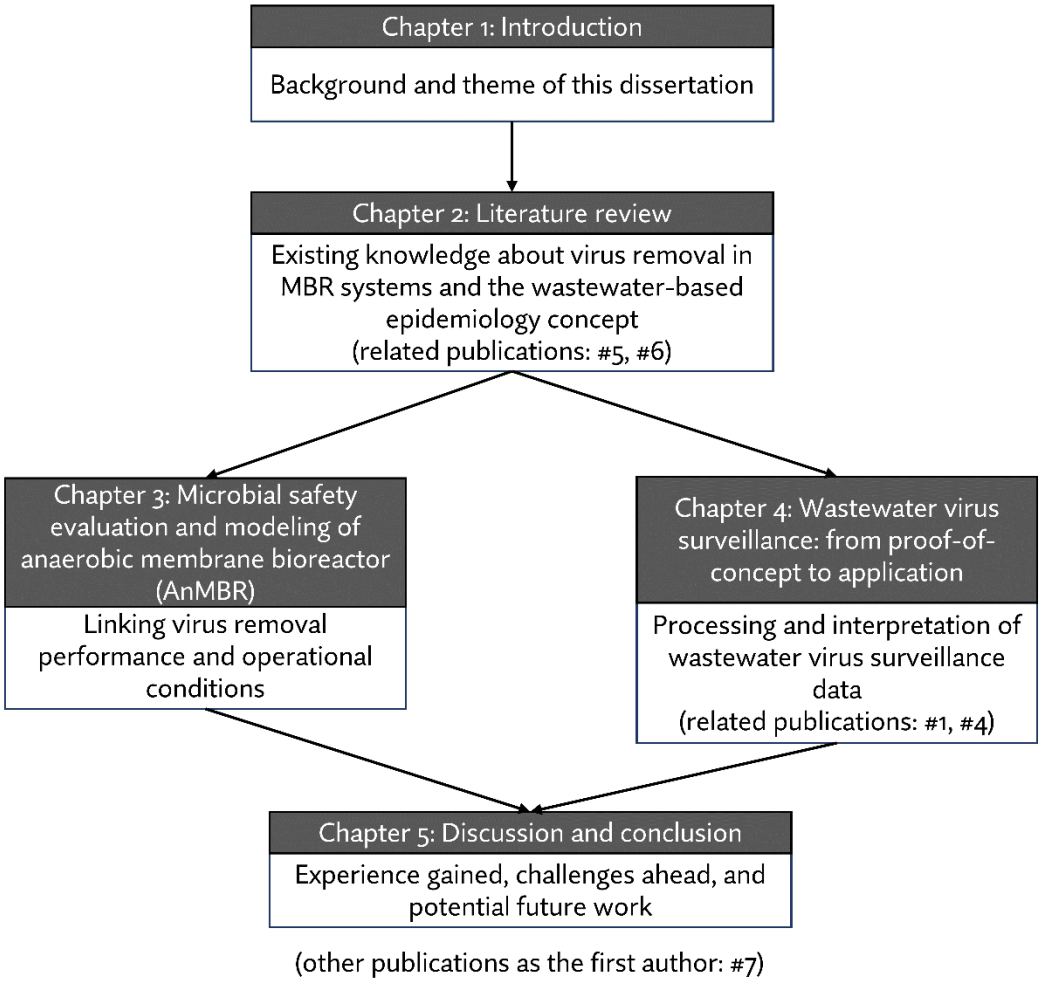

Fig. 1 Schematic of this dissertation.

2. Literature review

2.1 Virus removal in membrane bioreactors

2.1.1 Introduction

This section of the literature review focuses on the virus removal process in MBR systems as well as the related modeling efforts. Firstly, studies on MBR virus removal performance and the involved mechanisms are discussed to get a grasp on the microbiological safety factor of MBR technology, as well as to provide information on which factors contribute more significantly and thus should be paid more attention during model development. Secondly, historical and recent attempts to develop a model that connects other variables with virus removal efficiency via either conventional process-driven approach based on the physicochemical and biological relationship and equations, or novel data-driven modeling techniques are collected and reviewed.

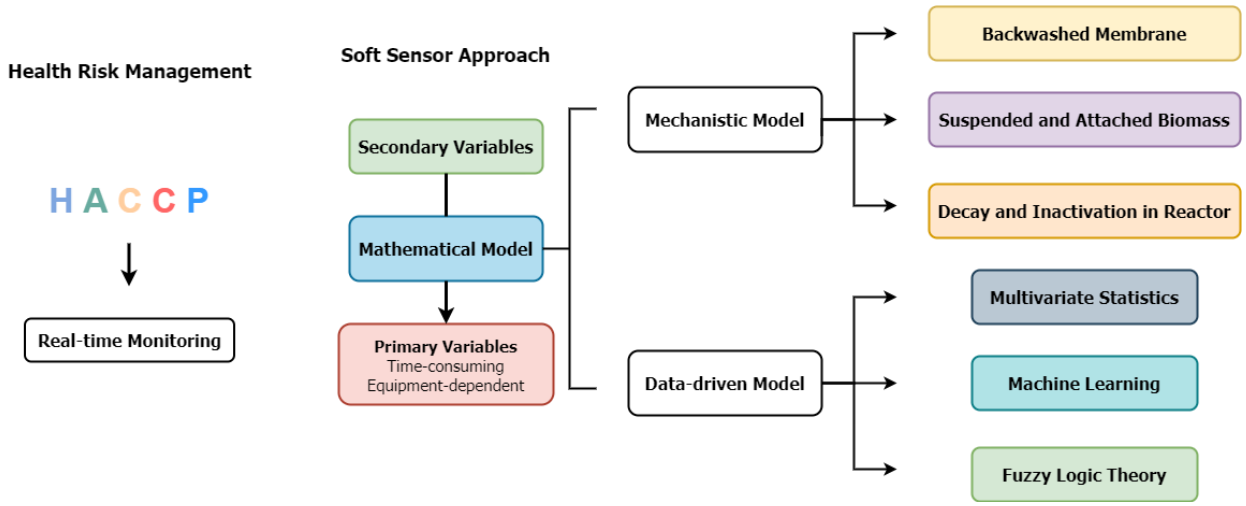

Fig. 2.1 The graphical abstract of literature review Section 2.1.

2.1.2 Mechanisms involved in MBR virus removal

In recent years, some studies have focused on the overall performance and contributing factors of the virus removal in MBR systems. Table 2.1 lists some recent studies that have covered a wide range of reactor scales, configurations, and model viruses. The mechanisms proposed based on experimental results, whether in AeMBR or AnMBR systems, can be classified into three major categories: the rejection and adsorption effect of the backwashed membrane, the adsorption of

virus particles to biomass, and the decay and inactivation occurred in the mixed liquor phase.

Three mechanisms are directly related to virus reduction by the membrane alone: size exclusion, adsorption, and electrostatic repulsion [60,81]. The principle behind size exclusion is rather intuitive: particles larger than the membrane pores get either rejected by the membrane or stuck in the pore channel; the larger the pores are, the easier the virus particles can pass through the membrane. The removal efficiency can, therefore, be significantly enhanced by choosing the membrane with a pore size close or smaller to the size of target virus. Lv et al. (2006) reported that under the same operating condition using T4 phage (average size 107.9 ± 12.9 nm) as the model virus, a 0.22 μm membrane provided only 1.7 log removal whereas a 0.1 μm membrane reached a much higher removal of 5.8 logs . When the diameter of the pathogen particles is at the same level as the nominal membrane pore size or less, other mechanisms such as mechanical sieving and the aggregation of virus particles start to take effect and facilitate this process. As reported by Da Silva et al. (2011) and Samandoulgou et al. (2015) [82,83], the aggregation of norovirus GI and GII particles is affected by pH and ionic strength, and the size of aggregates may greatly exceed the membrane pore size under certain circumstances. Chaudhry et al. (2015) reported a high removal rate by backwashed membrane with a 0.04 μm nominal pore size Chaudhry et al. (2015b), which is in line with the diameter of many enteric viruses. However, it is worth mentioning that AnMBR plants tend to use membranes with a pore size ranging from 0.1 to 0.4 μm to increase the flux and reduce the operation cost brought by membrane fouling [85], and under this circumstance, the membrane itself may only provide limited removal capability when dealing with viruses small in size.

Table 2.1 AeMBR and AnMBR virus removal studies in recent years (2009-2022)

Reactor Type	Nominal Membrane Pore Size	HRT	Virus	LRV	Reference
Bench-scale AnMBR	0.4 μm	12 h	MS-2 Phage	1.75 to 5.5	[86]
Bench-scale AnMBR	0.4 μm	12 h	T4 Phage	5 to >7	[86]
Bench-scale AnMBR	0.2 μm	8 h	MS-2 Phage	0.2 to 3.6	[87]
Bench-scale AnMBR	0.1 μm	8 h	Norovirus GI	4.64	[88]
Bench-scale AnMBR	0.1 μm	8 h	Norovirus GII	5.00	[88]
Bench-scale AnMBR	0.1 μm	8 h	Rotavirus	2.31	[88]
Pilot-scale AnMBR	0.03 μm	9 d	Somatic coliphage	3.7	[89]
Bench-scale AeMBR	0.04 μm	10 h	MS-2 Phage	1.7	[90]
Bench-scale AeMBR	0.04 μm	10 h	phiX174 Phage	2.3	[90]
Bench-scale AeMBR	0.04 um	10 h	Fr Phage	4.2	[90]
Bench-scale AeMBR	0.45 μm	100 day	Adenovirus	0.2 to 6.3	[91]
Pilot-scale AeMBR	0.4 μm	35 h	Norovirus GI	1.82	[92]
Pilot-scale AeMBR	0.4 μm	35 h	Norovirus GII	3.02	[92]
Pilot-scale AeMBR	0.4 μm	35 h	Adenovirus	1.94	[92]
Pilot-scale AeMBR	0.4 μm	7.2 h	Enteroviruse	0.3 to 3.2	[37]
Pilot-scale AeMBR	0.4 μm	7.2 h	Norovirus GII	0.2 to 3.4	[37]
Pilot-scale AeMBR	0.4 μm	7.2 h	Sapovirus	1.3 to 4.1	[37]
Full-scale AeMBR	0.4 μm	36 h	Rotavirus	>2.0	[93]
Full-scale AeMBR	0.4 μm	36 h	Sapovirus	>3.0	[93]
Full-scale AeMBR	0.4 μm	N/A	F-specific coliphage	5.13	[94]
Full-scale AeMBR	0.4 μm	N/A	Somatic coliphage	3.24	[94]
Full-scale AeMBR	0.4 μm	N/A	Enterovirus	3.40	[94]

Table 2.1 (continued)

Reactor Type	Nominal Membrane Pore Size	HRT	Virus	LRV	Reference
Full-scale AeMBR	0.4 μm	N/A	Adenovirus	3.67	[94]
Full-scale AeMBR	0.4 μm	N/A	Norovirus GI	3.02	[94]
Full-scale AeMBR	0.04 μm	0.18 h	Norovirus GI/GII	2.3	[63]
Full-scale AeMBR	0.04 μm	0.18 h	Adenovirus	4.4	[63]
Full-scale AeMBR	0.04 μm	11 to 12 h	Enterovirus	3.5 to 4.8	[95]
Full-scale AeMBR	0.04 μm	11 to 12 h	Norovirus GII	4.1 to 6.8	[95]
Full-scale AeMBR	0.04 μm	11 to 12 h	Adenovirus	4.1 to 6.3	[95]

The adsorption of virus particles onto the membrane surface is mainly governed by hydrophobic and electrostatic effects while non-specific interactions are of secondary importance [37,60,96,97]. Madaeni (1997) studied the removal of poliovirus by a 0.2 μm MF membrane and concluded that the physicochemical characteristics of the virus particle and membrane material, and the ratio of the pore diameter to virus particle diameter are the important influencing factors in the adsorption of viruses into the membrane [98]. The preferable condition for adsorption is when the two components have opposite charges or only a small amount of charges, and generally low pH level can facilitate this process [99–101].

Electrostatic repulsion works differently. When the membrane material and virus particles share the same type of charge, electrostatic repulsion would push the virus particles away from the membrane surface, contributing to virus retention [60,81]. Also, in contrast to membrane adsorption, the effect of electrostatic repulsion is more pronounced under increased pH level [102,103]. The other vital contributing factor, hydrophobic effect, works by minimizing the area of contact between water molecules and virus particles, and between water and membrane surface, thus increasing the potential of viruses to adsorb onto the membrane [104]. The magnitude of this effect leans on a variety of factors including ionic strength, virus surface characteristics, and membrane material [85,97,103,105].

It is also worth pointing out that the size of pores on the membrane is not consistent. During the production process, there might be abnormal pores on the membrane and these pores may lead to unexpected virus passage or decreased filtration performance, thus the membrane pore distribution is also a factor to be considered in membrane size exclusion [106,107]. The log-normal distribution is widely applied to describe the membrane pore distribution [108,109]. Based on that, Duek et al. (2012) investigated the actual pore size distribution on several UF membranes and reported that it does have a significant effect on the virus rejection property [110]. In the study, virus retention is more accurately predicted by the absolute pore size d_{100} than by d_{50} and d_{90},

indicating that abnormally large pores contribute more to virus passage through UF membrane. A similar result was reported by Kosiol et al. (2017) [111], who found that d_{99} values of a number of membranes showed a correlation with LRVs of bacteriophage.

As the biomass in the reactor grows, both the suspended solids and the gel/cake layer attached to the membrane surface develop. It has been well-acknowledged that the adsorption of virus particles to the biomass is a critical contributor to the virus removal in a number of ways [86,90,112–117].

Firstly, the adsorption of phage or enteric virus particles to the mixed liquor suspended solids (MLSS), which consist of such as bacteria and organic compounds that are larger than the membrane pores, makes their passage harder. For instance, Shang et al. (2005) reported a 0.8 log MS-2 phage removal by adsorption to the suspended biomass alone in a bench-scale AeMBR[118] , and in the study by Miura et al. (2018) [93], 1.5 log removal of norovirus GI was achieved after 60 min of mixing with the MLSS. In a similar manner, Hirani et al. (2010) recorded a higher removal rate of indigenous MS-2 coliphage compared to seeded MS-2 coliphage in several AeMBR systems and attributed it to the higher degree of particle association of indigenous coliphage [106]. MLSS concentration and virus characteristics have been reported to be influencing factors, Wu et al. 2010 found that the fraction of adsorbed somatic coliphage went up from 65% to 92% as MLSS concentration increased from 1.6 g/L to 9.6 g/L in their AeMBR [113]. In the study of Chaudhry et al. (2015), three bacteriophages, MS-2, phiX174, and fr, were fed into a bench-scale AeMBR, and a significant difference in their attachment to the mixed liquor biomass was observed [84]. While only 0.2 $\log_{10}$ removal can be attributed to suspended biomass attachment for MS-2, phiX174 and fr showed much higher removal (1.2 and 3.0 $\log_{10}$). Since the three bacteriophages have similar zeta potentials, the difference in surface composition of the phages was assumed to be the cause.

Secondly, the biofilm attached to the membrane surface also plays a pivotal role in the

removal process by adsorbing onto the inside of membrane pores or block the pores. The decreased effective pore size and the reduced number of available pores raise the membrane resistance, thereby making the passage of virus particles more difficult [119]. In addition, the accumulation of gel and cake layers on the membrane surface provides extra adsorption spots, as these layers are made up of soluble microbial products and extracellular polymeric substances that can potentially adsorb and trap virus particles [120]. Also, the presence of proteins in the mixed liquor inhibits the adsorption of the viruses on the membrane due to the competition between proteins and virus particles for adsorption sites [98]. In MBR systems where proteins make up a significant proportion of the extracellular polymeric substances (EPSs) and soluble microbial products (SMPs) [121], the inhibition caused by proteins can be a crucial factor. Furthermore, the high concentration of suspended biomass may lead to a high excretion rate of EPSs and SMPs. However, the interaction between them and viruses has not been explained clearly yet [37]. Ueda and Horan (2000) investigated the effect of biofilm growth on virus removal performance [122], and they found that the removal efficiency improved notably as the biofilm attached to the membrane surface grew and increased the filtration resistance; a 2.1 log removal was achieved by 21-day-biofilm whereas 9-hr-biofilm achieved only a 0.3 log removal.

It is worth mentioning that membrane fouling, despite the contribution to virus rejection, is considered detrimental with respect to the reactor operators because it leads to a decline in permeate flux and alteration of the reactor hydrological characteristics [123,124], eventually resulting in decreased handling capacity and higher operating costs [54]. Commonly employed fouling control strategies include membrane backwash, gas sparging, and chemical cleaning [125,126]. Also, in recent years, the addition of activated carbon in the reactor has received a considerable amount of attention for being both effective and financially economical [127]. Fox et al. 2015 investigated the effect of gas sparging rate on phage removal in AnMBR and found that MS-2 rejection increased

with the elevated sparging intensity after a 10-day operation at a low sparging rate [86]. Since high gas scouring relieves fouling, the result seems rather counterintuitive. The authors suggested that it can be attributed to the reduced concentration polarization at the membrane surface resulted from intense gas sparging. Similar findings have been reported by Cui et al. (2003) and Madaeni et al. (1995) who concluded that increasing stirring and gas sparging can have a negative impact on the membrane permeability for particles like protein and virus [128,129]. Simply put, if the virus particles are seen as a solute, a layer of high concentration will gradually build up in the vicinity of the surface of membrane during the filtration process, resulting in an increased concentration of virus particles in the effluent. When the gas sparging or stirring rate is increased, this layer can get disrupted, leading to a lower concentration of virus particles in the effluent. This, too, suggests that the virus removal process is highly complicated with multiple mechanisms working simultaneously, but nevertheless, the role of biofilm has been well-established [90,91,130]. Finding a delicate balance between virus particle rejection performance and membrane permeability will be a vital task for reactor operators and requires a more comprehensive interpretation of the dynamics in the reactor [114].

The major mechanisms responsible for the effect of mixed liquor on virus decay and inactivation are likely to be the predation by other microorganisms and enzymatic breakdown [90,131]. For MBR, Wu et al. 2010 found that the somatic coliphage decay was significantly accelerated in the presence of activated sludge compared to the spontaneous decay in the influent wastewater, which took about 10 days to achieve 0.72 $\log_{10}$ removal [113]. Likewise, Fox and Stuckey (2015) reported that phage concentration in the AnMBR mixed liquor phase decreased by about 2 $\log_{10}$ over the experiment period of two weeks, which is faster than the expected washout rate under the same hydraulic condition, suggesting that the anaerobic condition inside the reactor may facilitate the process of virus inactivation Fox and Stuckey (2015). Although conceptually, all virus particles

rejected by membrane and attached biofilm are subject to biodegradation, considering the dominating contribution of membrane/biofilm rejection and typical hydraulic retention time (HRT) of several hours to days in MBR systems, the effect of biodegradation on effluent virus concentration may not be so pronounced.

Compared to the number of studies dedicated to AeMBR virus removal performance, in the case of AnMBR, as a relatively new but thriving technology, only a few reports are currently available, covering only a limited range of configurations and operating conditions. Nevertheless, the existing studies have revealed that AnMBR and AeMBR have many things in common when it comes to virus removal, including the overall efficiency and the responsible mechanisms, although some differences are likely to exist due to their respective kinetics. The good thing is, as the potential of AnMBR being further recognized, more AnMBR plants are being built or planned in various configurations for research and development needs, and we can expect more studies on the topic of virus removal capability to be conducted in the near future because the safety aspects associated with this technology need to be thoroughly discussed and will play a central role in ameliorating public perception in the future.

Still, some vital information can be extracted from these past studies. The reported virus removal efficiencies are highly system-dependent and it makes parallel comparison very difficult, if not impossible at all. This is resulted from the diversity in reactor configurations (*e.g.*, plant scale, membrane material and pore size, hydraulic and solids retention time), and in the sources and characteristics of the wastewater being treated [22,85]. Sometimes, conclusions from different studies may even conflict. For instance, Chaudhry et al. (2015) reported that a 3.1 $\log_{10}$ reduction of norovirus GII was achieved solely by the backwashed membrane [84], making it the greatest contributor in the total removal, whereas Fox and Stuckey (2015) and Ueda and Horan (2000) both pointed out that the membrane provided only relatively poor phage rejection in their studies Fox

and Stuckey (2015) and Ueda and Horan (2000), although the discrepancy likely comes from the different pore sizes used (0.04 μm vs 0.4 μm) since the relative size of particles compared to membrane pore size matters greatly in size exclusion. Another example is the study conducted by Farahbakhsh and Smith (2004) [132], in which the adsorption onto the membrane surface or in membrane pores governed the coliphage removal when the membrane was pristine, but as the membrane gradually got fouled, the governing factor shifted to the interception by the cake layer. This discrepancy can also be observed when the relative contribution of each mechanism is calculated and sorted, but the order varies between studies [117,118]. All these indicate that the current understanding of the intricate process is still far from sufficient, and further research will need to view from a wider angle as multiple highly coupled components are involved with a wide selection of influencing factors [54,93,133], especially during the development of biofilm.

From previous studies, we conclude that the primary contribution comes from the adsorption to suspended biomass, and membrane retention, either by the membrane itself or the biofilm attached. Since the physical properties of membrane stay stable while the biomass growth is a highly active process, we speculate that to be more suited for the task, the model should keep a close eye on the biological kinetics and how it proceeds to impact the physical processes.

2.1.3 Efforts on modeling virus removal in MBR

Driven by the need to design, operate, and optimize WWTPs systematically and scientifically, the modeling of biological water treatment processes has long been of great interest to researchers [134,135]. The majority of the proposed models are mechanistic models expressed by numerical and analytical equations to provide information about the composition and structure of the system, the dynamics of each component, and the interactions connecting the components [136]. An early dynamic model considered only two state variables, degradation of the substrate and first-order biomass formation [137], but thanks to the growing understanding of the complicated process,

an increased number of state variables began to appear in later models, including the now widely applied ASM model family, which has been under continuous development since the 1980s [138–141]. Although ASM models were originally designed for activated sludge process, they have been applied to the MBR systems in recent years to describe the biomass kinetics with some adjustments made to accommodate the unique configuration of MBR [138,142,143], such as the addition of the fate of soluble microbial products (SMP) that play a critical role in membrane fouling, the high mixed liquor concentration and solids retention time, and gas sparging for membrane pressure relaxation.

Since in AnMBR the biological processes occur under the fundamentally different anaerobic condition, the models simulating them would have to be based on the kinetics of the anaerobic digestion process. The modeling of anaerobic process is considered a mature and well-established field after years of research, one widely accepted and discussed model is the IWA ADM1 developed by Batstone et al. (2002) [135,145].

Briefly, the models mentioned above share the same basic structure: the mass balance equations of components included in the system, either the influent composition or biomass in the reactor. The mass balance equations describe the inflow, outflow, reaction, and accumulation dynamics of substances in the reactor; biomass kinetics define the substrate transformation process; and physicochemical components construct the overall environment, including the interaction between different phases and ionic behavior. In practice, simplification is an inevitable step in modeling [146]. For example, 10 assumptions were made in ASM1 by the task group, mainly about environmental conditions and related coefficients that are fixed during the stable operation period [141]. Proper simplification could reduce the complexity of the modeling task and make the model more tractable [147], yet the assumptions are subject to system errors and failures and may lead to uncertainty [148]. The decision of what simplification should be made depends on the trade-off of accuracy and simplicity, and the focus of the model.

As membrane plays a central part in MBR systems, the physical process of membrane filtration should also be featured in a model dedicated to MBR systems [138]. In their extensive review of AnMBR modeling, Robles et al. (2019) introduced several candidate models, including pore blocking law models, resistance-in-series models, and critical-flux models [135]. Among these mechanistic models, resistance-in-series models developed on Darcy's law of filtration take into account the simultaneous and combined effects of multiple fouling mechanisms and thereby better mimic the reality than single fouling factor. In MBR systems, the filtration dynamics is under the influence of a variety of elements: the buildup of the cake layer, particle size distribution and hydrodynamics in the tank, and the operational factors including the aeration intensity and crossflow velocity.

For virus removal modeling, neither of the two models can be individually applied because biological and physicochemical factors are jointly involved. An integrated model that connects the two fields would be needed. Although both the biomass kinetic models and membrane filtration models are well-established in their own right, they are fundamentally different in terms of basic principles, which adds considerable difficulty to integrating the two components into a unified mathematical model. Some attempts have been reported in recent years, such as the AeMBR model developed by Mannina et al. (2011) [149], and the AnMBR model developed by [150], both models have fixed issues left by previous studies and lead to impressive TMP prediction performance ($R^2 \approx 0.9$ in the AnMBR model and ≈ 0.99 in the AeMBR model). Nevertheless, the complexity of the integrated models raises new concerns about the applicability due to the time and computational power required for fine-tuning and validation [151]. For the AeMBR model, 45 parameters and 9 state variables were used to carry out the model calibration, and similarly, a total of 53 parameters and variables are featured in the AnMBR model.

For the better interpretation and more accurate prediction of the virus removal performance

during wastewater treatment, researchers have long been interested in establishing models based on the understanding of the underlying mechanisms and kinetics. Here, we define a model as "process-driven" if it is constructed upon the understanding of the physicochemical and biological processes involved.

Kim et al. (1995) developed a simplified model based on amount balance equations to describe the virus transferring dynamics in the activated sludge basin [152]. The core equation is

$$V \cdot X_0 = V \cdot X_L + V \cdot X_E + V \cdot X_I \quad (2.1)$$

where V is the volume of the basin, X_0 is the initial virus concentration in the basin, and the mixed liquor in the activated sludge basin is divided into three parts; the liquid phase, the peripheral, and the inner region of the sludge flocs. X_L, X_E, and X_I in equation 2.1 stand for the virus concentration in these three parts, respectively. Virus particles in the liquid phase are assumed to have a reversible adsorption balance with the floc peripheral region. The floc inner region then encompasses the adsorbed virus particles into the inner part of the flocs. Also, the impact of predation is taken into consideration because the floc inner region is assumed to contain the protozoa and metazoan that uptake the viruses that are either dispersed in the liquid phase or adsorbed on the floc. Each virus transfer mechanism has an independent rate constant *K*, the values of *K* are assumed to be proportional to MLSS concentration and the amount balance is built upon the first-order equations describing the inflow and outflow of the compartments. Despite having established a dynamic balance of the virus behaviors in the mixed liquor, as the effect of environmental factors and the virus transfer mechanisms are overly simplified, this model still lacks some crucial features, including being able to respond to constantly changing reactor status and influent characteristics, and.

Regarding the kinetics of adsorption of virus particles adsorption onto suspended solids, Xing et al. (2019) used kaolinite and fiberglass as examples of colloidal particles present in the

aquatic environment and evaluated the adsorption property of MS-2 phage [153]. The adsorption kinetics can be described well by the Lagergren pseudo first-order model:

$$\frac{dq}{dt} = k(q_e - q) \tag{2.2}$$

$$\frac{dC}{dt} = k'(C - C_e) \tag{2.3}$$

In the equation, C is the concentration of unbound MS-2 phage in the bulk liquid phase at time t, and C_e is the equilibrium concentration. Similarly, q is the concentration of bound MS-2 phage at time t with q_e being the equilibrium concentration; k and k' are the observed pseudo first-order rate constants in the solid and liquid phases, respectively.

Despite having stated that the rate constants increased with increased kaolinite concentration, the authors did not integrate this relationship into the final model since a clear correlation between the two parameters was not found. Similarly, in another virus adsorption kinetic analysis conducted by Grant et al. (1993) [154], the reversible adsorption behavior of virus particles onto the solid surface was also described by the pseudo first-order model using the following equation:

$$\frac{1}{V}\frac{d\varepsilon}{dt} = k_f Q W n_f - k_b W n_s \tag{2.4}$$

where n_f and n_s indicate the number of virus particles in fluid and surface, respectively, and

k_f and k_b are pseudo first-order rate constants for virus adsorption and desorption. ε is the number of virus particles transferred from the liquid phase to the solids surface, Q represents the maximum adsorption capability per unit weight of the solid material, and W is the mass of suspended solids in the system.

Considering the adsorption media employed in these studies were stable solid materials, the use of fixed rate constants, despite not being ideal, makes perfect sense. However, in a real-

world context, the biomass in reactor is a highly dynamic complex that is sensitive to the fluctuation of operational status and influent characteristics [134,135]. Its composition and bioactivity actively vary over time, altering the adsorption behavior and kinetic parameters. Using fixed constants may not capture these dynamics and may eventually lead to insensitivity to the environmental changes.

Likewise, the first-order kinetic model was also applied to the virus inactivation process under various conditions with the following equations [90,113,155]:

$$\frac{dC}{dt} = -K_d C \tag{2.5}$$

$$C = C_0 \exp(-K_d t) \tag{2.6}$$

where K_d, C_0, and C stand for the inactivation rate coefficients (h^{-1}), the initial concentration of somatic coliphage in influent wastewater, and the somatic coliphage concentration at time t (PFU ml^{-1}), respectively. In the aquatic environment, the virus inactivation rate is closely related to temperature since the $\log_{10}$ inactivation rate has been found to hold a linear relationship with temperature [156], but it was not included in this model.

Regarding the effect of membrane filtration on virus removal performance, [81]) Elhadidy et al., (2013 introduced a model for UF membrane bacteriophage rejection based on a protein rejection model developed by Elhadidy et al., (2013. In the following equations, log removal is calculated from equation 2.7 by S_0, the sieving coefficient. S_0 is expressed as the ratio of the virus concentration in filtrate to that in the feed water. As expressed in equation 2.8, S_0 is related to $S_a(r)$, the convective transport coefficient of spherical solutes; r, the membrane pore radius; and $f(r)$, a log normal probability distribution that describes the membrane pore size distribution as in equation 2.9 [157]. $S_a(r)$ is derived using equation 2.10, where $\lambda = d_{particle}/d_{pore}$, $d_{particle}$ and d_{pore} stand for the diameters of the particle and the pore, respectively. The calculation

method of hydrodynamic coefficients K_s and K_t in equation 2.10 was described in Bungay and Brenner (1973):

$$\text{Log removal} = -log_{10}(S_0) \tag{2.7}$$

$$S_0 = \frac{C_{filtrate}}{C_{feed}} = \frac{\int_0^\infty S_a(r) \times f(r) \times r^4 \mathrm{d}r}{\int_0^\infty f(r) \times r^4 \mathrm{d}r} \tag{2.8}$$

$$f_r(r; \mu, \sigma) = \frac{1}{r \times \sigma \times \sqrt{2\pi}} e^{-\frac{(\ln r - \mu)^2}{2\sigma^2}} \tag{2.9}$$

$$S_a(r) = \begin{cases} 0 & 0 < r \leq a \\ (1-\lambda)^2 \times [2 - (1-\lambda)^2] \times \dfrac{K_s}{2 \times K_t} & a < r < \infty \\ 1 & r = \infty \end{cases} \tag{2.10}$$

The assumptions made for the model include the absence of concentration polarization and the effects of short-range intermolecular forces, uniform virus concentration inside the pore and in the permeate, and due to the properties of UF membrane, the exclusion of virus transport routes other than convective transport. On one hand, this study made a valuable point in establishing a baseline prediction model for membrane virus removal, but on the other hand, the authors also mentioned that under different pH settings, the removal of MS-2 coliphage observed in experiment contradicted the model prediction, indicating that electrostatic repulsion, despite not being included in the model, has an important role in membrane rejection of MS-2 coliphage.

Another simple virus filtration model developed by Rathore et al. (2014) assumes virus particles are colloidal particles without any specific interaction, Darcy's law is used to calculate membrane flux and the concentration of virus particles in the permeate is given by the equation:

$$C_p = K_i C_{mp} \tag{2.11}$$

$$K_i = -6.83 + 19.384\lambda - 12.518\lambda^2 \tag{2.12}$$

where C_p is the permeate virus concentration, K_i is a coefficient related to the hindrance of pore walls given by equation 2.12 using λ, and C_{mp} is the virus concentration inside the pore

mouth, which can be calculated by the equations below:

$$C_{mp} = \Phi C_s \tag{2.13}$$

$$\Phi = (1-\lambda)^2 \tag{2.14}$$

$$C_s = C_b \exp\left(\frac{J_v}{D}\delta\right) \tag{2.15}$$

where Φ is the ratio of virus concentration inside the pores to the virus concentration at the pore mouth, and the value is determined by the value of λ via equation 2.14. C_s is the virus concentration at the surface of the membrane, which can be calculated by equation 2.15, where C_b is the bulk virus concentration, J_v is the permeate flux, D is a coefficient for apparent diffusion of virus particles, and δ is the thickness of the concentration polarization (CP) layer formed by the rejected virus particles on the membrane surface, which can be given by the equation below:

$$\delta = at^b \tag{2.16}$$

where a and b are both constants, and t is the time of filtration. This equation indicates that as the filtration proceeds, the CP layer would grow thicker.

Wu et al. (2010) took a deep look into the removal process of somatic coliphages in a bench-scale MBR system and analyzed the contribution of each major mechanism. Both physical and biological processes were considered and fitted with mathematical models, although it is worth pointing out that this model is only partially process-driven because some relationships and coefficients are obtained via regression methods. The model starts with the mechanical sieving by the pristine membrane, a linear relationship between the log removal and λ was reported. Equation 2.17 shows the equation:

$$\text{Log removal} = 5.06 \cdot \frac{d_{particle}}{d_{pore}} + 0.03 \tag{2.17}$$

The decay and inactivation, either spontaneous or enhanced by activated sludge of somatic

coliphage, fitted well with the first-order kinetic model of equation 2.5 and 2.6. As for the coefficient K_d, the authors found the observed K_d value of sewage was higher than that of natural water and attributed it to the increased number of bacteria in sewage. However, the impact of water type was not packed into the model, because how environmental factors quantitatively affect the decay rate coefficient remains unclear. The adsorption of coliphage particles by activated sludge was fitted by the Freundlich isotherm equation shown in equation 2.18:

$$log_{10}Q = log_{10}K_a + \frac{1}{n} log_{10}C_e \quad (2.18)$$

In this equation, C_e and Q are the adsorption equilibrium somatic coliphage concentration and the adsorptive capacity at certain C_e, respectively, and n and K_a are constants. The authors also mentioned that the removal contributed by the fouled membrane is positively correlated with fouling degree, yet a mathematical model was not proposed.

Whereas the process-driven models provide great reference value in many ways, their applicability to real MBR systems still needs further validation before they can be useful in practical applications. The major obstacle is the model complexity when facing a process as complex as the virus removal in MBR systems. If all the contributing factors in both the biological and physical processes are integrated into an exhaustive and generalized mechanistic model, not only the number of active variables may outreach the scope of practical experiments design and routine monitoring [160,161], but the coordination and balance of components involved in the complex system would also significantly increase the amount of work and computational power needed. Moreover, the current understanding of the process is still far from adequate, the effect of some parameters on certain processes, such as membrane fouling, has yet not been clarified, and some processes may not even be able to be described by a mathematical model [138,143,151,162]. Bagheri et al. (2019) listed 28 parameters as important factors associated with membrane fouling, but they

also stated that available information is not enough to infer the relative importance of those parameters. Similarly, the membrane fouling model developed by Li and Wang (2006) takes into account the uneven distribution of aeration turbulence and the different rates of cake layer accumulation that follows. The final model consists of a large number of equations with 49 functioning parameters and coefficients, and even that, several assumptions, such as the absence of biomass properties variability and the effect of floc size on membrane fouling, are still made for simplicity. The simulation result shows that although the prediction of the general trend can be obtained, the fitness between the simulated result and experimental data was not satisfactory, further demonstrating the degree of complexity and nonlinearity of the membrane fouling process. The operating condition is generally set to be stable, which not only has limited tolarence for fluctuation, but also attenuates the potential effect of environmental factors that could alter the biomass behavior and the membrane physicochemical properties such as pH, conductivity, and chemical composition, making the model insensitive to the dynamic operating condition.

Since the virus removal process has not yet been clearly described by mathematical formulas due to its complexity [151,163,164], a chance for data-driven modeling approach may exist. Generally, a model can be classified as "data-driven" if the link between input and output variables is established via statistical methods using existing dataset, circumventing the need for studying the actual mechanisms. Due to this feature, some data-driven models are referred to as "black-box model" because the inner structure can be too obscure for further interpretation. Fig. 2.2 shows the typical workflow of designing and operating a data-driven soft-sensor model.

Considering the critical role of membrane filtration in the virus removal process, the efficiency of virus removal may be inferred from certain process indicators reflecting the membrane permeability, which can easily be put under real-time monitoring. Existing studies have supported such an idea, Shang et al. (2005) and Wu et al. (2010) both stated that when other

operational conditions remain unchanged, transmembrane pressure (TMP), a common measure of membrane fouling degree, could be used as an indicator for virus rejection, and the latter study reported a significant positive correlation (R = 0.693, p = 0.006) between the somatic coliphage rejection and TMP. A similar correlation between TMP and virus removal (R^2 ranges from 0.63 to 0.94) was also highlighted in the study of Yin et al. (2016) where human adenovirus was used as the model virus, but the authors pointed out that the quantitative relationship may be system-dependent and is hence challenging to establish. However, as pointed out by Fox and Stuckey (2015), it is also indispensable to find a way to incorporate other factors as well since the virus removal is not entirely dependent on TMP.

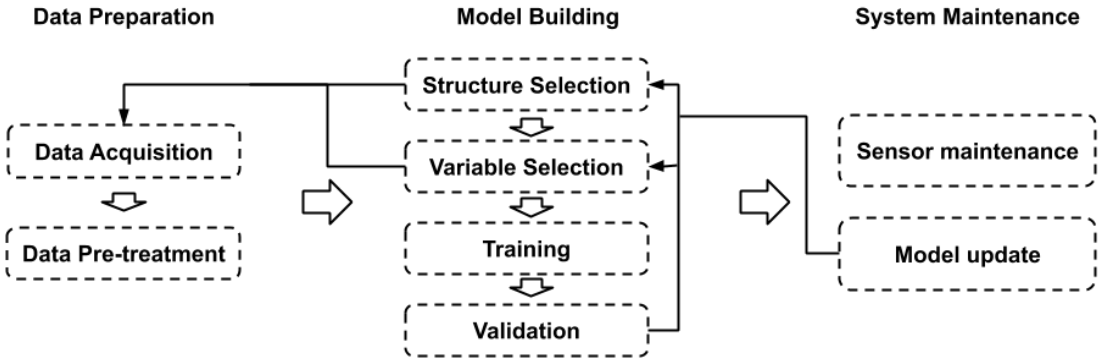

Fig. 2.2 The workflow of data-driven soft-sensor approach, from model design to application, adapted from Haimi et al. (2013).

Led by the increasing demand for online process monitoring and the inherent inadequacies of mechanistic models, the approach of data-driven modeling is gaining interest among researchers in various fields, and researchers working on water-related topics are no exception [165–167]. The main appealing aspect of data-driven models is that the connection between input and output variables is derived from available dataset by designated algorithms without the need for an understanding of underlying mechanisms, which could be either beyond current knowledge base or mathematically unsolvable [162,168]. In addition, data-driven models allow better handling of the

uncertainty and nonlinearity by comparison [169], this is especially intriguing when modeling a sophisticated process such as membrane fouling, which is closely related to the virus removal performance during the filtration process.

The data-driven modeling approach has seen a handful of successful applications regarding MBR systems with a special interest in automation and membrane-fouling control [124,169]. In the review paper by Naessens et al. (2012), several data-driven modeling methods already applied to MBR systems for different purposes are introduced. Generally, two types of methods can be considered data-driven: machine learning methods, and multivariate statistics. Machine learning techniques covered here include artificial neural network (ANN) and adaptive neuro-fuzzy inference system (ANFIS) while principal component analysis (PCA) and partial least squares (PLS) are discussed under the category of multivariate statistics. In essence, machine learning methods stand out in establishing nonlinear input-output relationships without prior knowledge, while the power of multivariate statistics lies in capturing the hidden relationship between inputs and output and finding the variables mostly correlated with the desired output. The two types of methods are often used together to offer better performance, for instance, the structure of ANN and ANFIS can be optimized by using PCA to reduce the dimensionality of data [124,166,167,170]. The power of these methods has been demonstrated in many cases, one example is the study conducted by Liu and Kim (2008), in which a comparison between ANN model and single blocking laws in TMP prediction was performed. While the ANN model took only three variables as input, its accuracy surpassed the single blocking law over the complete experimental period.

With all the progress having been made, though, applications related to MBR virus removal remain scarce in literature and the potential of such techniques is yet to be fully acknowledged. The closest example is the study by Madaeni and Kurdian (2011), in which virus removal by microfiltration membrane was predicted by a fuzzy inference system. Notwithstanding a decent

agreement was reached among the predicted and experimental data (RMSE = 15.81), the highly simplified filtration module design means there is still a long way to go before such a method could be employed for practical use.

Despite the competitive performance, data-driven models still suffer from some limitations. First, by nature, they need large training dataset to tune the internal parameters [172], which means when the availability of experimental data is less than ideal, the model may not perform as expected [161]. Secondly, since the understanding of the underlying process mechanisms is bypassed and the models are dedicated to existing data, the opaqueness of black-box models make them less easy to interpret when the interaction between process variables needs to be analyzed [167,173]. These drawbacks have raised the discussion among researchers about the potential of hybrid methods. Essentially, the objective is the convergence of mechanistic understanding of the process being modeled and the overwhelming superiority of data-driven models in learning from data and handling nonlinearity and uncertainty. Conceptually, in a properly built hybrid model, the mechanistic part and statistical part should complement each other, which means the resultant model can diminish the demand for training data and offer better extrapolation potential. Despite there has not been a study on applying hybrid model to virus removal in MBR systems, some efforts have been made for related topics such as membrane permeability prediction. Hwang et al. (2009) developed a hybrid model for membrane filtration performance forecasting, the model consists of a filtration model and an ANN model, two variables obtained from the physical model are fed into the ANN model as input variables, while the output is TMP predicted by 6 inputs in total. Another example of hybrid TMP prediction model can be found in the study of Chew et al. (2017), but in this model, the order is reversed. The ANN model was used to predict the specific cake resistance, α, a coefficient that both fluctuates with the characteristics of feed water and requires extensive works to determine via experimental method. The predicted value of α is then

used in a first principal model which gives TMP as output. By replacing the actual experiment with ANN model prediction, the model enabled rapid estimation and provided good agreement between experimental and predicted results.

2.1.4 Preferred features of future model and conclusions

From the viewpoint of maximizing the model capability and robustness, several merits would be of particular interest when conceiving and designing a pioneering model. Firstly, the model should be equipped with the ability to accurately grasp and approximate the intricate interactions between a large set of input and output parameters while being tolerant to data noise and fluctuation. In addition, it should have the capability to learn from available data and go beyond the scope of the current understanding of the virus removal process. Thirdly, as suggested by the HACCP concept, if possible, the model should take only easy-to-measure parameters or online sensor signals as inputs for real-time prediction. Finally, the model should have some flexibility to allow extrapolation to the conditions the reactor may encounter. Due to the wide range of reactor configurations and wastewater characteristics, the coefficients obtained from one reactor and one set of operational conditions might result in significant deviation when applied to others, so the ability to adapt to new configurations and operating conditions would be critical.

In conclusion, to ensure the safe use of the reclaimed water from MBR systems, an important task is to analyze and control the microbial risk, particularly the viral infection and disease risks. In addition to virus removal experiments as end-product inspection, prediction models based on the concept of soft-sensor needs to be developed for advanced risk management schemes. However, the high degree of complexity, nonlinearity, and uncertainty of the MBR-based wastewater treatment process makes establishing such a model an arduous task. There is no virus removal performance prediction model currently in existence that can fulfill all the requirements. Future studies on the understanding and integration of physical and biological virus removal

mechanisms and their joint impact on the final performance would be of great importance. Also, as the burgeoning data-driven and hybrid modeling approaches have shown their potential in this field, further research on this direction is needed.

2.2 Potential and challenges of COVID-19 wastewater surveillance

2.2.1 Introduction

COVID-19 is an infectious respiratory disease caused by SARS-CoV-2 infection. Due to its highly contagious nature, following the initial cases reported in Wuhan, China at the end of 2019, COVID-19 has swept the world. The World Health Organization (WHO) officially declared a global pandemic of COVID-19 on 11th March 2020, but it had spread to more than 200 countries and regions with a whopping worldwide case count of more than 500 million as of June 2022 despite all the measures taken to control its transmission [175].

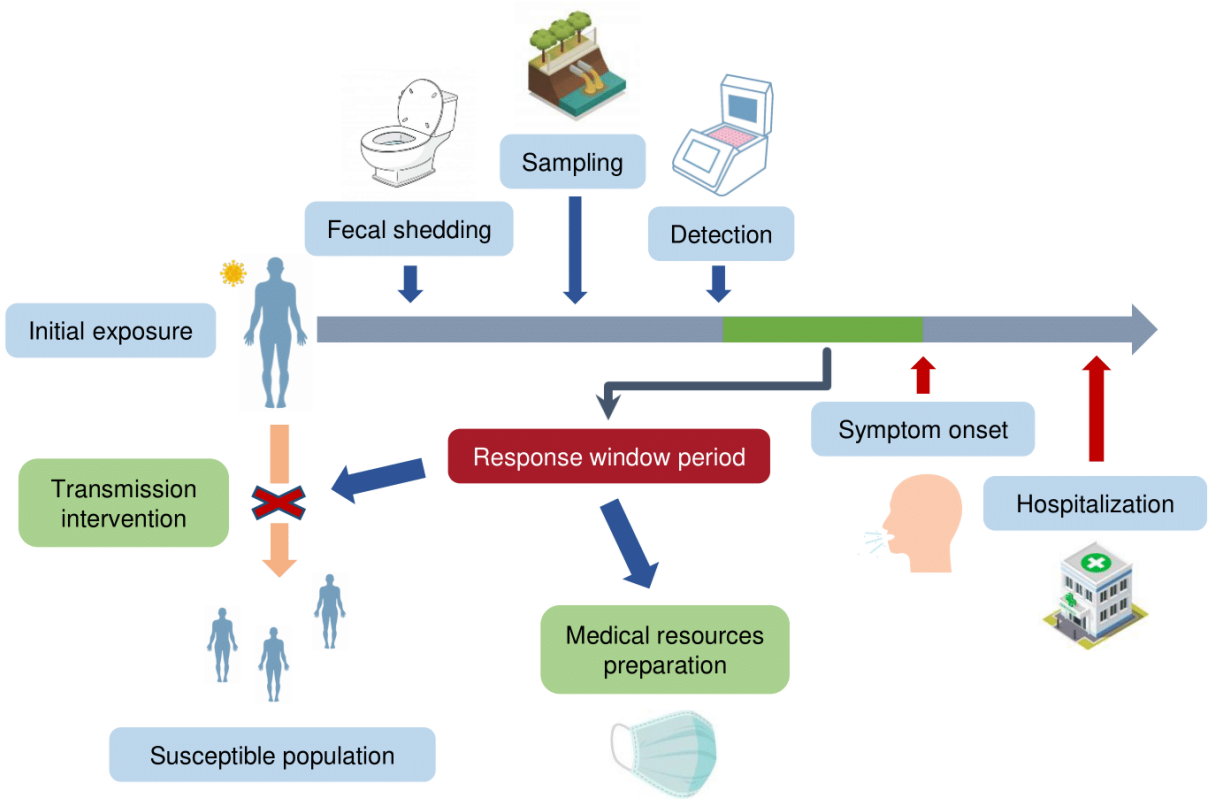

Fig. 2.3 A graphical abstract of literature review Section 2.2.

Among the efforts to contain the COVID-19 pandemic and mitigate its adverse impact

on society in the absence of an effective vaccine, the ponderance of a reliable and timely epidemic surveillance system has been stressed. Conventionally, the epidemic surveillance relies heavily on clinical testing either conducted by existing healthcare facilities or temporarily established testing sites, and for COVID-19, using reverse transcription quantitative polymerase chain reaction (RT-qPCR) on nasopharyngeal swabs to detect RNA signal has been accepted as the standard testing procedure [74]. However, the high contagiousness and the presence of asymptomatic virus carriers have made the clinical testing capacity largely lag behind the demand, raising the concern about the grievous outcomes of underreporting, which has been suggested by both statistical analysis and seroprevalence surveys [176,177]. Acknowledging the importance of filling the gap and lifting the pressure on testing facilities, recent studies have underlined the potential of wastewater-based epidemiology (WBE) as a solution complementary to clinical testing [68,69,178,179]. Following its successful early applications of tracking illicit drug usage and lifestyle factors, WBE is gradually gaining popularity among researchers in the water-related field. Blessed with its community-wide coverage, ability to "see" the underreported and asymptomatic patients, and low-cost nature, WBE has been proposed to be a promising tool in infectious diseases surveillance, and unsurprisingly, high hopes are placed for its capability of helping combat COVID-19 as well [67–69].

The basic concept of WBE centers around this principle: certain chemical or biological agents (also referred to as 'biomarkers') excreted by human bodies can be collected by the sewage network and end up entering the wastewater, making it a rich source of these substances. Via physicochemical methods, biomarkers can be recovered from wastewater and the measured concentration can then be used to infer the size of the shedding population and provide community-level health information [66]. For SARS-CoV-2, although antigen testing is also emerging [68], the viral genome has been widely accepted as the biomarker. To date, a handful of

studies have reported the detection of the SARS-CoV-2 viral genome in sewage networks [70–74,76,180,181].

However, some believe that the true standout of WBE is the early warning capability. The term "early warning" can be interpreted in two ways in the context of COVID-19 surveillance: (1) signaling an early stage of an outbreak. Presymptomatic/asymptomatic transmission of COVID-19 is considered a key factor behind its rapid spread [182]. Arons et al. (2020) recovered viable virus from 71% (17 in 24) of presymptomatic individuals 1 to 6 days prior to the symptom onset [183], and He et al. (2020) estimated that 44% (95% CI 25-69%) of secondary cases were infected when the index cases were in their presymptomatic stage [184]. While asymptomatic and presymptomatic virus carriers can easily hide in the population due to the absence of appreciable symptoms such as fever and dry cough, by nature, WBE can indiscriminately detect their presence as long as they develop viral RNA shedding [185]. Therefore, if a positive wastewater viral load is spotted in a region previously experiencing no or a low prevalence, it may indicate an unnoticed initial circulation of the virus in the community. This information can be made use by the local authority, who can take intervention by issuing warnings or administrative orders accordingly to inform the public of the potential threat and reduce the chance of invisible transmission. Also, as many countries and regions suffer from limited resources needed for a large-scale clinical testing program which greatly helps monitor the epidemic development and control the spread, getting a rough location of an initial circulation can help ease the burden and make the testing more efficient by guiding the valuable testing capacity to where it is most urgently needed; (2) foreshadowing an impending increase in infected individuals. The basic assumption behind this is: since infectiousness predates symptom onset, so can the viral shedding. Thus, if proper sampling tactics and quantification methods are adopted, an increased wastewater viral load may be observed and reported before

the newly infected individuals develop symptoms and seek medical attention. Since there may be a correlation between wastewater viral load and the number of infected individuals, in addition to supporting the administrative and resource deployment measures previously described, from the perspective of disease treatment, the quantitative information also allows the healthcare facilities to take measures aimed at improving preparedness and coping with the anticipated new patients beforehand so that the facilities are less likely to be overwhelmed.

Both interpretations of early warning have been backed up by recent studies and events. Table 2.2 lists some selected recent wastewater surveillance studies that highlight the potential of WBE early warning of COVID-19. In terms of practical application, the University of Arizona made headlines in August 2020 when researchers there detected SARS-CoV-2 viral genome in the wastewater from a student dormitory, the university quickly took action and tested all 311 residents living and working in the said building and found two asymptomatic carriers among them, likely having prevented a potential outbreak and making it the first true application of WBE in COVID-19 early warning [186].

Table 2.2 Recent wastewater surveillance studies that indicate the potential of COVID-19 early warning via WBE

Region	Sample type	Primary concentration method	Sampling period	Population size in the WWTP catchment area	Major findings related to early warning potential	Reference
Murcia, Spain	Grab raw sewage	$Al(OH)_3$ adsorption-precipitation	2020/03/12-2020/04/14	Multiple, from ~ 28,000 to ~ 530,000	Wastewater samples from three WWTPs were tested positive 12-16 days before COVID-19 cases were reported in the respective catchment regions	[71]
Amersfoort, The Netherlands	Composite raw sewage	Ultrafiltration	2020/02/05-2020/03/25	~ 234,000	Sewage signaled virus circulation 6 days before the first cases were reported	[72]
Milan, Italy	Composite raw sewage	PEG/dextran precipitation	2020/02/03-2020/04/02	~ 1,050,000	Samples were tested positive when the COVID-19 infections were very limited (29 in a larger area)	[70]
Ishikawa, Japan	Grab raw sewage	PEG precipitation	2020/03/05-2020/04/21	Multiple, from ~ 31,000 to ~ 233,000	Samples were tested positive when the prevalence was lower than one confirmed case per 100,000 people	[75]
Bozeman, MT, USA	Composite raw sewage	Ultrafiltration	2020/03/30-2020/06/12	~ 50,000	SARS-CoV-2 RNA levels in wastewater precede clinical PCR test results by 2–4 days	[187]
New Haven, CT, USA	Primary sewage sludge	N/A	2020/03/19-2020/06/01	~ 200,000	SARS-CoV-2 RNA concentrations in sludge predate hospital admissions by 1-4 days	[188]

2.2.2 Limiting factors, current knowledge, and research needs

When used for detecting newly introduced virus carriers and initial virus circulation in a low-prevalence community, the viability of WBE and the confidence it offers largely lean on the lowest possible prevalence level that enables viral RNA detection. This threshold is governed by many factors including the sewage network layout and capacity, shedding profile of infected individuals, sewage characteristics, sampling strategy, the recovery efficiency of the concentration and quantification methods, and the detection limit of the instrument. A relatively reliable estimate requires the latest knowledge about the pathology of COVID-19, verified experimental method, as well as support from the local water agency. Some estimates have been given by previous studies, Hart and Halden (2020) performed a computational analysis with the City of Tempe, Arizona, USA being the studied region and estimated that a sensitivity of 1 in 144 to 2 million individuals can be achieved, depending on the assumptions used [189]. Similarly, Ahmed et al. (2020a) reported an estimated prevalence level of 0.028% (95% CI 0.019–0.039%, 1 in 3571 individuals) based on viral RNA detection [73]. However, these estimations may be too optimistic as some factors that can significantly affect the detection sensitivity are missing while others face significant uncertainty. For instance, neither of the two studies counted the recovery efficiency of the experimental method, the latter study also did not consider the natural degradation of the viral RNA. As for the example of the University of Arizona, despite a detection sensitivity of 0.64% (2 in 311) on paper, as further details (*e.g.*, sampling strategy) remain undisclosed, it is unclear whether the same level of sensitivity can be expected under other conditions. Besides, in a quantitative sense, as an extension of calculating the lowest prevalence level that enables successful detection, a back-calculation model that projects the obtained wastewater viral load to the active shedding population is of foremost importance [66], yet so far, very few studies have challenged this issue.

Another measure of the viability of WBE in COVID-19 early warning is how responsive it can be. Even if the detection sensitivity is adequate for low prevalence detection, the value of detection can be seriously undermined, even nullified, if the result cannot reach the correct hands in time. Also, in regions where prevalence level is high enough to enable consistent viral RNA detection, WBE can still shine from its quantitative side; if the wastewater viral load is closely monitored and there is a surge in infections, as fecal shedding may predate symptom onset, an increase in viral load may appear before the newly infected individuals develop symptoms, seek medical attention, and be admitted to healthcare facilities after diagnosis, and the number of them may be inferred from the viral load. Different from the low prevalence detection which only gives a qualitative result, the quantitative outcome gives local healthcare facilities and their supervising agencies a response window period and an anticipated capacity demand. Just as in the case of testing capacity, in a time when many regions are having logistic difficulty handling the rapid increase in infections with limited resources, being able to forecast the demand may help get an upper hand and improve the preparedness as local healthcare facilities can make use of this time to (1) prepare necessary medical supplies and equipment including beds, ventilators, protective clothing, and masks; (2) arrange human resources to make sure there would be adequate health workers for the increased workload. In addition, from a higher angle, this community demand forecast may enable regional reallocation of available resources which can come in handy if there is an overall shortage.

However, both measures of the feasibility of WBE early warning face considerable uncertainty. In the previously mentioned studies regarding the lead of viral RNA in primary sewage sludge compared to local admissions, the analysis was performed in a retrospective way: the accumulated longitudinal SARS-CoV-2 quantification data were compared with the clinical reports during the same period. For WBE to be an active early warning tool, though, it needs to

be performed in a timelier manner. One important index in the timeline of COVID-19 infection is the incubation period, which is the time gap between virus exposure to symptom onset. Some studies have reported very similar median or mean values of approximately 5 days [190–192]. After the symptom onset, there typically will be another period until the testing result comes out or the patient gets admitted to a hospital, Lauer et al. (2020) reported a mean value of 1.2 days [190], but it may vary greatly depending on the testing policy and the capacity of the hospital in question. Adding the two intervals up sets a reference for WBE; whether the workflow can be streamlined to beat this time largely affects its viability, although to what extent the outcome is useful also depends on how long is the response window period left behind.

In the following sections, factors that may become bottlenecks, their significance, what previous and recent studies have revealed, and what awaits to be addressed and clarified by further studies are summarized and discussed to provide readers with a brief roadmap towards the final application of WBE as a part of the COVID-19 early warning system.

2.2.3 Shedding profile of infected individuals

The shedding profile of infected individuals directly determines the wastewater viral load and is hence regarded as one of the most critical factors in WBE. The shedding profile consists of three parts: the shedding rate, the beginning of shedding, and the shedding duration. When the shedding profile is relatively predictable and stable while showing finite between-person variation, it will greatly simplify the modeling process, but on the other hand, if the shedding profile bears significant stochastic fluctuations and between-person discrepancy, substantial extra efforts would be needed to handle the data noise and uncertainty.

So far, reports regarding shedding rate have mainly focused on hospitalized symptomatic patients due to the availability. Walsh et al. (2020) summarized in their review that while some studies reported little to no difference in the viral loads of symptomatic and asymptomatic patients,

there are also studies that found the severity of symptoms can affect viral load, indicating substantial heterogeneity. Generally speaking, fecal viral shedding shows significant uncertainty, and the overall pattern is more erratic than respiratory shedding. One of the earliest assessments of the rate and duration of fecal shedding was conducted by Wölfel et al. (2020), while the highest recorded viral load among 9 hospitalized patients reached 10^7 copies/gram of stool sample, the results also show significant variation between cases; the viral load of one patient had always stayed below 10^4 copies per gram of feces. In a review by Parasa et al. (2020), the recorded viral load in stool samples also ranges from 550 to 1.21×10^5 copies per mL of feces. The viral shedding in the gastrointestinal tract seems more erratic than that in the respiratory tract [193]. In addition to the variation in shedding rate, it has also been stated that not all infected individuals will develop fecal shedding. In the aforementioned study by Wölfel et al. (2020), the stool specimen of one patient was negative during the entire testing course. A meta-analysis by van Doorn et al. (2020) reported that 51.8% (95% CI 43.8-59.7%) of patients have their stool specimens tested positive while another systematic review by Gupta et al. (2020) reported a similar percentage (53.9%), but very limited information is available about the shedding ratio among asymptomatic virus carriers. Not only is this uncertain fecal shedding a hindrance to the estimation of achievable detection sensitivity, it also means that when the number of infected individuals is low, statistically, there is a chance that none of them sheds viral RNA into wastewater, making their presence undetectable by WBE no matter how sensitive the assays are.

Also, the timing of fecal shedding has a decisive role in determining how “early” the shedding can be detected. As the routine testing of fecal shedding typically only focuses on symptomatic patients after their hospitalization, solid evidence remains scarce as to the actual starting point of fecal shedding, especially among asymptomatic virus carriers. Alternatively, the timing of infectiousness development (respiratory shedding) may be used as a proxy. He et al.

(2020) estimated that the infectious period begins at 2.3 days prior to symptom onset and peaks at 0.7 days before it. Nevertheless, it is important to keep in mind that respiratory shedding does not perfectly represent fecal shedding and may not exactly parallel it, related information hence must be interpreted and used prudently until more medical evidence becomes available.

As another critical aspect of the shedding profile, the persistency of shedding should also be given some consideration. It has been revealed that the shedding of SARS-CoV-2 in fecal specimens can outlast that in respiratory specimens [185,197–200]. The long-tailed fecal shedding may cause a masking effect on newly infected individuals, making their presence indistinguishable from the patients in their post-infection phase, especially when an infection peak has recently ended and the shedding population remains large. Although according to previous medical reports, the intensity of shedding steadily declines during the infection course, further clinical evidence is still needed to confirm whether the long-tailed shedding will become a concern for WBE application.

Because the shedding rate and duration determined from clinical case reports may be subjected to stochastic error and person-to-person variation, if possible, packing available data and biological explanation into a mathematical model for better generalization and easier extrapolation of the shedding dynamics is preferable. Currently, available information about this approach is very limited and further study is needed. Recently, Miura et al. (2020) fitted a shedding dynamics model originally developed by Teunis et al. (2015) for norovirus fecal shedding.

$$C(t|\alpha,\beta) = C_0 e^{-\alpha t}\left(1 - e^{-(\beta-\alpha)t}\right)(\beta - \alpha) \tag{2.19}$$

This model assumes that virus particles first accumulate at an infection site and are then released from the intestinal tract into the environment. $C(t|\alpha,\beta)$ is the virus concentration in feces at time t, α and β are constants that are defined by the transport rate and effective volumes of the compartments within the intestinal tract, and C_0 is a constant controlling the height of peak

virus concentration. The shedding curve features a rapid increase in the initial stage of infection, followed by a downward slide until the virus concentration falls below the detection limit. Other mathematical models have also been developed for virus shedding into saliva and blood based on the understanding of the infection process [202,203]. However, although these previous models have provided some insights, as mentioned above, the fecal shedding of SARS-CoV-2 may have its own distinct characteristics and follow a different biological mechanism, it is unclear whether the same pathologic assumptions and consequently these mathematical models can be applied to SARS-CoV-2.

In conclusion, though much information has been made available, the current knowledge is still far from enough to support successful WBE application in absolute calculations. A heavy workload still lies ahead until the uncertainty in the fecal viral shedding can be properly addressed. However, it should be clearly stated that there is no guarantee that such a goal will finally be achieved therefore the worst scenario also needs to be considered: if the shedding profile is eventually found to be too erratic and unpredictable, as some existing literature suggests, to be clearly described and properly modeled, the prospect of WBE will be critically impaired as it lacks the ability to be a tool for absolute quantitative analysis. But to proceed from where we are now, a more comprehensive and holistic image of the shedding profile, including the rate, starting time, and duration is needed, which will benefit from further clinical evidence.

2.2.4 Recovery efficiency and instrument detection limit

Stable and efficient recovery and detection of the viral RNA is a decisive factor in wastewater surveillance. The recovery efficiency and instrument detection limit provide a critical reference when estimating the threshold prevalence level and back-calculating the shedding population from the viral load. For primary concentration and RNA extraction, several research articles and reviews have looked into this technical issue, focusing on either surrogates or other coronavirus strains [204–

[207]. Ahmed et al. (2020d) recently compared the recovery efficiency of some commonly used methods for wastewater virus concentration using murine hepatitis virus (MHV) as the surrogate for human coronavirus, the average recoveries varied from 26.7 to 65.7%, with the method having the highest recovery efficiency being an adsorption-extraction method supplemented with $MgCl_2$. Torii et al. (2020) conducted a similar study, in which *Pseudomonas* phage φ6 was used as the surrogate, and a method combining polyethylene glycol (PEG) precipitation and acid guanidinium thiocyanate-phenol-chloroform extraction achieved a mean recovery efficiency of 29.8 to 49.8%. From the standpoint of quantitative analysis, this means if the recovery efficiency is not considered, in other words assuming a 100% recovery, the estimated detection limit would be lower than the actual value, which may lead to a falsely high sense of security. However, even though both MHV and φ6 are enveloped viruses and may better resemble the behavior of SARS-CoV-2 than nonenveloped surrogates, discrepancy may still exist and the measured recovery efficiency should be used discreetly and only as a reference.

It is also worth mentioning that many established primary concentration methods were originally developed and validated for nonenveloped waterborne gastrointestinal viruses. Due to the distinct structure and surface property of enveloped viruses such as SARS-CoV-2, their behavior in the wastewater matrix may also be different, including the partitioning [208]. This has been reflected by recent reports of the detection of SARS-CoV-2 in sewage sludge [74,188,209]. However, it is important to point out that due to the sedimentation process, the viral load in primary sludge may be the result of an accumulation over several days and does not reflect the real-time change in the wastewater matrix. As for the wastewater solids, Kitamura et al. (2021) and Westhaus et al. (2021) recovered SARS-CoV-2 RNA from both the solid and liquid fractions of wastewater and the results suggest that wastewater solids may support more sensitive SARS-CoV-2 detection. Therefore, an extra step that helps release viral RNA from the solids (*e.g.*, heat treatment and

adsorption-elution) may improve recovery efficiency [212,213], but additional research needs to be conducted to verify the efficacy for SARS-CoV-2.

The last barrier of the quantification assay is the detection and quantification limit. For RT-qPCR, a standard curve is necessary for converting the cycle threshold (Ct) value into virus titers, but if the signal intensity is below a certain Ct value, it would be indistinguishable from the potential noise. In practice, this Ct value limit is usually translated to gene copies per unit volume by referring to the standard curve. However, if the dilution series is not well configured, there could be a difference between the limit of detection (LoD) and the limit of quantification (LoQ). Attention should be paid to reduce or eliminate the gap between LoD and LoQ. PCR reaction inhibition is also a concern in wastewater surveillance, the introduction of process control, whether applied to the whole process, before RNA extraction and/or before RT-qPCR, has been proposed to help evaluate the extent of inhibition [214]. In addition, the design of RT-qPCR assay [73,180,210,215] and nucleic acid extraction kit [216] can also affect the detection sensitivity. As in the case of the primary concentration method, at the current stage, a consensus of optimal recovery-detection assay has not been reached, researchers may need to conduct their experiments to determine the assay suitable for the lab condition and wastewater characteristics.

Some recent studies have employed droplet digital PCR (ddPCR) for the detection of SARS-CoV-2 RNA in clinical samples [217–220] and suggested that ddPCR is a superior choice for clinical diagnosis for its higher sensitivity and other benefits such as not needing a standard curve for quantification. However, D'Aoust et al. (2021) compared RT-ddPCR and RT-qPCR using wastewater sludge samples and the results did not support the statement that RT-ddPCR performs better than RT-qPCR. It is possible that the low detection limit offered by ddPCR can enhance the performance of the WBE approach, but related research needs to be further extended to investigate the effect of factors such as inhibition and optimize the assay.

2.2.5 Dilution factor and sampling strategy

Once the viral RNA is released from shedding individuals, it will enter the sewage network and get mixed with the rest of the wastewater. In its simplest form, the dilution factor can be determined by assuming a complete and homogeneous blend of the viral RNA shed by all shedding individuals in one day and the daily wastewater flowrate which is usually obtainable from the sewage network operator. But in practice, the mixing and dilution process is significantly influenced by the uneven diurnal wastewater flowrate and the timing of toilet flushing. There are two options of sampling: composite sample and grab sample. Composite samples are favored in recent detection reports and are generally considered more suitable for the task as multiple wastewater samples over a period of time are collected, this increases the success rate of detection given the high uncertainty of shedding, especially when the sampling period is set to 24 h and a flow-proportional sampler is used [69,176,221]. However, considering the biological rhythm and living habits of human beings, the variance may, in turn, be beneficial and the grab sample may offer a higher chance of detection if the sampling time is optimized to capture the peak hours of the toilet flushing. In the aforementioned study of Hata et al. (2020) in which a positive signal was detected when the catchment area had a low prevalence level (less than one confirmed case per 100,000 people), grab samples were used. However, due to the unevenly distributed in-sewer travel time in a large sewage network, this specific method may be more applicable to confined environments (*e.g.*, dormitories and nursing homes). An early study on defecation concluded that defecations are more likely to occur in the early morning [222], and Campisano and Modica (2015) reported that there are three toilet flushing peaks during a day, although it is necessary to point out that the result is merely based on a case study of a household and whether it also applies to a larger community needs further verification.

Previous studies have employed different sampling frequencies, from taking samples on

discrete dates [70,224], to routine sampling with a relatively stable interval [71,74,180] and daily sampling [188]. For retrospective analysis, frequent sampling over a long period (*e.g.*, several months) may unnecessarily increase the total workload required for sample processing, therefore lower frequency is acceptable and more realistic. But under the premise of using the measured viral load for early warning, especially considering the rapid progression of the COVID-19 epidemic and the potential social significance of the measures to be taken, daily or similarly frequent sampling is highly recommended as long as the laboratory capacity allows.

Apart from direct measuring, human fecal indicators may also help normalize the flowrate as well as help identify the peak flushing hours in a day if there are any. Some previous studies have opted for the usage of pepper mild mottle virus (PMMoV) as an internal control because of its universal and stable presence in the wastewater matrix [225,226], but more options including crAssphage, HAdV, JCPyV, human microbiome-specific HF183 *Bacteroides* 16S ribosomal rRNA, and eukaryotic 18S rRNA may also be used [74,176,227,228], although it is worth mentioning that because their nature may be very distinct from that of the target biomarkers, these internal control targets cannot be used for signal normalization.

2.2.6 In-sewer travel time and degradation

Once the viral RNA is released from infected individuals and enters the wastewater, it will spend some time traveling in the sewer pipes until it reaches the designated sampling site. The in-sewer travel time is a function of many characteristics of the sewage system in question, such as the spatial configuration of the sewer network and wastewater flow rate in a given time, hence its value may vary greatly among sewage networks and is highly recommended to be determined for each WBE project individually if needed. Although its importance in WBE has been underlined [229], the in-sewer travel time for a given sewage network has rarely been reported, presumably due to the difficulty of performing an experiment or establishing a hydrological model. But according

to limited existing estimates made for multiple purposes including WBE application, the mean value of in-sewer travel time, or wastewater residence time, typically falls within several hours. For instance, it has been estimated that the national median in-sewer travel time for the U.S. is 3.3 h [230], and the approximate sewer transit times of the UK and Rome have also been estimated to be ~2 h and 3-5 h, respectively [231,232]. Also, in the case of grab sampling, the mean or median value does not consider the population heterogeneity, the wastewater produced by those living close to the sampling site will have significantly shorter in-sewer travel time compared to that from people living in the upstream area. To offset the potential impact, the demographic and geographic distributions of the population may also be considered a factor.

Wastewater is a complex matrix with a high concentration of microorganisms and substances that are either organic and inorganic, all of which may contribute to the natural degradation of viral RNA. Previous studies have investigated and reviewed the degradation of human coronaviruses including SARS-CoV and SARS-CoV-2 and their surrogates such as murine hepatitis virus (MHV) in the wastewater matrix [233–235], as the results suggest, the viral RNA of SARS-CoV-2 is more persistent than viable virus particles and can stay in wastewater for a relatively long period, and the decay rate increases as the wastewater temperature goes up. Bivins et al. (2020) recorded a 26.2 days T_{90} value in untreated wastewater at 20 °C, which is comparable to the study by Ahmed et al. (2020) in which the T_{90} values in untreated wastewater at 15 and 25 °C were 20.4 and 12.6 days, respectively [235,236]. Because the typical residence time of wastewater is several hours, the effect of degradation may not be as pronounced as other factors, but it is still recommended to take the degradation kinetics into consideration for better accuracy. For instance, in a long-term monitoring project, the seasonal change in wastewater temperature may bring change to the prevalence estimation as the degradation during summer would be more significant and may reduce the measured viral load [189].

Although the majority of existing studies took samples from wastewater treatment plants (WWTPs) for better coverage and convenience, they are not the only option. If a better spatial resolution or a shorter response time is required, the strategy of 'upstream sampling' can also be employed, which means samples are taken from locations closer to the origins, such as sewer pumping stations and maintenance holes, to narrow down the coverage and shorten the in-sewer travel time [69,176].

2.2.7 Turnaround time for sample treatment and quantification

The turnaround time for sample treatment consists of sample transportation, virus concentration, quantification, and data analysis and organizing. Primary concentration methods can take anywhere from about an hour (ultrafiltration, electronegative membrane vortex) to overnight (PEG precipitation) [205,206], the time required for subsequent steps varies depending on the reagent kits and instruments used but is also typically in the range of several hours if all steps are done consecutively. The time needed for sample transportation and data analysis depends heavily on real-life factors including the transportation method, the distance between sampling site and laboratory, and the way of data processing, so far, very limited information about these two steps is available from existing literature. Due to the varied conditions, although it is possible for the WBE approach to predate symptom onset and hospital admission, the entire workflow is subject to significant uncertainty and different settings hence an estimated time cannot be given. We encourage future studies to include the information of the time required for each step to give a better image of the total turnaround time.

Worrying that the standard off-site RT-qPCR method may not fulfill the demand for rapid detection, recent studies have discussed alternative methods. Mao et al. (2020) and Bhalla et al. (2020) discussed the potential of paper-based analytical devices, which are easy-to-carry tools that can be deployed for rapid on-site nucleic acid testing. Yang et al. (2017) reported a paper-based

"sample-to-answer" platform for the detection of human genomic DNA in untreated wastewater based on the loop-mediated isothermal amplification (LAMP), through which the result can be yielded within 45 min. Nguyen et al. (2020) shared similar optimism about LAMP, specifically stating that LAMP can be a potential candidate for COVID-19 early detection. While alluring on paper, compared to the conventional laboratory apparatus, the reliability of new methods and devices remains unverified, and very limited information is available regarding the practical application despite the strong interest. Although the development of novel devices and methods that can enable rapid and reliable detection of SARS-CoV-2 genome RNA is highly encouraged, considering that the derived information will be used to help make crucial decisions, the application must be proceeded with caution.

2.2.8 Data analysis

After obtaining the quantification result, the final step is data analysis. If the SARS-CoV-2 signal in a low prevalence region is positive for the first time, it indicates a high possibility that the predetermined threshold prevalence level has been exceeded, but for better dependability, especially considering the information will be used to support critical decisions that may leave a permanent impact on the society, an additional validation step may be employed at the cost of longer response time. As for long-term monitoring in a middle-to-high prevalence region where the viral load is consistently higher than LoQ, the concentration of viral RNA, or the active shedding population if a back-calculation model can be successfully established and validated, should be combined with previous results to assemble a longitudinal pattern.

Although in theory qualitative and semi-quantitative analysis can be performed without a back-calculation model that connects the viral load to the active shedding population [68], the lack of quantitative projection would certainly impair the usefulness of the result. Although lagged correlation has been found in wastewater viral load and reported patient number [187,188], there is no

model currently in existence that can infer the size total infected or shedding population, which could be much larger than reported cases due to undertesting and asymptomatic virus carriers. Previous WBE projects have used excretion-dilution-recovery mass balance models for the back-calculation of chemical biomarkers [241–243], but in the case of COVID-19 surveillance, the same model may suffer greatly from the limited understanding and the variance of some parameters (mainly the shedding profile and dilution factor) as well as the potential data noise. One reason is that due to the persistent fecal shedding, the wastewater viral load is likely to be contributed by patients in different infection stages, this population may even include those who have the virus cleared in the respiratory tract. Thereby, not only modeling tools that help reduce the uncertainty (*e.g.*, Bayesian inference and maximum likelihood estimation) are highly recommended, other mathematical models featuring different structures are also worth looking into as long as they offer a decent capability of capturing the correlation between viral load in wastewater and the shedding/infected population and dealing with the noisy data. Here, we not only encourage researchers who are already working on COVID-19 wastewater surveillance to reach out and look for potentially suitable modeling techniques but also call on experts from other disciplines, such as epidemiology and statistics, to join in and tackle the challenge together.

Knowing the *de facto* population size in the catchment area also helps reduce the uncertainty when doing quantitative analysis [68,176,244,245]. Census data or estimation based on facility capacity can be used as an approximation, but they may deviate from reality. Another option is to use certain population biomarkers including exogenous markers such as nicotine and caffeine, and endogenous markers 5- hydroxyindoleacetic acid (5-HIAA) and ammonia [244], but it should be kept in mind that significance discrepancy may exist between regions and countries due to various lifestyles. Apart from the *de facto* population, in regions with high mobility (*e.g.*, tourist attractions and transportation hubs), the frequent movements of people not only increase the risk of virus

introduction but also introduce a new source of uncertainty for quantitative analysis [243]. Further studies will need to employ appropriate methods to estimate and validate the population covered by the studied sewage network and consider how to incorporate the dynamics of the population into the result interpretation process.

As mentioned previously, WBE should not be considered as a standalone solution, but rather as a complementary data source in public health management [69,74,246]. Therefore, the result obtained from WBE should be viewed and assessed along with other supporting materials such as clinical reporting and estimation made with epidemic models before reaching any final decision.

2.2.9 Conclusion

While certainly holding potential, the prospect of using wastewater-based epidemiology as an early warning system for COVID-19 surveillance still has many hurdles to overcome. As a result, we encourage experts from different disciplines to work together and share knowledge for the further refinement and validation of this novel approach as humanity continues to battle the ongoing COVID-19 pandemic.

3. Microbial safety evaluation and modeling of anaerobic membrane bioreactor (AnMBR)

3.1 Introduction

In this project, the aim is to testify the applicability of soft-sensor approach in the real-time monitoring of virus removal performance in AnMBR. We employed a pilot-scale AnMBR treating municipal wastewater as the testing platform, the concentration of two indigenous viruses was quantified using RT-qPCR. Then, operational variables acquired from reactor operators were analyzed for their potential connection with the virus reduction performance. Finally, data-driven modeling methods were tested to verify whether virus reduction can be predicted from the operational conditions of AnMBR.

3.2 Materials and methods

3.2.1 AnMBR overview

In this study, a pilot-scale submerged AnMBR plant located in Sendai, Japan was employed. The reactor has a total volume of 5,000 L, featuring a hollow fiber PVDF membrane with a pore size of 0.4 μm and a total area of 72 m^2. The influent is pre-screened municipal wastewater from a local sewage treatment center that serves a population of about 150,000. Before sampling, this pilot-scale plant had been operated for about 500 days and had entered a stable stage. More information about the configuration and operation of this AnMBR plant can be found in previous studies [247,248].

3.2.2 Sample collection strategy

Influent and effluent samples were collected from the AnMBR plant from September 06, 2020 to February 01, 2021 (duration: 149 days). The sampling frequency was once a week with exceptions due to holidays and reactor maintenance. Considering the potential difference in virus concentration, the volumes collected for influent and effluent are 40 mL and 1 L, respectively. Upon collection, samples were kept in ice and transported to the laboratory and were concentrated on the day of collection.

3.2.3 Sample concentration

Influent and effluent samples were concentrated using two methods due to different collected volumes. Influent samples were concentrated by a previously described polyethylene glycol (PEG) precipitation method. Briefly, a 40 mL of influent sample was added with 3.2 g PEG 6000, 0.92 g NaCl, and 100 μL of pre-prepared murine norovirus (MNV) strain S7-PP3 stock suspension for recovery calculation. The mixture was stirred overnight at 4 °C using a magnetic stirrer. Subsequently, the mixture was centrifuged at 8,000 × g for 30 min at 4 °C. The supernatant was then removed, and the pellet was resuspended with 1 mL of MilliQ water. The resuspension was further centrifuged at 9,000 × g for 10 min at 4 °C. The supernatant, with its volume measured, was used for following RNA extraction and RT-qPCR.

Effluent samples were concentrated by a double membrane filtration assay [249]. Briefly, one liter of effluent was added with 10 mL of 2.5 M $MgCl_2$ and 1 mL of MNV stock suspension. The sample was then concentrated by suction filtration using a 0.45 μm membrane (HAWP-090-00, Millipore). Following the filtration, the membrane was washed by 200 mL of 0.5 mM H_2SO_4. Finally, 10 mL of 1 M NaOH was added to elute the absorbed virus into 10 mL TE buffer with 100 mM H_2SO_4, the final volume is about 20 mL. Then, the filtrate underwent a secondary filtration using CentriPrep YM-50 at 2,500 rpm for 10 min. Note that due to a shortage of CentriPrep, two effluent samples (collected on) were concentrated by Amicon Ultra-15, MWCO 30 kDa for 15 min at 2,500 × g. The volume of the final filtrate was recorded for recovery calculation.

3.2.4 RNA extraction, cDNA synthesis, and RT-qPCR

PMMoV and norovirus GII were chosen to be targets because they are: (1) indigenous in the wastewater matrix and (2) representative of the fecal content (PMMoV) and waterborne human virus (norovirus GII) [226,250]. The RNA extraction and cDNA synthesis were conducted

using QIAamp Viral RNA Mini Kit (Qiagen) and iScript™ cDNA Synthesis Kit (Bio-rad), respectively. RT-qPCR was performed on a CFX Connect system (Bio-rad) using the SsoAdvanced Universal Probes Supermix (Bio-rad). The details of RT-qPCR, including the sequences of the primer/probe set for each target virus, formula of the mix, and thermal cycling conditions can be found in Appendix Table S2. All RT-qPCR reactions were performed in triplicate and the mean Ct value was used for subsequent calculations.

3.2.5 Virus removal performance and modeling

The virus concentrations measured in RT-qPCR were first converted back to the concentrations in samples using the following equation:

$$C = 1000 \times \frac{V}{V_w} \times \frac{V_{f,ex}}{V_{s,ex}} \times \frac{V_{f,syn}}{V_{s,syn}} \times C_{qPCR} \quad (3.1)$$

where V is the volume of sample after concentration, C_{qPCR} is the concentration of cDNA applied to qPCR [copies/μL], V_w is for the original sample volume [mL]. $V_{f,ex}$, $V_{s,ex}$, $V_{f,syn}$, and $V_{s,syn}$ are all the volume of samples in the intermediate steps [μL]. Subscripts *f* and *s* stand for final and starting volume, while subscripts *ex* and *syn* stand for RNA extraction and cDNA synthesis, respectively. Then the virus removal performance was defined by the log reduction value (LRV) calculated using the following equation:

$$LRV = logC_{inf} - logC_{eff} \quad (3.2)$$

where C_{inf} and C_{eff} are the virus concentration in the influent and effluent samples, respectively.

The record of operational variables of the AnMBR plant during the study period was acquired from reactor operators. The record includes a total of 36 variables (Appendix Table S1), ranging from reactor conditions like the pH of influent to operating strategy such as HRT. The devices and experiments performed to obtain these variables had been described in previous studies [247,248].

A variable screening and selection step was first conducted by calculating its Spearman's rank correlation coefficient with LRV. The modeling was performed in three ways: 1) only variables found to be strongly correlated with LRV were used as the inputs while LRV was the output; 2) 50% of all variables, selected by their absolute correlation coefficients, were used as inputs; 3) all variables were used as inputs. The goal was to see whether using more variables in the prediction model offers better prediction. Two data-driven regression models (artificial neural network (ANN) and random forest (RF) were tested for comparison. Briefly, ANN features a network structure and three layers: input layer, output layer, and one or more hidden layers. Each layer has a certain number of nodes and the input and output layers are connected via the hidden layer. By tuning the weights between the nodes, the output can be indirectly connected to the input layer. This gives ANN the ability to establish complex and potentially nonlinear relationship between the input and output. On the other hand, random forest is based on a large number of decision trees. Using bootstrap aggregating, the final outcome from random forest is the collective decision of all individual decision trees. To ensure the randomness in model training and reduce overfitting, repeated random sub-sampling cross validation method was used. In each iteration of model training, only a part of the dataset (80%) was randomly selected to train the model, the model was then used to perform prediction on the inputs of remaining 20% dataset. The training process used 500 iterations. The prediction performance was evaluated by the root-mean-square error (RMSE) between the predicted and actual LRV, a grid search step was used to find the optimal model configuration under each setting.

3.3 Results and discussion

A brief overview of some key AnMBR performance indicators and the virus quantification results can be found in Fig. 3.1. The reactor had been in stable operation during the study period with only minor adjustments of the operating strategy. Specifically, as the air

temperature decreased during the winter, the MLSS temperature was also turned down to save the electricity consumed by reactor heating and test whether the reactor performance is still stable under a lower temperature. On the first sampling day (September 09, 2020), the recorded air temperature was 31.0 °C, representing a typical summertime working condition in the local environment. After that, air temperature continued to decrease until reaching a low point at 2.0 °C on December 13, 2020. The low temperature condition (≤ 6.5 °C) lasted to the end of study period. In response to this, the reactor heating setting was changed from 25 °C to 20 °C. A common index used for AnMBR performance evaluation, COD removal efficiency, retained at a high level (~90%) during the majority of study period with only one exception when a low MLSS concentration was recorded. But overall, there was no significant variation in reactor operation status, providing a stable platform for virus removal test. Regarding virus recovery efficiency, after adjusting for the volume change in the quantification steps, the MNV recovery efficiency was relatively stable, ranging from 18.37% to 47.96% in influent samples. However, in effluent samples, the range is 0.14% to 4.39%, lower not only than that of influent samples, but also reported in previous literature for other viruses [249].

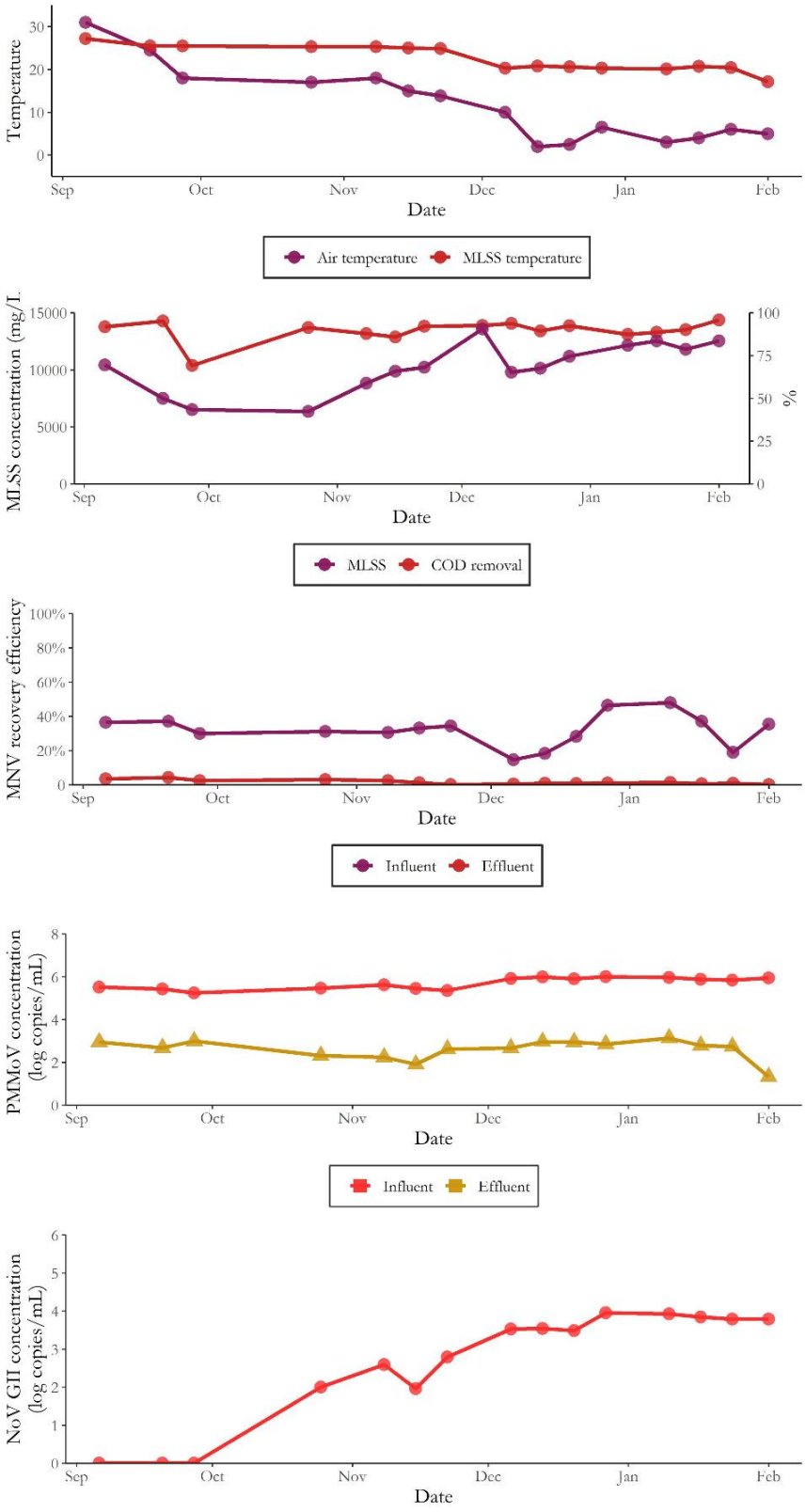

Fig. 3.1 The summary of the reactor operation conditions and virus quantification results.

Regarding virus quantification results, during the study period, PMMoV had a consistent and significant presence (> 5 log copies/mL) in influent samples. In effluent samples, the concentration of PMMoV dropped to 1.32 to 3.13 log copies/mL. After counting in the volume conversion involved in the concentration-quantification process, the LRV ranges from 2.25 to 4.61. On the other hand, the presence of norovirus GII in influent samples showed an upward trend during the study period, from the negatives recorded in September 2020 to around 4 log copies/mL during the wintertime. Despite the presence in influent samples, all effluent samples were negative for norovirus GII, suggesting a complete reduction by AnMBR. Because a correct LRV could not be calculated for norovirus GII, the following LRV model was established upon PMMoV removal.

In the correlation analysis (Fig. 3.2), out of all operational variables, only two (MLSS pH and influent pH) showed strong and significant correlation with PMMoV LRV (Spearman's rank correlation coefficient $\rho > 0.7$ and p-value ≤ 0.05). Although some other variables also showed some degrees of correlation with LRV, as nine operational variables had Spearman's rank correlation coefficient $\rho > 0.3$, their correlations were not significant. The grid search result indicates that ANN model performs better with only two inputs while RF model performs better using 9 inputs and is insensitive to the number of trees used.

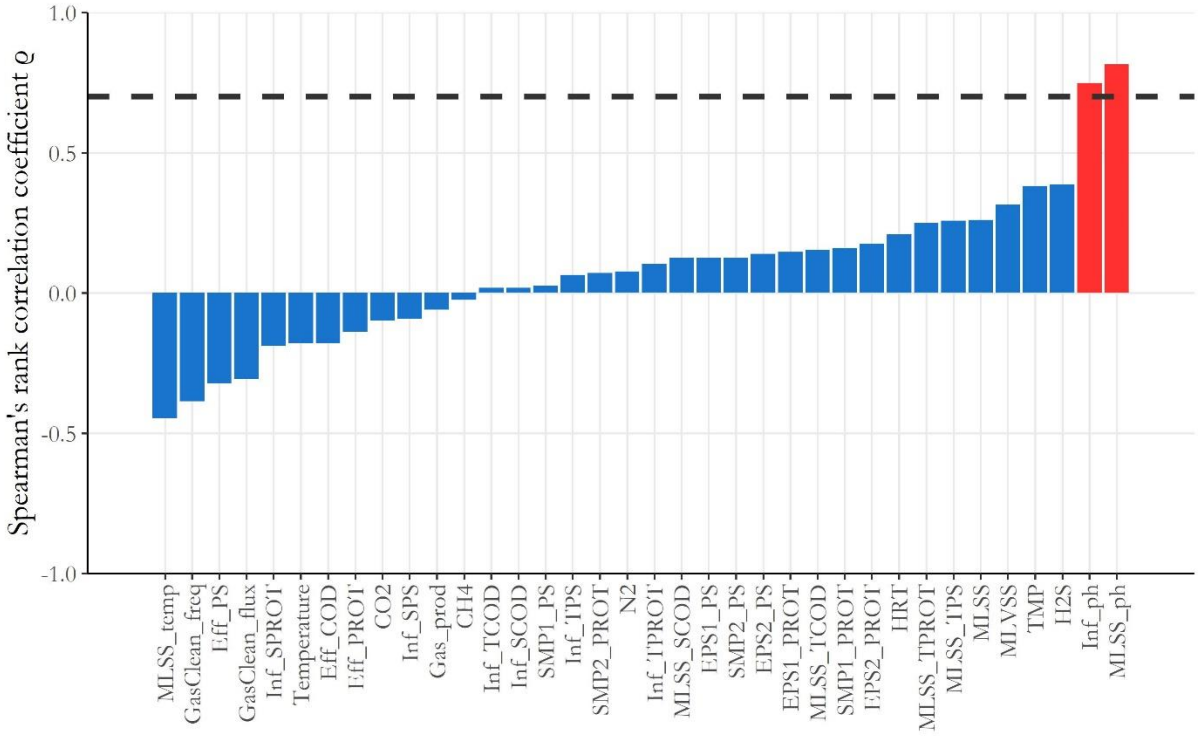

Fig. 3.2 Correlation analysis results. The two operational variables (influent pH and MLSS pH) that have strong and significant correlation with PMMoV LRV (Spearman's rank correlation coefficient $\rho > 0.7$ and p-value ≤ 0.05) are marked by red color.

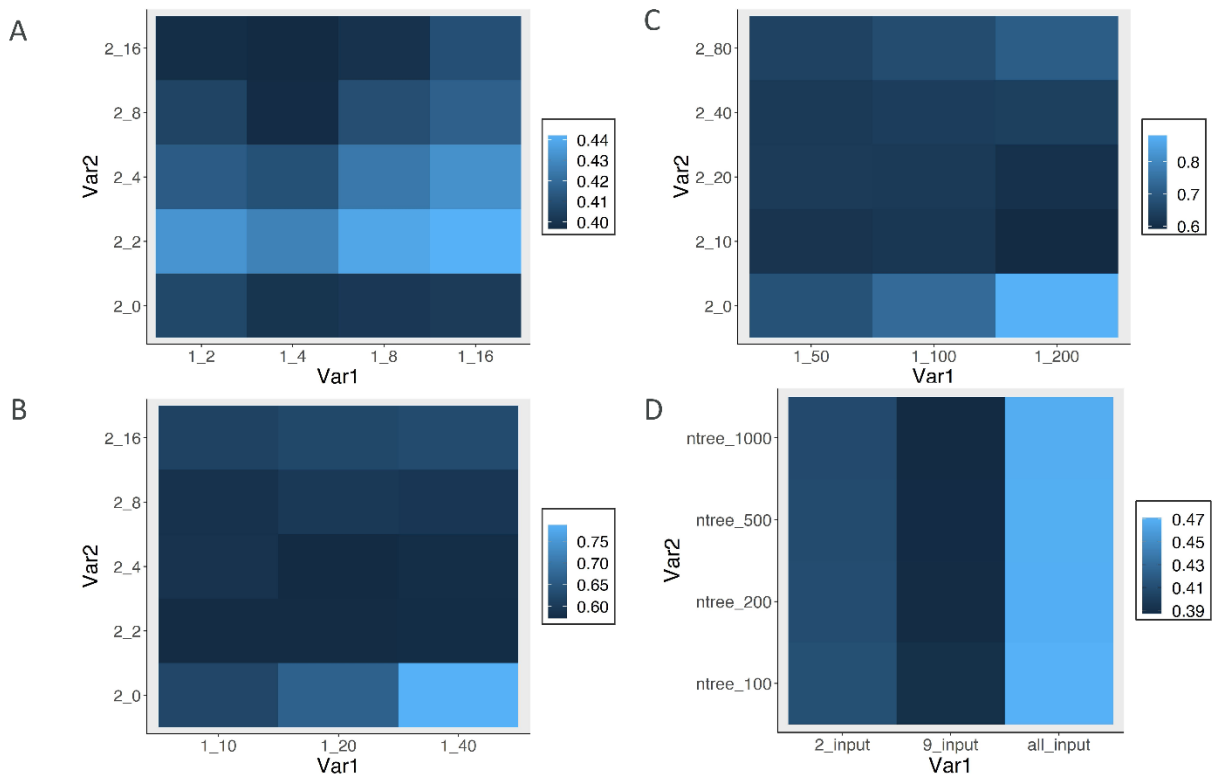

Fig. 3.3 The grid search result for model configuration optimization. A-C: RMSE values from different hidden layer settings. The X-axis (Var1) stands for the number of neurons in the first hidden layer while the Y-axis (Var2) represents the number of neurons in the second hidden layer. A value of zero in the Y-axis means only one hidden layer is used in the model. D: RMSE values from random forest models with different numbers of decision trees.

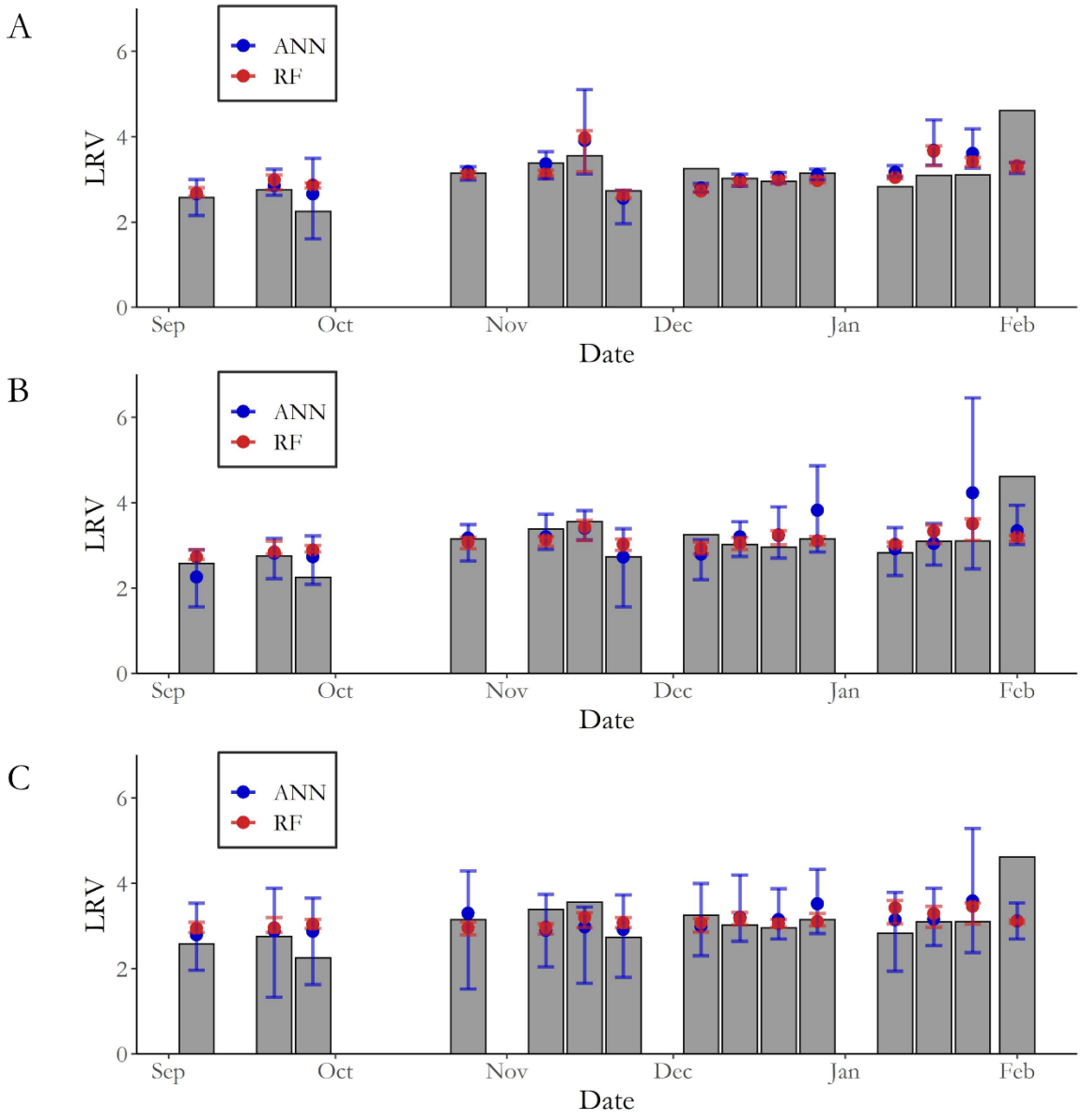

Fig. 3.4 The performance of PMMoV LRV prediction by different data-driven models. The point and error bar stand for the median and 95% confident interval (CI), respectively. A: only two operational variables with strong correlation with LRV (influent pH and MLSS pH) were used as inputs; B: nine variables with Spearman's rank correlation coefficient $\rho > 0.3$ were used as inputs; C: all operational variables were used as inputs.

The prediction performance of the two data-driven regression models tested in this study is shown in Fig 3.4. For ANN, as more variables are used as inputs, the prediction performance

decreases. When only two variables were used as inputs, ANN had the lowest average RMSE = 0.367. When the number of inputs increased to 9 and 36, the average RMSE also increased to 0.506 and 0.617, respectively. In comparison, under every input setting, RF offered better prediction performance. However, for RF, the RMSE value did not increase as the number of inputs increased like ANN. When two inputs were used, RF offered an average RMSE of 0.348, lower than ANN under the same condition (0.367), but when more inputs were used, the average RMSE first decreased to 0.273 then increased again to 0.394. Overall, the best prediction performance was offered by RF using nine operational variables with an average absolute error of 0.303 LRV and a mean absolute percentage error of 10.7%.

In the present study, we investigated the virus removal performance of a pilot-scale AnMBR. Furthermore, to test the feasibility of putting it under real-time monitoring, which is advocated in modern sanitation frameworks, we established a prediction modeling framework that connects the LRVs with the monitored operational variables. Overall, the pilot-scale AnMBR had a stable virus removal efficiency. We found that the virus removal efficiency is strongly correlated with the pH values of both MLSS and influent. The modeling result showed that it is feasible to circumvent the mechanistic understanding of virus removal process and predict LRV given the operational conditions, validating the soft-sensor approach.

AnMBR has already passed the proof-of-concept phase and is currently being verified under real-world conditions in terms of reactor configuration and influent characteristics. Many technical challenges, such as start-up optimization, fouling control, and operating strategy, are being tackled by a growing number of scholars from all over the world. However, for this technology to make its way into real-world implementation, there are other practical factors that need to be taken into consideration with one being the microbial safety evaluation. As mentioned earlier, considering that past studies have proposed using AnMBR effluent for agricultural

irrigation [251,252], the performance and consistency of virus removal in AnMBR is pivotal in deciding whether tertiary treatment is needed, and if so, to what extent. However, there is a significant lack of academic considerations, both in terms of the number of studies and the conditions (reactor configuration, virus type, operational condition, etc.) covered. We intended to contribute to addressing this issue by conducting virus removal experiment in a pilot-scale AnMBR and introducing a modeling framework that can be adopted by future studies. As far as we know, this is the first study that investigated the virus removal performance in a pilot-scale AnMBR and connected the performance with operational variables.

The occurrence of norovirus showed a wintertime seasonality in influent samples, which is consistent with past literature on both norovirus wastewater monitoring and clinical testing [253–256]. However, no effluent sample was tested positive for norovirus GII, showing that AnMBR is capable of effectively and reliably removing viruses from municipal wastewater to a low level. This is also consistent with a recent virus removal study featuring a bench-scale AnMBR [88]. Conceptually, the reactor can be further optimized to yield higher virus reduction rate (e.g., using membrane that has a smaller pore size or maintaining a thicker biofilm), but the improved virus removal performance may come at the cost of other aspects (higher membrane purchase and maintenance cost, higher electricity consumption due to increased TMP, etc.). Therefore, a balance needs to be found in operation. Also worth mentioning is that introducing bacteriophages for fouling control and reactor performance enhancement was discussed in recent studies [252,257]. If this approach comes to fruition, the reactor will need to remove not only indigenous viruses but also added bacteriophages, demanding an even higher and more reliable virus removal capability.

As for the modeling, although several studies have attempted to model virus removal performance in membrane systems via either mechanistic, statistical, or data-driven modeling

[113,159,162], limited progress has been made regarding the real-time monitoring aspect. The complexity of the system, especially when it features biomass, has greatly hindered the development of mechanistic models. Therefore, the data-driven modeling approach was chosen in this study because it circumvents the need for understanding the underlying mechanisms and learns directly from the data.

Due to the relatively stable operation at the AnMBR plant employed in this study, the sampling interval in this study was chosen to be one week to cover the potential long-term operation variability. Indeed, from September 2020 to February 2021, the recorded air temperature ranged from around 2.0 °C to 31.0 °C, which resulted in a series of minor performance changes, most noticeably in the operating temperature. Although the operating temperature was closely associated with the overall performance of AnMBR [248], in terms of virus removal, no strong correlation was found between it and LRV, indicating that the microbial safety of AnMBR is consistent throughout the operating temperature range.

The experimental results have several implications. Firstly, the fact that the virus removal performance was strongly correlated with the pH of influent and MLSS indicates that electrostatic interactions play an indispensable role in the virus removal process, which was also identified in our review article and other previous studies [63,93,97,104]. Since TMP largely indicates the permeability of the membrane module, it was originally expected to be a crucial factor because membrane rejection was recognized as a main virus removal mechanism, but a poor correlation between TMP and LRV was found in this study. Considering the pH values of both influent and MLSS were found to be strongly correlated with PMMoV LRV and the reactor was in stable operation at the time of sampling, a plausible explanation is that the electrostatic interaction-driven virus absorption onto either the suspended or attached biomass was the dominating virus removal mechanism in AnMBR. This also explains the moderate correlation

between MLSS concentration and LRV, albeit not significant. In addition, from the perspective of AnMBR operating strategy, this means a temporary drop in TMP, which can be a result of membrane cleaning or sludge discharge, may not greatly affect the overall virus removal performance. But on the other hand, this may rise the necessity of pH adjustment for virus removal purpose. In this study, a positive correlation was found between LRV and influent/MLSS pH, meaning increasing the pH will likely result in better virus removal efficiency. However, whether this will affect the activity of the microorganisms in the reactor remains unclear. Further studies are needed to investigate whether there is a tradeoff between virus removal efficiency and wastewater treatment performance for operation optimization.

Two limitations of this study should be mentioned. Firstly, since norovirus GII was reduced below the detection limit in all effluent samples, making the virus removal data left-censored, the modeling was performed with PMMoV as the target instead due to its consistent presence. However, the removal of PMMoV may not well represent the removal of human pathogens due to different physicochemical characteristics, especially the affinity for MLSS. Nevertheless, we should point out the absence of norovirus GII in all effluent samples suggests this pilot-scale AnMBR achieved high removal of norovirus GII throughout the entire study period, adding credibility to the claim about its microbial safety. In this case, PMMoV removal may serve as a conservative indicator. Secondly, the measured virus concentration, and by extension LRV, can be greatly influenced by the virus recovery efficiency. Although we employed previously reported virus concentration methods, some extent of variation in recovery efficiency still exists, which may affect the robustness and reliability of the subsequent modeling.

3.4 Conclusion

As the interest in AnMBR technology continues to grow, follow-up research needs to catch up and that rightly includes its microbial safety assessment and verification. We hope the

findings made in the current study will expand the understanding of the role AnMBR can play in the grand scheme of wastewater reclamation and reuse.

4. Wastewater virus surveillance: from proof-of-concept to application

4.1 Introduction

Being one of the greatest global health crises in the 21st century so far, the raging pandemic of COVID-19 has left a mark on virtually everyone's life in 2020 and its profound impact will likely extend to at least the next few years. Following the initial reports from Wuhan, China, COVID-19 has promptly spread to other countries and regions. Japan, being a close neighbor of China, is one of the first countries to be affected. The first COVID-19 cases in Japan were reported at the end of January 2020, most of them had travel history to Wuhan. In the following days, as the highly contagious disease found its way to proliferation in a country famous for the highly urbanized and concentrated population, domestic cases started to surge. Despite various efforts to slow down the transmission, including stringent border control, the declaration of a nation-level state of emergency, and the promotion of a contact tracing smartphone application, as the later waves continue to hit and a vaccine had yet to reach the general public, the national cumulative cases have surpassed 9 million as of June 2022 [175].

To intervene with the spread, proactive measures such as travel restriction, stay-at-home order, and mask mandate have been adopted and imposed by authorities at different levels. But as effective as these measures can be, the concern and growing evidence about their far-reaching impact on the economy, people's livelihoods, and their mental health mean the authorities need to find a delicate balance between epidemic containment and the social order. To achieve that, knowing the optimal timing to impose those measures is essential. Timely intervention would effectively flatten the epidemic curve while minimizing unwanted social disruption.

One important data source for planning containment measures is how the epidemic has progressed over time. This relies heavily on dependable epidemic surveillance. However, due to the turnaround time needed for sample collection, transportation, analysis, and data organizing,

adding to the fact that some infected individuals may not receive a test, the current reporting of clinically diagnosed patients may significantly lag behind the true progression of the epidemic. When the sheer number or the trend of reported cases triggers an alarm, the circulation of the disease may have already passed a critical threshold. Beyond that, interventions may only receive limited efficacy as the base number of infected individuals is already too large. Recent studies endorse wastewater-based epidemiology (WBE) as a complementary monitoring method. Studies have found that infected individuals, regardless of their symptoms, can persistently shed viral RNA into the environment from the early stage of the infection via defecation. Once the feces enter the sewage network, it gets mixed with the wastewater from other people in the same catchment area. This means, conceptually, the wastewater provides a probe of the infection condition of the community.

Timely information disclosure and update has been an indispensable part in COVID-19 response. Thanks to advanced data collection and visualization tools, a plenty of COVID-19 dashboard pages have been established to inform the public of both epidemic progression (e.g., daily confirmed cases and hospitalizations) and measures being taken to control it (e.g., clinical testing and vaccination rate). In addition, researchers and corporations are also reporting relevant data (e.g., mobility reports issued by Google (https://www.google.com/covid19/mobility/) and Apple (https://covid19.apple.com/mobility/), even model-based COVID-19 forecasts (Google U.S. and Japan COVID-19 Public Forecasts (https://g.co/covidforecast) to help society acquire knowledge about different dimensions of the pandemic. As wastewater surveillance is showing its potential as a complementary data source, a similar data sharing strategy may raise the public interest in this approach and promote the further development and deployment of it.

To date, more than 100 dashboards either dedicated to or containing COVID-19 wastewater surveillance results have been set up, according to data aggregation site "COVIDPoops19" (https://www.covid19wbec.org/covidpoops19). These dashboards cover a great variety of scale (national, state-wide, city-wide, or institutional) and data disclosure strategies (quantification results only, quantification results and trend, variant detection results, or with other epidemic metrics such as reported cases and testing rate). To date, most dashboards are operated by high-income countries. For example, U.S. is in the absolute lead with more than 50 dashboards established at different levels. It is worth noting that some countries and regions have established COVID-19 wastewater surveillance sites, even networks, yet the results are currently only for academic uses and not publicly accessible. In addition to the experimental data, the site "COVIDPoops19" also acts as a platform on which researchers can share the latest scientific advancements as well as relevant resources such as data visualization tools.

As stated, wastewater surveillance results are mainly communicated in the raw form (positive/negative or viral titers in sewage sample) so far as data sharing primarily occurs among researchers. However, when adopted as a public information source, some extent of quantitative interpretation or expert knowledge-based annotation may be needed to provide a context for the results.

One major challenge faced by researchers in this field is the difficulty in quantitative data processing and interpretation. Conceptually, the wastewater viral load would be proportional to the size of the shedding population. Although this was the basis of back-calculation model in many chemical-based wastewater surveillance projects, it has been repeatedly mentioned that under the influence of many pathological, physical, and environmental factors in the complex wastewater matrix, measurements are far from consistent [258]. For instance, only about half of

infected individuals would develop fecal shedding and the shedding rate shows significant intra-host variability [185,259]. Also, as an enveloped virus, SARS-CoV-2 particles have a greater tendency to partition to wastewater solids compared to non-enveloped viruses [204,208]. The result is significant inter-day fluctuations [260]. As far as we know, no back-calculation model has yet to be verified for COVID-19 wastewater surveillance.

It should be noted that even in the absence of back-calculation model, qualitative or semi-quantitative results can still add new dimensions to the epidemic progression and potentially guide epidemic response. An increase in detection frequency in a low-prevalence level may suggest the circulation of virus in the catchment area, and for quantifiable viral load, an upward or downward trend may reflect the change in the shedding population base, and by extension, the prevalence level [261], although the threshold can only be empirically decided at present. The Ohio Department of Health (ODH) issues a notification when a tenfold increase in wastewater SARS-CoV-2 load is observed, a similar approach is taken in Utah where wastewater SARS-CoV-2 RNA level is used to direct clinical testing [262]. It was also proposed that detecting the occurrence of SARS-CoV-2 RNA in the aircraft wastewater may enhance the screening of inbound passengers, preventing the importation of new COVID-19 cases [263]. Also, from the perspective of variant tracking, the occurrence or increasing ratio of a variant among others may also serve as a warning to the healthcare sector of a phase transition or potential outbreak [264]. One project based in Berlin, Germany reports the change in the detection frequency of VOC over time [265].

Another challenge is that most findings regarding the connection between wastewater surveillance results and the epidemic status were made through retrospective analyses, therefore, when wastewater surveillance is applied to guide future public health practices, such as issuing projections of prevalence level or the possibility of an outbreak, additional uncertainty may

apply. Also, there are caveats and inherent limitations of wastewater surveillance that an average person may not know about. For instance, one may posit that a positive signal means the presence of contagious individuals in the community, while the shedder(s) may have left the catchment area by the time of information disclosure, especially when the catchment area covers sites with heavy traffics such as tourist attractions or transportation hubs. Considering the points mentioned above, when communicating the results, expert knowledge-based data annotation may help avoid unnecessary confusion and panic. Many dashboards have a Q&A section or provide an information sheet to help audience understand the benefits and limitations, as well as the methodology used in the project.

The disclosure strategy should also be decided in accordance with the grand scheme of COVID-19 response. As stated above, preferably, wastewater surveillance should complement other surveillance routes rather than being as an isolated information source. Thereby, the results should be presented and interpreted along with other epidemiological metrics. This can be achieved with multidisciplinary dashboards that integrate the data from multiple sources. Another factor worth considering is the spatial heterogeneity of data. While the lateral comparison of wastewater surveillance data may lead to further understanding of the epidemic, like the spatial heterogeneity, laboratories are often differently equipped, making using a unified experimental method challenging. The result is that data from different wastewater surveillance projects are often not comparable, adding difficulty to the spatial integrating of data. While using verified and standardized methodology is strongly encouraged, if this is not feasible, city- or institution-wide data integration may be the viable option to provide a relatively consistent context. On this matter, one recent study proposed a normalization method for data comparison across sampling sites, but further research is needed to validate its applicability [266].

The recognition and support from the public and authority should be highlighted as the former is the beneficiary and the latter often operates the information disclosure platforms and the sewage system, as well as provides logistic support for wastewater surveillance. Open and effective communication about the benefits offered by wastewater surveillance in the forms like media coverage and public seminar is needed to educate and persuade both parties that wastewater surveillance can greatly contribute to COVID-19 response. Notably, emphasizing the cost-effectiveness and wide coverage of wastewater surveillance in low- and middle-income countries may add to its appeal and improve acceptance in local communities, although the applicability of wastewater surveillance may be limited by the coverage of sewage system. In the previously mentioned cases where wastewater surveillance is used to issue notification or direct medical resources, introducing these practical applications is also in favor of gaining support. Also, as a tool with a direct impact on the society it serves, wastewater surveillance may also raise ethical concerns, thereby early engagement of social scientists and public health experts is critical [267].

At different stages of an epidemic, wastewater surveillance may serve different purposes. In pre-peak period, the priority should be identifying the potential starting point of local circulation by monitoring the entry of infected individuals into the catchment area. Amid the outbreak event, the focus may shift onto the estimation and prediction of the epidemic trend.

Since the two research fields have distinct purposes, methodologies, even limitations, the significance of interdisciplinary collaboration for further data interpretation should be highlighted. Particularly, since wastewater surveillance has wide coverage and is immune to the change in testing policy, it may serve as an extra input to improve existing epidemic models. Conversely, information obtained from the healthcare sector can also empower wastewater

surveillance. For instance, the time lags in the infection-shedding-onset course obtained from medical reports may be used to calibrate the lead time offered by wastewater surveillance [268]. To achieve all these, however, novel models need to be developed.

With the rapid development in computational power and modeling tools, data-driven methods have been actively employed in Berlin, Germany. Amid the COVID-19 pandemic, various modeling techniques, notably compartmental model and network model were employed for various tasks including simulating epidemic progression, studying the transmission dynamics, and evaluating the efficacy of restrictive measures [269,270]. On the other hand, researchers in water field have long been using data-driven models for forecasting and decision-making purposes [271]. Regarding the high uncertainty of wastewater surveillance results, data-driven methods such as fuzzy logic and Bayesian inference may also be incorporated for anomaly identification [272]. Several studies on the topic of using data-driven modeling to facilitate wastewater surveillance have been reported. The potential of augmented wastewater surveillance was demonstrated in one study in which the detection results and external variables were fed into multiple data-driven models for prevalence prediction [273], yet the authors also noted that wastewater surveillance result alone is likely inadequate to generate reliable result. Another recent study proposed a model that helps identify vulnerable communities where wastewater surveillance may yield maximum benefit [274]. The capability of data-driven modeling tools to address uncertainty and bypass the causality of input–output pairs may greatly enhance the research at the intersection of two fields. But in general, studies aimed at this research gap are still rare and more efforts are needed to further explore the connection between the two disciplines and the form of data integration.

The aim of this project is to assess the applicability of WBE in the early warning and containment of COVID-19. Particularly, it comprises two steps: the first step is a theoretical

calculation that uses available information about the transmission pattern and pathology of COVID-19 to perform a preliminary feasibility assessment; the second step is to establish a short-term COVID-19 prediction model using actual SARS-CoV-2 wastewater surveillance data to test the real-world applicability of data-driven modeling.

4.2 Theoretical calculation of feasibility

4.2.1 Methodology

This calculation focuses on the city of Tokyo, where the first COVID-19 cases were reported in late January 2020 following the initial outbreak in China. The infected individuals reported in this period were mostly tourists who came or had returned from Wuhan, and subsequently, local cases began to appear and rise in the middle of February 2020.

The dataset of daily reported cases was acquired from the COVID-19 information website maintained by the Tokyo metropolitan government (https://stopcovid19.metro.tokyo.lg.jp/). It includes information on the report date, whether the individual dwells in the Tokyo metropolitan region, age group, sex, and whether the individual has already been discharged from quarantine/healthcare facilities. Apart from three travelers from China reported in late January 2020, the dataset contains a total of 101,417 cases. The report date ranges from February 13, 2020 to February 3, 2021.

To date, Tokyo has experienced three waves of outbreak. The first one struck between late March and late May 2020 and as the situation quickly escalated, a state of emergency was declared in seven prefectures including Tokyo on April 7, 2020. The state of emergency was subsequently expanded to nation-level on April 16, 2020 before it was elevated in Tokyo on May 25, 2020. During that time, the weekly new cases in Tokyo dropped to ~50, which is substantially lower compared to the peak week of April 6-12, 2020 when the total new cases exceeded 1,000. However, in June 2020, the epidemic made a comeback as daily new cases started to rise again. On July 9,

2020, 224 new cases were reported, surpassing the previous daily new case record of 206 during the first wave. Subsequently, a temporal peak of 472 daily new confirmed cases was recorded on August 1, 2020. The second wave lasted until October 2020 when the daily new cases plateaued at ~200. Unfortunately, at the end of 2020, the third and by far the most serious wave hit Tokyo once again. On January 7, 2021, 2,447 new cases were confirmed, marking an all-time high since the beginning of the epidemic. In response to this surge, the state of emergency was declared again, and it is expected not to be elevated until March 2021.

To provide an additional index that helps illustrate the efficacy of intervention measures, the openly accessible mobility dataset provided by Apple (https://covid19.apple.com/mobility) was used. The dataset contains the numbers of daily navigation route requests (driving, transit, and walking) in major cities and regions including Tokyo received by Apple since January 13, 2020.

Many recent studies assumed that all shedders have the same shedding rate, and the inter-individual variation can be modeled by uniform and log-uniform distributions. However, it is unclear whether the actual shedding follows the same distribution. It has been revealed that the viral shedding in stool specimens can outlast the shedding from the respiratory tract, and clinical reports suggest the shedding dynamics is erratic and varies greatly among individuals [193], making modeling it a tough task. In this study, a mathematical model (equation 4.1) reported by Miura et al. (2020) was used. The model was originally developed by Teunis et al. (2015) for the fecal shedding of norovirus.

$$C(n|\alpha,\beta) = C_0 e^{-\alpha n}\left(1 - e^{-(\beta-\alpha)n}\right)(\beta - \alpha) \quad (4.1)$$

$C(n|\alpha,\beta)$: concentration of viral RNA in the fecal specimens (copies/g)

n: the nth day into the fecal shedding course

$C_0,\ \alpha,\ \beta$: curve shape coefficients

The coefficients were estimated by fitting the model to the existing SARS-CoV-2 fecal

shedding reports. For more detail of the calculation process and the biological explanation, refer to Miura et al. (2020) [275].

As the fecal shedding of SARS-CoV-2 RNA is persistent, the wastewater viral load on a given day is contributed by patients in various infection stages who should be viewed as individuals with different shedding rates rather than a group of homogeneous shedders. Therefore, in this study, the viral load is considered the sum of fecal shedding from all active shedders. Patients on their day *n* of the infection will be assigned a shedding rate C_n calculated using equation 4.1, the viral load and the number of active shedders can be expressed by the following equation 4.2 and 4.3:

$$L_t = \sum_{n=1}^{26} N_{n,t}\, MRC_0 e^{-\alpha n}\left(1 - e^{-(\beta-\alpha)n}\right)(\beta - \alpha) \tag{4.2}$$

$$N_{s,t} = \sum_{n=1}^{26} N_{n,t} R \tag{4.3}$$

L_t: the total viral load on day *t* (copies)

$N_{n,t}$: the number of infected individuals in the day *n* of the fecal shedding course on day *t*

M: the average weight of feces produced by one individual per day (g)

R: the ratio of infected individuals who develop fecal shedding

We assumed that the shedding lasts for 26 days [275], and $N_{n,t}$ can be obtained from Re_m, the 7-day moving average of new cases on another day *m* via a matrix-based infection status model (Fig. 4.1a). To convert fecal shedding rate into wastewater virus concentration, an average daily feces production of 2.11 $\log_{10}$ gram per person [276] and a daily wastewater flow of 4,378,893 m^3 are used (Bureau of Sewerage, Tokyo Metropolitan Government). Briefly, because the status of infected individuals changes every day and all of them would be or would have been the reported

cases on a certain day, the number of them on a given day can be converted to *Re* on another day. The conversion is controlled by the expected shedding course. The active shedders $N_{s,t}$ is defined as all individuals that contribute to the total viral load on a given day *t*, calculated from multiplying the sum $N_{n,t}$ on all day *n* (1 to 26) by the shedding ratio R, for which 50% was used in this study based on previous reports [185,199,277–279].

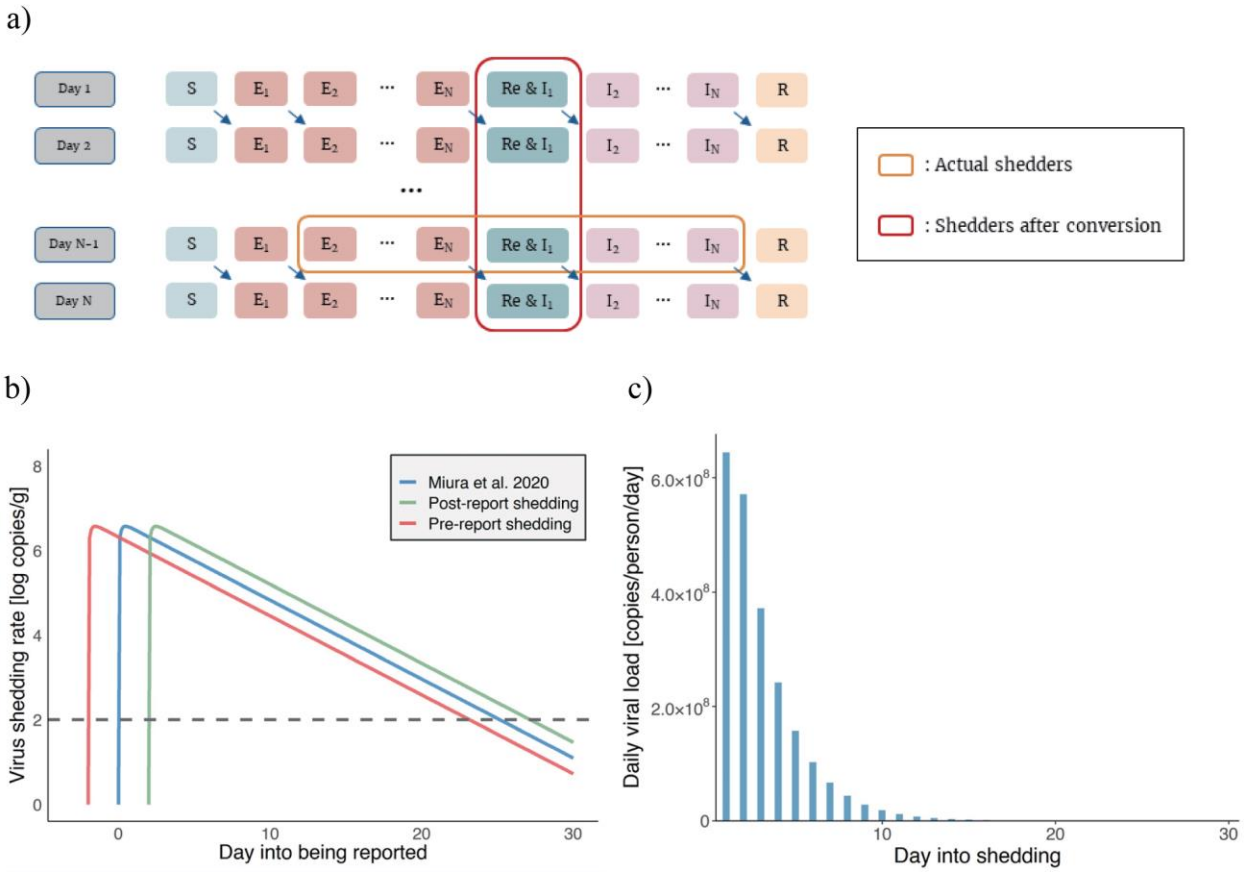

Fig. 4.1 a) an illustration of the matrix-based infection status model used to convert the individuals in different shedding statuses on the same day to *Re*, the number of reported cases, on several consecutive days. b) the three shedding settings used in this study, based on the shedding model developed by Miura *et al.* (2020). The starting points of fecal shedding were set to be 1): 2 days before being reported 2): the same day of reporting, and 3): 2 days after being reported, to reflect different shedding scenarios. c) the estimated daily viral load from one shedder throughout the course of fecal shedding. As a result of the high initial shedding rate, most of the fecal shedding occurs within the first 10 days.

It had been reported that the infectiousness likely develops and even peaks in the early

stage of the infection [184,280]. Thus, a setting under which fecal shedding starts 2 days before the individual is clinically confirmed was used. The shedding curve was horizontally moved by 2 days to reflect the change of the starting point of fecal shedding. In the meantime, as clinical evidence does not give a conclusive starting time of fecal shedding [185,193,281–283], two additional settings were tested. One follows the original shedding model and places the start of fecal shedding on the report date while the other assumes the shedding occurs 2 days after being reported, considering that the possibility that the fecal shedding starts relatively late cannot be ruled out completely. The shedding curves under all three settings are shown in Fig. 4.1b.

The efficacy of administrative orders varies greatly depending on the specific regulations and how strictly are they enforced. In this study, the time-dependent reproduction number (R_t) was chosen as the index. R_t was estimated using the R package "R0", the serial interval was assumed to follow a lognormal distribution with the mean and standard deviation (SD) of 4.7 and 2.9 days, respectively [284]. The average R_t value between the two courses of the state of emergency (the first one started on April 7, 2020, and ended on May 25, 2020, the second one was announced on January 7, 2021, and was expected to end on February 7, 2021) was calculated as the baseline level of intervention. The average R_t during each of the two periods of state of emergency were also calculated to show the impact of intervention measures on the transmission pattern of COVID-19.

4.2.2 Results

This study aims to evaluate whether WBE is a feasible tool for COVID-19 early warning. To do that, we developed a dynamic wastewater viral load model and tested it on Tokyo's epidemic dataset. The total viral load (pre-report shedding setting) and the size of the active shedding population are shown in Fig. 4.2. The correlation between the total wastewater viral load and the number of the 7-day moving average of reported patients (Spearman's ρ: 0.9879) is stronger than that with the number of daily reported patients (Spearman's ρ: 0.9343) and the number of active

shedders (Spearman's ρ: 0.9591). This indicates that individuals in their early infection course contribute more to the viral load.

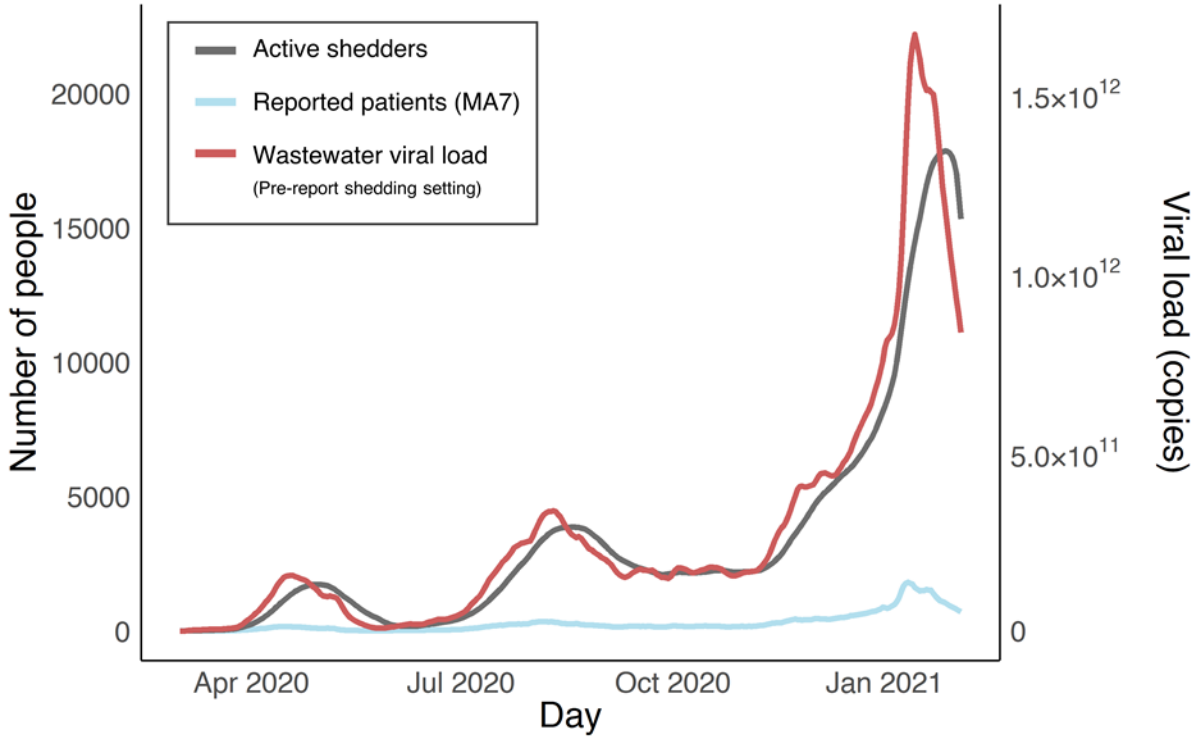

Fig. 4.2 The 7-day moving average (MA7) of reported cases, the total wastewater viral load calculated from the dynamic shedding model under the pre-report shedding setting, and the total number of active shedders considering the duration of fecal shedding.

The 7-day moving average of the confirmed cases and R_t are shown in Fig. 4.3. At the beginning of the epidemic, R_t is highly uncertain and fluctuates drastically, this likely results from the limited confirmed cases, disordered testing, and rapidly changing policies. As time went by, estimated R_t became stable, allowing for critical information about the transmission to be inferred. During the two rounds of the state of emergency, the average R_t is well under the threshold value of 1.0 (0.816 for the first and 0.963 for the second), indicating the epidemic will eventually die out if the situation stays that way. Compared to the average R_t in between (1.104), it suggests that the measures taken during the state of emergency effectively hampered the progression of the COVID-19 epidemic. The efficacy likely comes from a lower contact rate because of reduced overall

mobility. The mobility index in Tokyo is significantly lower during both rounds of the state of emergency (Fig. 4.4), meaning that fewer people were going out, whether by transit, driving, or walking during that time.

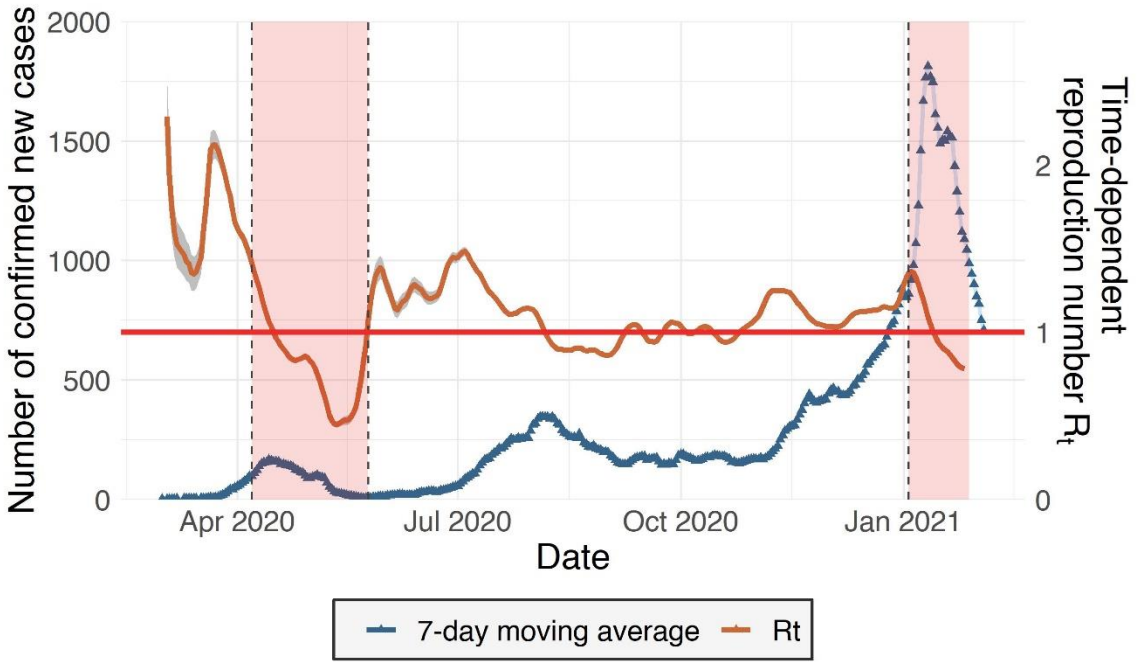

Fig. 4.3 The 7-day moving average of daily reported cases and the time-dependent reproduction number R_t from March 1, 2020 to February 3, 2021 (data source: Tokyo metropolitan government). The red line indicates the threshold value $R_t = 1$, the two periods of the state of emergency (April 7, 2020-May 25, 2020, and January 7, 2021~) are also marked out. The gray area near the R_t line is the 95% confidence interval.

The total viral load only represents the amount of viral RNA in the entirety of daily wastewater flow, for WBE application, a more important aspect is whether the concentration of viral RNA is higher than the detection limit of the quantification method. In this study, the wastewater viral load is simply calculated by dividing the total viral load by the total volume of wastewater from all residents in the Tokyo metropolitan region. To date, the lowest detection limit is 1.9 copies/100 mL sewage sample reported by Ahmed et al. (2020) [73]. If this detection limit and the pre-report shedding model *(i.e.*, highest sensitivity and earliest fecal shedding) are adopted, the

concentration of viral RNA of SARS-CoV-2 in Tokyo wastewater would surpass the detection limit on April 5, 2020, when Tokyo had just entered the first wave of COVID-19 outbreak and the daily reported cases had reached 141. Under the other two shedding settings, there would be a slight delay as the same surpassing would occur on April 7, 2020 and April 9, 2020, respectively. It is worth mentioning that the simulated detection dates coincide with the first state of emergency, which was not put into effect until April 7, 2020. This means that under the best scenario, the current detection method can theoretically provide an epidemic warning as early as other clinical and societal indices do. Realistically speaking, however, wastewater surveillance project may not be put into effect in time due to various reasons (*e.g.*, lack of essential resources or reliable testing protocol). But even if the first wave is missed, as the wastewater virus concentration surges again when the second wave hits, the wastewater viral load would nevertheless surpass the detection limit on July 4, 2020, prior to the peak of the second wave. Besides, between the second and the third waves, a plateau of wastewater virus concentration would form, during which time the wastewater viral load would stay above the detection limit. The potential detection opportunities may signify the underlying danger, indicating the threat has not gone away and the next outbreak could be around the corner. The decision-making process to devise and implement preventive measures may be reinforced, especially if other potential information sources are jointly used.

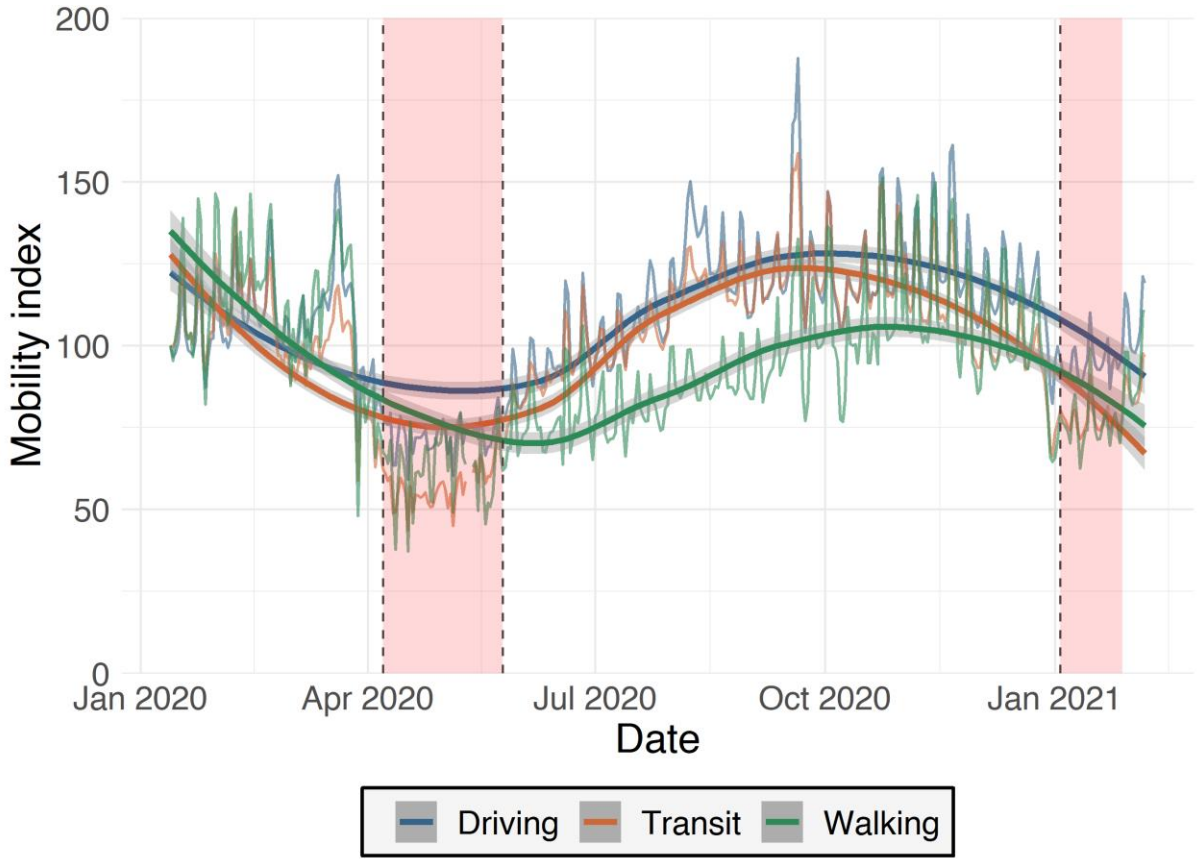

Fig. 4.4 The mobility indices (driving, transit, and walking) represent the number of navigation route requests received each day by Apple. The values are standardized with the data on January 13, 2020 being used as the baseline and set to 100. The smoothed lines are drawn with the "geom_smooth" function included in R package "ggplot2". During the first state of emergency, all types of transportation underwent a significant drop, but as it ended in late May, the indices resurged, although walking, which may cover a large portion of non-essential short trips, did not recover as much as driving and transit. It should be noted that the data are potentially biased and may not accurately represent the mobility of all Tokyo residents (*e.g.*, users of other devices and navigation applications, and people who do not need navigation).

However, taking 1.9 copies/100 mL as the standard detection limit for WBE may be risky, considering that only one reference has reported such a low value so far. The detection limit of our recent in-house quantification experiment is estimated to be about 8,000 (~$10^{3.9}$) copies/100mL, and other studies have reported their respective detection limits from 10^1 to 10^4 copies/100 mL sewage sample [75,181,187,210,285–287]. Therefore, a more moderate detection limit (~$10^{2.5}$ copies/100 mL) was also evaluated. Under this new premise, the wastewater viral load would not be higher

than the detection limit during the entire studied period (Fig. 4.5), meaning that WBE may not be a feasible approach for early detection and warning. However, we had recorded a positive signal in our routine monitoring program in Sendai, Japan (data not shown) when the reported cases-based prevalence level would only give a wastewater viral load of 6.7 copies/100mL wastewater, which means that the observed wastewater viral load is about 1,200 times higher than the estimation. This highlights the importance of recalibration of some critical factors for the further refinement of the model. We have previously listed and discussed some bottlenecks halting the application of WBE in COVID-19 early warning in a preliminary review article [288]. In the following paragraphs, we would like to provide a brief insight into some of the factors that may contribute to this disparity.

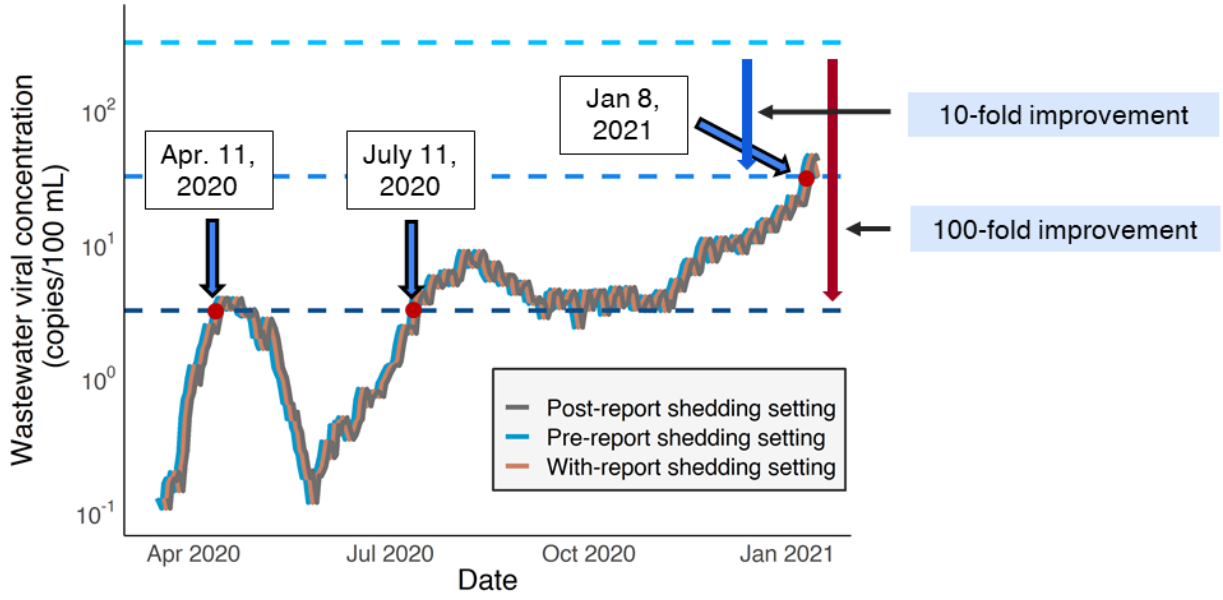

Fig. 4.5 The wastewater virus concentration under the three different shedding settings. The modest detection limit is assumed to receive a 10- or 100-fold improvement ($10^{2.5}$ to $10^{1.5}$ and $100^{.5}$ copies/100 mL). With the 100-fold improvement, the viral RNA would be detected from wastewater as early as on April 11, 2020 for the first wave, and on July 11, 2020 for the second, the plateau of wastewater virus concentration between the second and third waves would also be noticed as it would still stay above the new detection limit from late August and early November 2020. But if the detection method would only receive a 10-fold improvement, the successful detection would not occur until Jan 8, 2021.

First, admittedly, the assumption of homogeneous mixing of viral RNA and wastewater may not match the reality. This has been supported by the previous detection of SARS-CoV-2 RNA in low prevalence regions. For instance, Hate et al. (2020) [75] detected the presence of SARS-CoV-2 RNA in the wastewater of Ishikawa prefecture, Japan when the prevalence level was lower than 1.0 reported cases per 100,000 people. By the same standard, the detection in Tokyo would have occurred before the daily reported cases surpass 140, which happened on April 5, 2020. The uneven mixing of wastewater underlines the importance of introducing detection methods and strategies that can improve the sensitivity and reliability of wastewater surveillance, especially when used as an early warning tool. The use of auto-samplers that collect 24-h composite samples has been favored by recent studies as they can maximize the opportunity of capturing viral RNA [289], but it also means that viral RNA may be highly diluted. On the contrary, in the studies of Hata et al. (2020) [75], Ahmed et al. (2020) [73], and Torii et al. (2021) [206], grab samples were used. Although using grab samples is at the risk of giving false-negative results, it may provide better sensitivity under certain circumstances. The reason being that viral load is not uniformly distributed throughout a day as a result of people's biological rhythms and modern lifestyles. It had been reported that toilet flushing has two peaks in a day, one in the morning and the other at night [290]. If the sampling strategy is optimized to match the hours with high toilet flushing rates with the consideration of in-sewer traveling time, the chance of successful detection may increase as the fecal content would be more concentrated. However, it is unclear how effective this strategy is and further research and validation are needed. Also, statistically speaking, when the wastewater viral load is close to the detection limit, left censoring and data noise may affect the result. There could be temporal fluctuation in the wastewater viral loading which may result in false-negative. In such cases, statistical methods that help handle this issue, such as Bayesian inference, are worth looking into [291].

So far, most studies have employed 'downstream' sampling, meaning the samples were taken at locations where wastewater originated from different regions or sources merges (*e.g.*, WWTPs). This provides better coverage at the cost of less targeted monitoring [69]. Our model simulation suggests that under downstream sampling, the viral RNA concentration may not be high enough to enable successful detection. Upstream sampling, which refers to taking wastewater samples at locations closer to the end-users (*e.g.*, sewer pumping stations and maintenance holes), is therefore proposed as an alternative approach [176]. Rather than providing coverage for an entire city or a relatively large catchment area, upstream sampling offers better flexibility and resolution by focusing on a smaller population or area, sometimes a single facility, although the workload would be higher. Upstream sampling may be better suited for certain confined environments such as prisons and student dormitories where the presence of unidentified infected individuals may cause a serious outbreak. This strategy had a successful implementation in August 2020 when researchers at the University of Arizona found a wastewater sample from a student dormitory was tested positive for SARS-CoV-2 RNA. Actions were quickly taken to test all the residents dwelling in that dormitory and two asymptomatic virus carriers were later identified [186]. This likely prevented an outbreak in the campus before it happens. Considering all the uncertainties surrounding the detection sensitivity of WBE at this point, redirecting the focus of wastewater surveillance to certain critical points such as transportation hubs or major business districts rather than an entire city or a similarly large region, may make more sense from an efficiency perspective.

In this study, the calculation of viral load is solely based on reported cases. However, underreporting should not be overlooked as the real number of infections may be significantly larger [292–294]. Underreporting can be attributed to various factors such as the limited testing capacity (especially in the early stage) and the presence of asymptomatic individuals. Counting in

its impact may give a higher wastewater viral load and potentially, an earlier detection. The problem is, given the limited available information, it is very difficult to estimate an accurate ratio between actual and reported cases. Lau et al. (2020) [295] did an estimation for several countries and reported that in Japan, the actual number of cases is 12 times larger than reported as of March 17th, 2020. This means the unreported shedders have an effect similar to a 10-fold improvement of the detection limit. Additional investigation, such as seroprevalence study, is critical for giving a clearer image of the extent of underreporting. For instance, a seroprevalence study conducted in India found a case-to-report ratio of 26-32, and the value was even higher (82-130) at the early stage when testing was less available [296]. This, in turn, emphasizes the potential benefit of WBE as a community-covering monitoring tool because conventional clinical methods are often both time and resource-consuming for identifying and tracking unidentified cases. An accurate estimation of case number will help us finetune the viral load model, and the calibrated model may be used to perform back-calculation of actual cases based on wastewater viral load. However, this is another huge challenge in the application of WBE and is currently subject to significant uncertainties [258], more thorough studies are needed to take the model to the next stage.

Improving the assay sensitivity has also been proposed as a solution. A pre-amplification step that precedes qPCR was previously used to enhance the detection of SARS-CoV in clinical samples [297]. The results showed a 100-fold improvement in detection sensitivity can be achieved. Besides, it has been suggested that droplet digital PCR (ddPCR) can provide a 10 times higher sensitivity than conventional qPCR for SARS-CoV-2 RNA detection [74,220]. If these approaches can be implemented, the successful detection may occur earlier.

Assuming addressing the aforementioned issues can have a combined effect equivalent to a 10 or 100-fold improvement to the modest estimation of the detection limit ($10^{2.5}$ to $10^{1.5}$ and $10^{0.5}$ copies/100 mL), we performed another simulation based on the same shedding settings (Fig.

4.5). With the 10-fold improvement, the concentration of viral RNA in the wastewater would indeed exceed the detection limit, but it would not happen until January 8, 2021. By that time, Tokyo had already been hit by the third wave of COVID-19 outbreak. Daily confirmed cases reached an all-time high of 2,447 and the second state of emergency had just been declared one day before on January 7, 2021. Therefore, the possible detection would not quite qualify as "early" and may not have much significance. With the 100-fold improvement, though, the detection limit would be surpassed as early as April 11, 2020 under the pre-report shedding setting while the other two would result in a 2-day and 4-day delay, respectively. In a retrospective view, this potential detection, albeit much earlier, may also only have a limited effect on the epidemic trajectory as the state of emergency had already come into effect. However, after the first wave, the wastewater virus concentration would drop and stay below the detection limit until July 11, 2020. On that day, the confirmed cases reached 206, which is also the peak number during the first wave lasting from March to May 2020. Meanwhile, a plateau can be observed between late August and early November 2020 when the virus concentration is consistently higher than the detection limit. While no large-scale special action was taken during that time, which explains the resurgence of mobility indices in these months (Fig. 4.4), if the warning signal provided by WBE is taken seriously by the authority, the second and third waves might have been effectively suppressed, even avoided.

The impact that COVID-19 has had and will have on Japan's society is profound. Recent studies have investigated and discussed it from various angles including the change in mobility [298,299], the stigma associated with not obeying the social pressure of not going out [300], the mental wellbeing of the general public and workforce [301,302], and the adoption of personal hygiene practices [303]. Moreover, it has been documented that even though population-based interventions including lockdown and mask-wearing order can be taken, they are far from a panacea as the household transmission is hardly affected [280]. From a realistic standpoint, policies around COVID-

19 containment would go far beyond merely a medical concern due to the sheer scale of the epidemic. Containment measures that aim at lowering the contact rate and transmission risk can slow down the economy and social activities, even putting them to a halt, which may lead to serious consequences such as financial and mental burden. As society will likely have to keep functioning under the impact of COVID-19 in the foreseeable future, harsh constraints such as total lockdown, albeit effective, cannot fulfill the long-term needs. Acknowledging this, the way public health management is handled in this new era will be fundamentally different than what we had seen in the past year. Authorities may need to lean more on self-discipline and mild population-level constraints while strict measures will only be taken when an outbreak is likely to occur if no action will be taken. Choosing the appropriate timing, no matter through which method, can efficiently lower the basic reproduction number and flatten the epidemic curve without sacrificing the vigor of the economy too much.

4.3 Data-driven wastewater surveillance-based COVID-19 prediction

4.3.1 Materials and method

A total of 51 influent wastewater samples were collected from a municipal wastewater plant (WWTP) in Sendai, Miyagi, Japan that receives approximately 69 percent of wastewater generated in the city. Samples were taken twice a week, at 10 a.m., on Tuesday and Thursday from August 2020 to February 2021, from an influent line that serves the major urban area and about 360,000 people. All samples were grab samples (250 mL). Samples were immediately transported to the laboratory after collection and stored at -80°C until analysis.

SARS-CoV-2 RNA was recovered from 40 mL influent wastewater sample. Suspended solid was concentrated by centrifugation at 5,000 g for 10 minutes at 4°C. After the supernatant was removed, 1 mL of TRIzol reagent (Thermo Fisher Scientific, MA, USA) was added to the concentrated suspended solid, then the suspension was homogenized using a vortex mixer. The

total volume of the suspension was less than 3.5 mL. A 140 µL aliquot of the concentrate was processed for viral RNA extraction using the QIAamp Viral RNA Mini Kit (QIAGEN, Hilden, Germany) following the manufacture's instructions, and the viral RNA was eluted in 60 µL of elution buffer provided in the kit. The whole process recovery of the SARS-CoV-2 RNA was verified based on the concentration of Pepper Mild Mottle Virus (PMMoV) in wastewater samples, 140 uL aliquot was extracted from samples both before and after concentration. A 10 µL of extracted RNA was used to obtain 20 µL of cDNA with the High-Capacity cDNA RT Kit (Thermo Fisher Scientific). To synthesize cDNA for the SARS-CoV-2, the random primer included in the kit was substituted to CDC nCOV_N1-R Primer (CN 10006831, Integrated DNA Technologies, Inc., Iowa, USA) (10 µM) [304].

PCR-based preamplification method was applied to cDNA prior to the qPCR assay. The preamplification was performed with *TaKaRa Ex Taq*® Hot Start Version (Takara Bio, Kusatsu, Japan) and the CDC nCOV_N1 Primers (CN10006830 and CN10006831, Integrated DNA Technologies, Inc.) [304]. Each 50 µL reaction contained 20 µL of cDNA, 0.25 µL of *TaKaRa Ex Taq HS* (5 U/µL) (Takara Bio), 5 µL of 10 × Ex Taq Buffer (Mg^{2+} plus) (20 mM) (Takara Bio), 4 µL of dNTP Mixture (Takara Bio), 400 nM of forward and reverse primers. The PCR cycling condition was 2 minutes at 94°C, followed by 10 cycles of 30 seconds at 94°C, 30 seconds at 55°C, and 1 minute at 72°C. The preamplification step was simultaneously applied to 18 µL or 20 µL of standard DNA (2.0 to 2.0 × 104 copies/µL) created via 10-fold dilution series of 2019-nCoV_N_PositiveControl (CN10006625, Integrated DNA Technologies, Inc.). The pre-amplification step also was applied to 20 µL of TE buffer as the negative control for the pre-amplification and qPCR.

The concentrations of SARS-CoV-2 and PMMoV viral RNA were determined by real-time qPCR on a CFX96 Real-Time PCR detection system (Bio-Rad, Hercules, CA, USA). The

amplification reaction was performed with SsoAdvanced Probes Supermix (Bio-Rad). For SARS-CoV-2 viral RNA, we used the same forward/reverse primers from the previous preamplification step with nCOV_N1 Probe Aliquot (CN10006832, Integrated DNA Technologies, Inc.) [304], RT-qPCR was performed only on pre-amplified samples. Each 20 µL reaction contained 5 µL of pre-amplified cDNA, 10 µL of SsoFast Probes Supermix (Bio-Rad), 500 nM of forward and reverse primers, and 200 nM of fluorogenic probe. The PCR cycling condition was 30 seconds at 95°C, followed by 40 cycles of 10 seconds at 95°C and 30 seconds at 60°C. The number of SARS-CoV-2 genome copies was determined by a standard curve generated with the pre-amped standard samples (1.0×10^1 to 1.0×10^5 copies/reaction). Each sample was quantified in triplicate. The amplification efficiency in the real-time PCR was at least 80%.

The concentration of SARS-CoV-2 viral RNA in influent wastewater sample, $C_{v,w}$ (copies/mL), was determined by the following equation:

$$C_{v,w} = 1000 \times \frac{V}{V_w} \times \frac{V_{f,ex}}{V_{s,ex}} \times \frac{V_{f,syn}}{V_{s,syn}} \times \frac{V_{f,pre}}{V_{s,pre}} \times C_{qPCR} \quad (4.4)$$

where V is the volume of concentrated wastewater suspended with TRIzol regent [mL] (1.1-3.5 mL), C_{qPCR} is the concentration of cDNA applied to qPCR [copies/µL], V_w is the volume of raw wastewater [mL]. $V_{f,ex}$, $V_{s,ex}$, $V_{f,syn}$, $V_{s,syn}$, $V_{f,pre}$, and $V_{s,pre}$ are all the volume of samples in the intermediate steps [µL]. Subscripts *f* and *s* stand for final and starting volume, while subscripts *ex*, *syn*, and *pre* stand for RNA extraction, cDNA synthesis, and pre-amplification, respectively. The limit of quantification (LoQ) was 118-375 copies/mL based on the quantification limit in a qPCR assay (2 copies/µL of pre-amped standard samples) and equation (1).

For the quantification of PMMoV viral RNA, the cDNA was applied to real-time qPCR without preamplification. The amplification reaction was performed with SsoFast Probes Supermix (Bio-Rad), the reverse and forward primers, and probe. Each 20 µL reaction contained 5 µL of cDNA, 10 µL of SsoFast Probes Supermix (Bio-Rad), 500 nM of forward and reverse primers, and 200 nM of fluorogenic probe. The PCR cycling condition used for detection of CDC N1 was also used for PMMoV. The number of PMMoV genome copies of one reaction was determined by a standard curve generated with the standard samples (1.0×10^2 to 1.0×10^6 copies/reaction). Each sample was quantified in triplicate.

The concentration of PMMoV viral RNA in influent wastewater samples was determined by the following equation.

$$\text{PMMoV, copies/mL} = 1000 \times \frac{V_{f,ex}}{V_{s,ex}} \times \frac{V_{f,syn}}{V_{s,syn}} \times C_{qPCR} \quad (4.5)$$

where C_{qPCR} is the concentration of cDNA applied to qPCR [copies/µL].

For datapoints with quantified SARS-CoV-2 RNA concentration, the patient viral load calculation method mentioned in Section 4.2.1 (equation 4.1-4.3) was used.

To test whether wastewater surveillance can provide information about how the epidemic may unfold, for data points with positive yet unquantifiable result, a prediction model framework was established (Fig. 4.6). First, the correlation between the reported cases and positive rate was assessed by Spearman's rank-order correlation and generalized linear model (GLM). Rolling two- and four-week were used to ensure enough data points in a calculation window. The positive rate was calculated as the number of positive signals divided by the total sample number in the given calculation window (rolling two- or four-week). Then, the positive rates from consecutive calculation windows were used as inputs to predict the reported cases in the last calculation window. Both the positive rate and reported cases were assigned to the last week of the calculation

window.

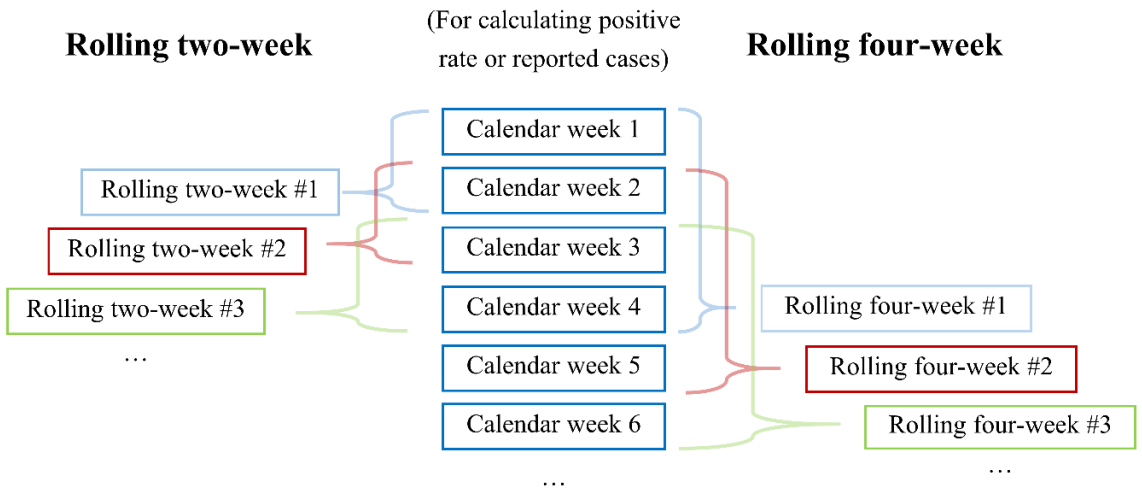

Input 1	Input 2	Output
Positive rate *p* (rolling four-week #1)	*p* (rolling four-week #2)	Reported cases *n* (rolling four-week #3)
p (rolling four-week #2)	*p* (rolling four-week #3)	*n* (rolling four-week #4)
p (rolling four-week #3)	*p* (rolling four-week #4)	*n* (rolling four-week #5)
p (rolling four-week #4)	*p* (rolling four-week #5)	*n* (rolling four-week #6)

Fig. 4.6 A brief illustration of the model framework. The positive rate and cumulative cases in a rolling week are calculated from a calculation window of two or four weeks, the values are assigned to the last week included in the calculation window. For example, when using rolling two-week, the positive rate during calendar weeks 1 and 2 is denoted as *p* (rolling week #1). In the prediction models, the model inputs are the positive rates in consecutive calculation windows (in chronological order) while the output is the cumulative cases of the following calculation window.

Three models, GLM, artificial neural network (ANN), and random forest (RF) were employed to perform the prediction tasks for their ability to solve nonlinear regression problems and learning from available data. For each model, a pre-determined portion of the dataset (80%) was randomly selected for model training; the trained models were then used to perform prediction on the remaining part of the dataset (testing data). This random sampling-training-prediction process was repeated 5,000 times. The mean squared error (MSE) of actual value versus predicted

value was calculated each time for performance evaluation. The optimal number of inputs was determined through a performance analysis (Appendix Table S3). The data pre-treatment, model configuration, prediction, and statistical analysis were all performed using the R programming language, related code is also provided in the Appendix.

4.3.2 Results and discussion

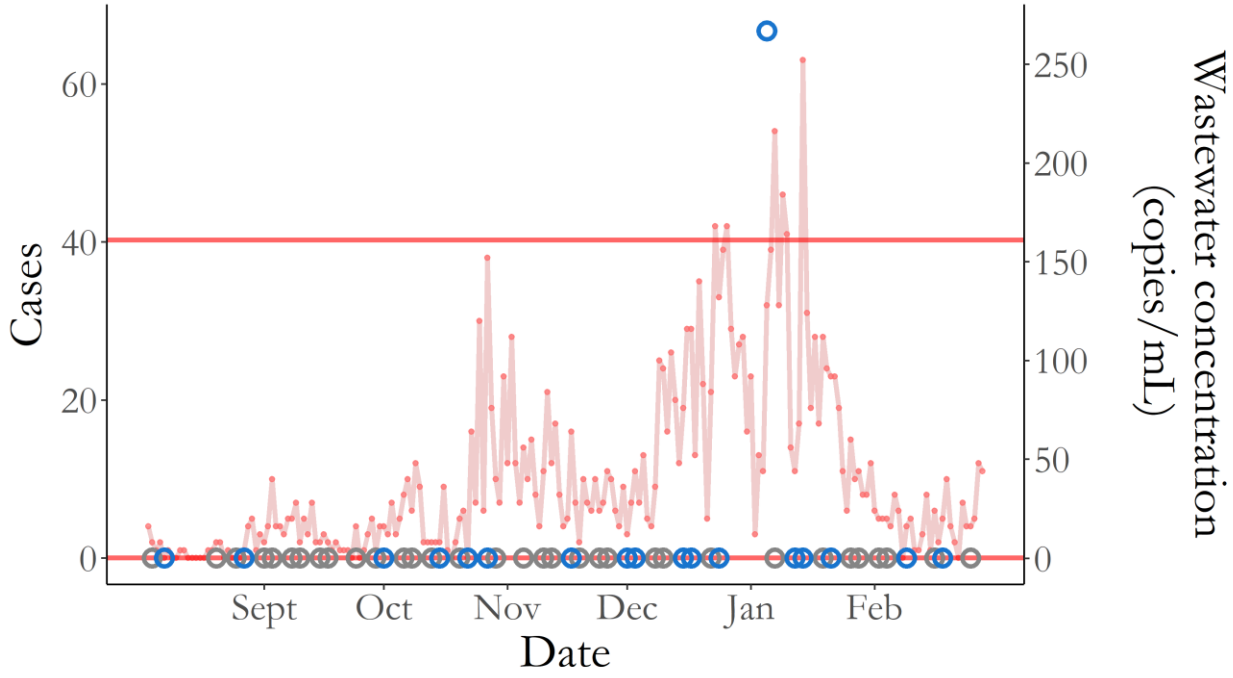

Fig. 4.7 The time series of the SARS-CoV-2 RNA occurrence in wastewater influent and daily reported cases (red line and points). Positives are shown as blue circles while negatives are grey. The upper and lower red horizontal lines represent the LoQ (median) and qualitative sensitivity, respectively.

As a low prevalence region, Sendai was not severely hit by COVID-19 during the study period. A total of 2,142 cases were reported in Sendai city from August 3, 2020, to February 28, 2021 and can be approximately assigned into two outbreak events (Fig. 4.7). The first one lasted between late October and late November 2021. The peak appeared on October 27, 2020, when 38 patients were reported. The second outbreak event that struck between mid-December and late January was more critical with a higher daily case count. There were eight days when the daily

reported cases exceeded the peak in the first outbreak, and 63 cases were reported on January 14, 2021, marking an all-time high. It is worth mentioning that although the daily reported patient number had a temporal dip during the New Year holiday, it was more likely due to the reduced testing capacity and delayed reporting rather than actual ease of epidemic. Following the second outbreak event, the daily reported cases dropped to a low level and remained that way until the end of the study period.

The concentration of PMMoV RNA in wastewater influent ranged from 5.2 $\log_{10}$ to 5.8 $\log_{10}$ genome copies/mL, while in concentrated influent samples ranged from 5.4 $\log_{10}$ to 6.4 $\log_{10}$ genome copies/mL. As the occurrence of PMMoV RNA in concentrated wastewater samples was stable, this may suggest there was no significant loss of SARS-CoV-2 RNA in the whole quantification process.

In total, 51 samples were examined throughout the surveillance period, and 33 of them were negative. The genome concentration corresponding to the highest Ct value in our assay (referred to as qualitative sensitivity hereafter) was estimated to be 0.025 copies/mL by extrapolating the standard curve. Seventeen samples recorded Ct values greater than this, but still lower than the limit of quantification (LoQ), ranging from 1.18×10^2 to 3.75×10^2 copies/mL with a median of 1.61×10^2 copies/mL. The amplification efficiency in real-time PCR was from 80% to 120% which was the acceptable range according to the MIQE guidelines [305]. The coefficient of determination of the standard curves was greater than 0.99 in each assay. No PCR products were detected in negative controls. We considered samples that were tested positive in at least one well in triplicate analysis as positive.

During the study period, the measured viral RNA concentration exceeded the LoQ only once on January 05, 2021 (Fig. 4.7). With a concentration of 2.67×10^2 copies/mL, the daily wastewater viral load calculated from equation 4.4 would be 6.74×10^{13} copies. However, the viral

load contributed by reported patients on that day, calculated using equation 4.3, would be 3.40×10^9 copies with 203 cumulative cases in the 26-day patient viral load calculation window, meaning a L_w/L_p value of 1.98×10^4. Also, this quantifiable signal occurred prior to the peak of reported cases which came nine days later, on January 14, 2021. The wastewater virus concentration did not exceed the LoQ again despite a higher daily case count reported in the following days.

On the other hand, due to the lack of quantifiable data points, non-quantitative detection gave us a more consistent dataset to work on. The first positive signal occurred on August 07, 2020, with just 21 cumulative cases in the patient viral load calculation window and an estimated patient viral load of 3.42×10^8 copies, which translates into a theoretical wastewater virus concentration of only 2.70×10^{-3} copies/mL, far below the qualitative sensitivity. However, assuming the concentration sits somewhere between the qualitative sensitivity and LoQ, the wastewater viral load would have a range of 6.32×10^9 to 4.06×10^{13}, thus a L_w/L_p range of 1.85×10^1 to 1.19×10^5, covering the L_w/L_p value estimated from the quantifiable detection on January 05, 2021. Over the study period, a total of 18 (35.29%) samples were tested positive. Although a positive signal does not directly translate into wastewater viral concentration, consecutive positives may indicate a high viral load with higher confidence. In that sense, two consecutive positives appeared four times and all of which occurred during the two outbreak events.

A stronger correlation was found between the four-week positive rate and cumulative cases than that between two-week positive rate and cumulative cases (Fig. 4.8). Therefore, the prediction models were used to predict the cumulative cases using four-week positive rate. By testing different amounts of input numbers, we found the optimal value was two. Among the three models, ANN offered the best overall performance (median MSE: 7520.22) followed by the other two (median MSE: 9038.60 for GLM and 12021.26 for RF, Fig. 4.9). For about half of the datapoints (45.83%, 11 in 24), the actual four-week cumulative cases were within the 95% CI

range of the prediction. For the remaining data points, the average error was 17.51%.

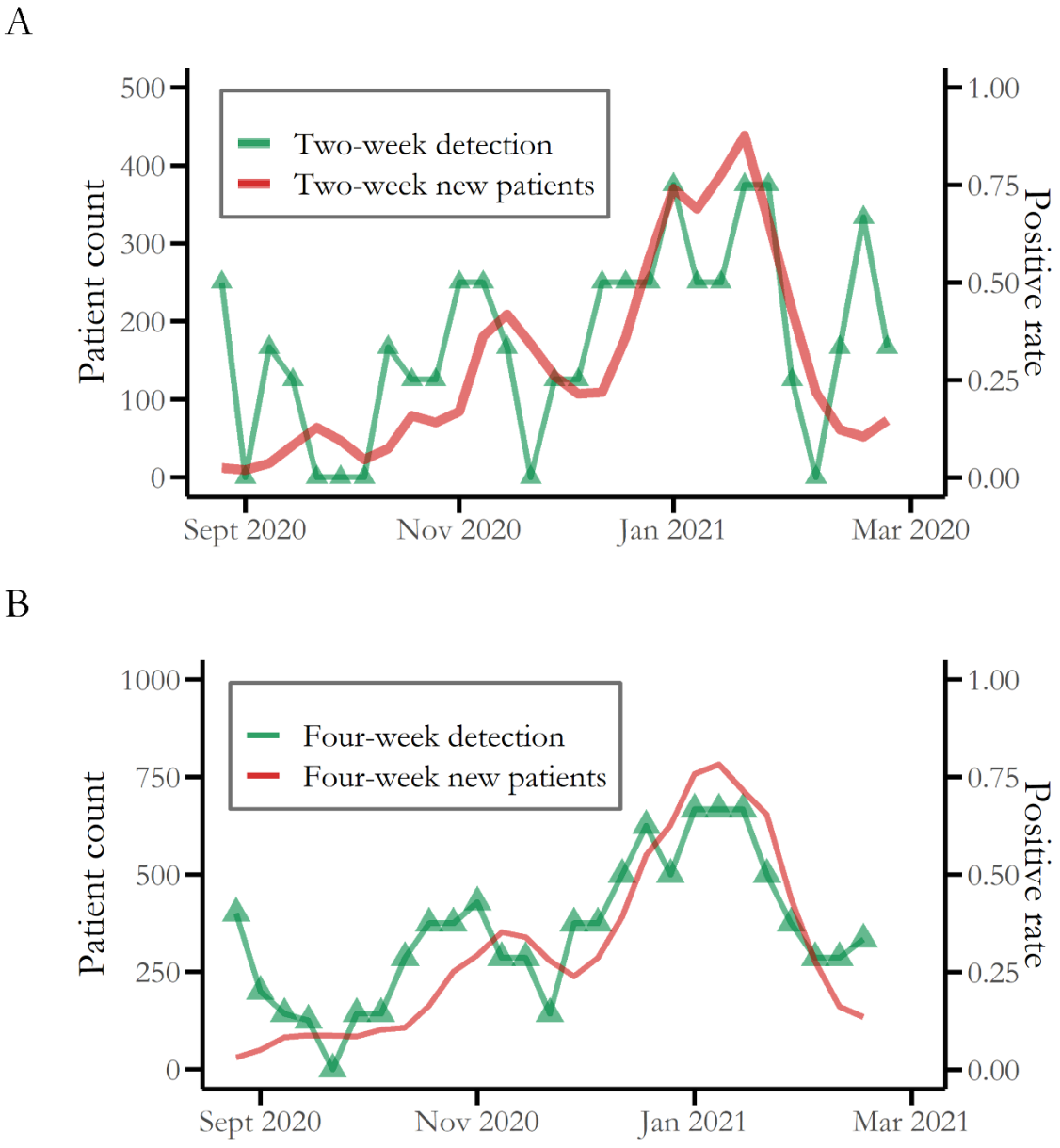

Fig. 4.8 The time series of positive rate and cumulative cases. a: the calculation window is rolling two-week. b: the calculation window is rolling four-week. Spearman's rank-order correlation coefficients: 0.4996 (two-week, $p < 0.05$) and 0.7598 (four-week, $p < 0.05$).

By employing a highly sensitive detection method, we monitored the time series of SARS-CoV-2 RNA occurrence in wastewater influent from an urban community with a population of 360,000. Eighteen out of the 51 influent samples yielded positive signals, and

seventeen samples had SARS-CoV-2 RNA concentrations lower than the LoQ. By examining the reported cases, we found the positive rate of detection has a strong correlation (four-week rolling window, $\rho = 0.7598$, $p < 0.05$) with the cumulative cases in the same time frame and established prediction models, hoping to extend the knowledge on WBE implementation strategies.

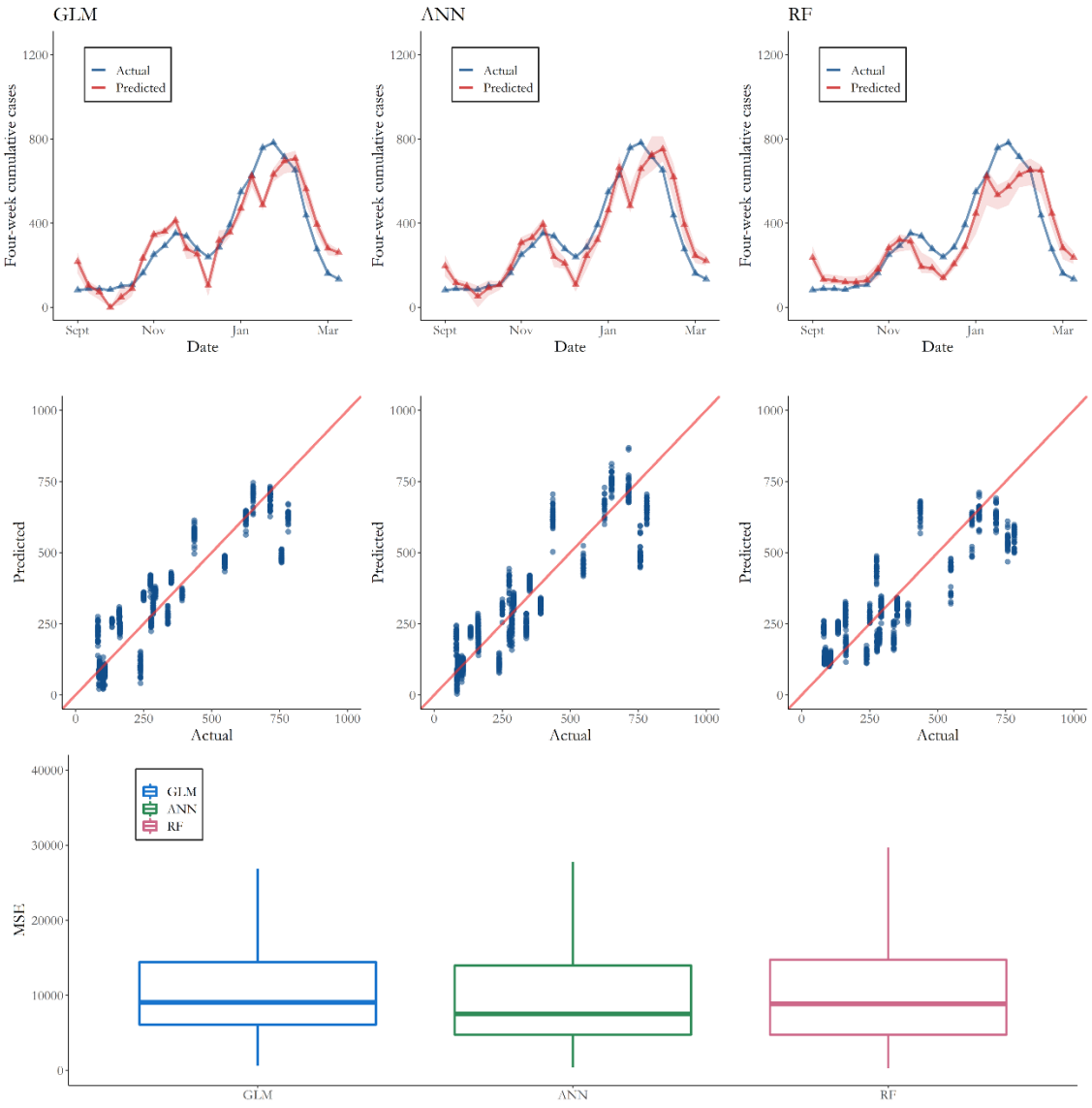

Fig. 4.9 The cumulative cases predicted by the three models. The inputs were the positive rates in two consecutive rolling four-weeks while the output was the within the latter. Normalization was applied to inputs and output before model training and all data were denormalized back to

the original scale once the prediction was conducted. The three rows of figures are the time series of actual versus predicted (median and 95% CI) four-week cumulative cases for each model, the scatter plot of 1,000 randomly selected pairs of actual and predicted values, and the boxplot of MSE distribution from the 5,000 predictions for each model, respectively.

In this study, the LoQ was around 1.61×10^2 copies/mL, about 1 log above the data reported in the previous studies [73,306]. This is due to the decreased volume of a sample considered throughout the analysis in this study. Specifically, the volume of a sample input was approximately 1/10, 1/6, and 1/10 of the total volume of a suspension obtained in a previous step, in RNA extraction, cDNA synthesis, and qPCR, respectively. The LoQ may improve by using other different extraction kits that use a larger volume of sample for extraction. Nevertheless, the method we employed is a feasible option because the data is obtained within 1 day, and our analysis has not been restricted by the stock shortages of manufactures.

We used PMMoV as an internal process control for SARS-CoV-2 detection from suspended solids. PMMoV are detected throughout a year and abundant in wastewater (10^6- 10^{10} copies/L) [225,226,307], which may allow for using it as an internal control of RT-qPCR for a wastewater sample [308]. A previous study reported that the recovered load of PMMoV correlated with that of murine hepatitis virus, suggesting that PMMoV is the potential indicator of the efficiency of SARS-CoV-2 [309]. We concluded that there was no significant loss throughout the analysis because the PMMoV concentration was consistent in both influent and concentrated samples. Future studies should decide the best whole process control for extraction from suspended solids. The better options are human coronaviruses 229E and HKU1 although the longitudinal concentration has not reported [310,311].

The pre-amplification employed in this study increases the number of amplicons in the downstream qPCR. The theoretical qualitative sensitivity should have the same Ct value as that

obtained from one copy per reaction, which in this study is 32.9. However, this value was surpassed by multiple samples whose Ct values reached up to 40.0. A possible explanation for the results was that organic compounds in the influent samples inhibited the amplification efficiency in PCR. We evaluated the effect of inhibitors using a commercially available RNA positive control following a previous study but did not observe lowered efficiency in pre-amplification and qPCR of the positive control RNA, indicating that other reasons were responsible for the greater-than-expected Ct values [312]. It may be explained by the different affinity efficiency of primers and polymerase to the target amplicons between the cDNA derived from viral RNA and plasmid DNA used as the positive control.

From the perspective of early warning, getting a positive signal from wastewater can be a solid proof that the virus has started circulating in the community [71,261]. So far, different studies have reported varied sensitivity. Hong et al. (2021) [313] reported that a positive signal in hospital wastewater requires 253-409 positive cases out of 10,000 individuals while Hata et al. (2021) [180] detected the presence of SARS-CoV-2 RNA in municipal wastewater when the number of cases was <1.0 per 100,000 people, and Betancourt et al. (2021) [78] reported a positive detection when there were only one symptomatic and two asymptomatic individuals among a total of 311 residents in a student dormitory. In practice, the varied detection sensitivity can be mainly attributed to the different experimental methods used as well as the characteristics of the sewage system in which samples are collected. A standardized method may contribute to the comparison and integration of studies [314]. In this study, when the first positive signal was recorded, the number of active shedders estimated from the clinical reports was only 21 in the catchment area with about 360,000 people. Nevertheless, a bigger active shedder base does not guarantee a positive signal in subsequent detections. Even during the summit of the second outbreak event which enabled the only signal above LoQ, negatives were still recorded. Such inconsistent detection had also been reported in

other studies [261,313], adding another layer of complexity.

Despite the strong interest in quantitative wastewater surveillance, a streamlined solution has yet to be formed. Especially, although the experimental side has received substantial attention which led to more sensitive and reliable detection, the analytical side still lacks adequate investigation and verification. There is a noteworthy knowledge gap in how to associate the measured wastewater virus concentration with the epidemic size in the catchment area. So far, most studies had tried directly correlating the abundance of viral RNA with reported cases. However, the following findings in our study: (1) a positive signal occurred when the speculated active shedder group was supposedly far from large enough to enable a successful detection, (2) higher reported cases did not translate to high wastewater virus concentration, and (3) there is a significant yet uncertain gap between the observed wastewater viral load and the viral load contributed by the supposed active shedder base, presented as L_w/L_p in this study, all point to a conclusion that at the current stage, the uncertainty associated with the wastewater viral load is still a great hindrance to reliable back-calculation.

The dimensionless metric L_w/L_p largely determines the robustness of back-calculation. Although a stable L_w/L_p is ideal for back-calculation and was therefore assumed in some recent studies, its value seems to be both time- and location-specific due to various factors. For instance, in Sendai, August and September are the rainy season, because the major urban area is served by a combined sewer, this likely aggravated the dilution of viral RNA and led to a lower L_w/L_p. This is supported by the lower bound of L_w/L_p estimated for August 07, 2020 when the first positive signal appeared. The way patient viral load L_p was calculated also implies it can be impacted by societal factors. For instance, a high level of underreporting may occur under limited testing capacity, leading to a smaller speculated active shedder base, thus a smaller L_p and a larger L_w/L_p. Similarly, if the asymptomatic infection ratio increase, a larger L_w/L_p can also be

expected. Knowing this, some critical epidemic-related information may be drawn by keeping a close eye on L_w/L_p. Nevertheless, it should be pointed out that our calculations of L_w and L_p were based on a set of assumptions including the shedding profile, which may be further refined once more medical evidence becomes available.

As shown in this study, in wastewater surveillance projects, researchers may obtain positive yet unquantifiable signals, especially in low-prevalence period/region. As far as we know, no wastewater surveillance study has utilized binominal data other than as occurrence indicator yet. But, the detection frequency, or positive rate, might serve as a suitable indicator of the virus occurrence upon which further analysis can be performed. This indicates that binominal result may also be utilized to help with epidemic surveillance while establishing a precise connection between wastewater viral load and prevalence level remains challenging and entails further research. Rolling four-weeks were used as the calculation window in this study, but it may be shortened by increasing the sampling frequency or the number of samples collected each time, albeit more time and resource consuming. It should be noted, though, that using positive rate as an indicator may only be feasible in a low prevalence region or at the early stage of an outbreak event. There exists an upper bound of epidemic size beyond which its linear correlation with positive rate becomes invalid, which may explain why the epidemic peaks were not successfully modeled in this study. On the other hand, a higher prevalence level means a higher chance of getting quantifiable signals and back-calculation models should take over once developed.

When a causal relationship between input and output is difficult to establish, data-driven methods like those used in this study may be employed. However, being data-driven also means training data need to be accumulated to finetune the model, and prediction does not always match the reality. With all the uncertainties, it should be reiterated that wastewater surveillance ought not to be a stand-alone tool and its outcome should be interpreted along with other information sources

before reaching any conclusion. For instance, in the early stage of an epidemic when clinical testing capacity is often compromised, wastewater detection may be put into action quicker and cover a larger area. Nevertheless, our study shows that positive rate may be an important indicator, as also recognized by a recent study [261]. Also, in terms of prediction accuracy, as stated above, environmental and societal factors may affect the detection result, thus adding explanatory variables into the model may improve the model performance.

Several limitations of this study should be noted. First, the lag between symptom onset and reporting was not included in modeling. Counting in the delay in case reporting may explain the 9-day delay between the quantified virus concentration and the case peak, it may also improve the correlation between positive rate and cumulative cases, as cases would be assigned to an earlier date. However, existing studies about the delay between symptom onset and hospitalization had varied estimations ranging from 7 days [315] to a much shorter 1.2 days [190]. Therefore, without enough information about the local testing and reporting practice, integrating this factor into the model may introduce further error. Second, grab samples are prone to short-term heterogeneity of viral RNA abundance, which may affect the representativeness of samples. But while composite samples collected by an autosampler may improve the consistency of detection, the viral RNA may also get highly diluted as toilet flushing mainly occurs during certain times, resulting in false negatives. Designing a sampling strategy that captures the toilet flushing peak, therefore, may be a viable solution as suggested by recent studies [78].

As the world is still under the shadow of COVID-19, on top of timely medical and societal intervention, each and every tool that helps monitor the situation and alerts the society is worth looking into. In this study, using a highly sensitive assay, we (1) monitored the occurrence of SARS-CoV-2 viral RNA in the wastewater of an urban area in Japan for over seven months and (2) established a model framework to help extend the existing knowledge base about analyzing

and interpreting the surveillance results. Particularly, we found that although quantitative epidemic size estimation based on measured virus concentration is still challenging, the positive rate of wastewater virus detection is strongly correlated with reported cases and can be used for its prediction, which may guide towards novel wastewater surveillance strategies. Our findings may not only strengthen the application of wastewater surveillance in the current COVID-19 pandemic but also help the scientific community prepare for other public health challenges.

4.4 Weekly COVID-19 case prediction in Sendai, Japan

4.4.1 Method

Building upon this detection frequency-based modeling framework, a program aimed at providing short-term COVID-19 prediction was initiated. The data collected in the one-year period from August 2020 to July 2021 for model improvement internal verification and the output was changed to weekly new cases. For this new task, while the same overall modeling approach was inherited from Section 4.3, a few key modifications were introduced: 1) one additional sampling point (pipeline) in the wastewater treatment plant, which receives wastewater from a resident/industrial area, was included (named line 2 hereafter, the original sampling point is referred to as line 1). This means a larger portion of the population is under wastewater surveillance; 2) instead of using two calculation windows as mentioned in Section 4.3, three consecutive calculation windows (rolling four-week) were used as inputs; 3) because the goal is to verify the feasibility of short-term prediction, multiple models of different assumptions and structures were used in parallel for performance comparison. For example, compared to the last study period, quantifiable detection results appeared more frequently. To preserve this extra information without changing the fundamental data processing structure, in one assumption, a simple algorithm was introduced to divide the data into one of the four categories: negative, positive, low concentration, and high concentration, rather than the original setting where only two options are available

(negative/positive). Therefore, the detection information now has three variables (positive rate R_P, R_L, and R_H); 4) because the time span greatly exceeds the previous trial study, explanatory variables (vaccination rate and the case count from the previous week) were introduced to see whether they help bring down the uncertainty, and; 5) in addition to the ANN model that showed the best overall performance in the previous trial study, long short-term memory (LSTM) and recurrent neural network (RNN) were also introduced later because they can maintain an internal memory which may help with time series forecasting. To reduce overfitting, all ANN models featured repeated random subsampling with 5,000 iterations while LSTM and RNN models used forward chaining and 100 iterations. The details of the models, including the assumptions made in ANN and the model configurations, are shown in Fig. 4.10 and Table 4.1.

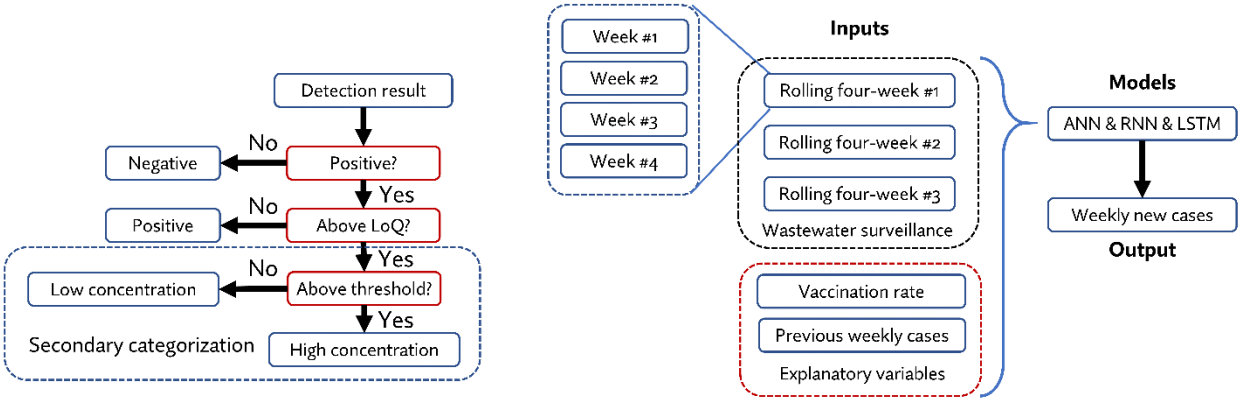

Fig. 4.10 The flow chart of detection result processing and the model structure.

Table 4.1 The configuration and assumption in each model.

Model	Input number	Hidden layer	Platform	Library	Cross validation	Assumption & explanatory variable	Iteration
ANN #1	20	[30,10,25]	R	neuralnet	Repeated random subsampling	N/A	5,000
ANN #2	20	[30,10,25]	R	neuralnet	Repeated random subsampling	Vaccination	5,000
ANN #3	20	[30,10,25]	R	neuralnet	Repeated random subsampling	Vaccination expiration	5,000
ANN #4	20	[30,10,25]	R	neuralnet	Repeated random subsampling	Secondary categorization	5,000
RNN	25	[40]	Python	TensorFlow	Forward chaining	Secondary categorization	100
LSTM	25	[50]	Python	TensorFlow	Forward chaining	Secondary categorization	100

4.4.2 Data overview

A total of 326 wastewater samples were collected and analyzed during the study period. Among them, 161 samples were tested positive (49.4%), and 28 samples had quantified concentration (8.6%). This low occurrence level was expected to some extent due to the relatively low prevalence level in Sendai and Japan. As for new COVID-19 cases, several outbreak events occurred during the study period. The most serious one started in the beginning of 2022 despite about 80% of the residents had received at least two shots of mRNA vaccine, primarily because the more contagious Omicron variant made its way into Japan around this time.

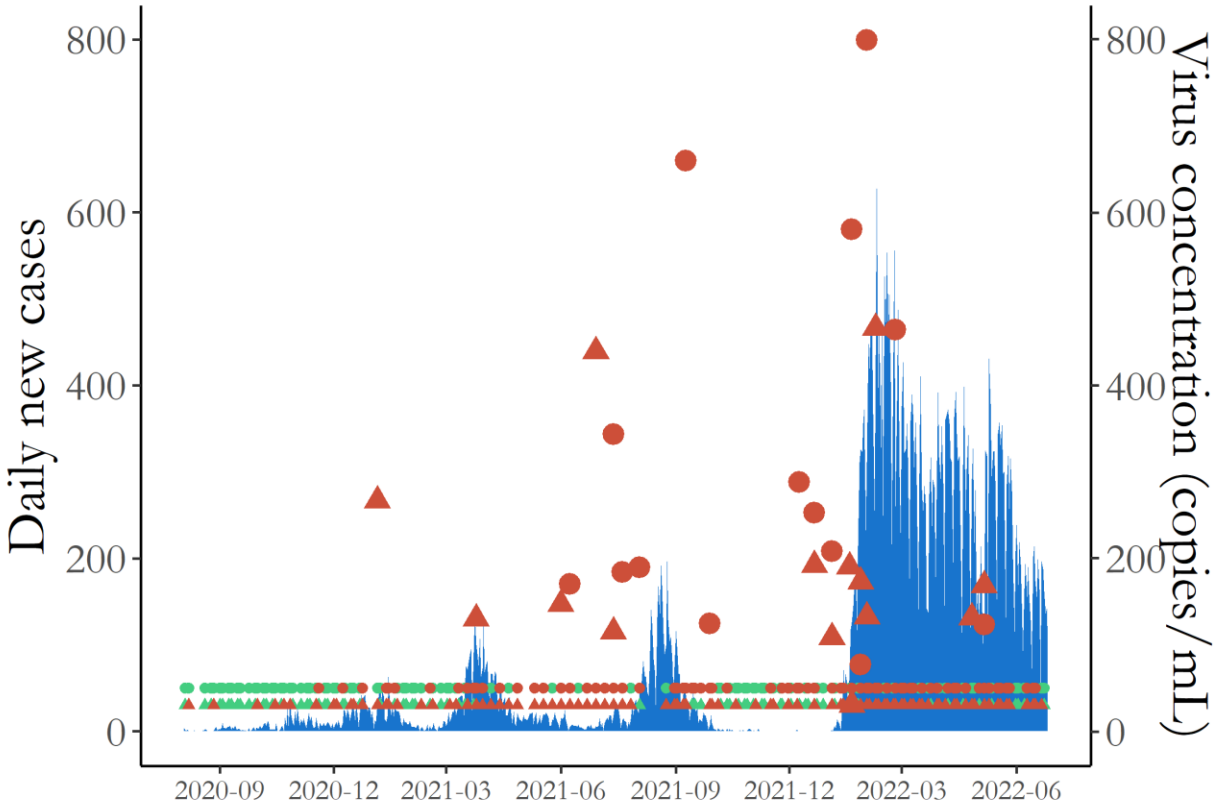

Fig. 4.11 The wastewater SARS-CoV-2 detection results during the study period. Positive detections are shown in red while negative detections are shown in green. The two sewage pipelines are marked by different point shapes. Triangle points represent line 1 while round points stand for line 2. Small red points close to the X-axis represent detections that are positive yet below LoQ.

4.4.3 Weekly COVID-19 case prediction

Starting from September 2021, weekly new case prediction is issued on every Monday and shared online on a designated website as well as news outlets, although for stability and consistency reasons, only the predictions generated by model #4 were shared with the public while the other predictions were only used for internal evaluation and comparison. As of June 27, 2022, a total of 43 predictions have been issued by ANN models and 27 have been issued by RNN and LSTM (Fig. 4.12). Among, model #4 provided the best overall fitting with RMSE = 294.4 and low residual autocorrelation (Fig. 4.13 and 4.14), although other ANN models also came close (RMSE = 310.6, 321.9, and 310.7, respectively). In comparison, RNN and LSTM have higher RMSE quite different from the ANN family.

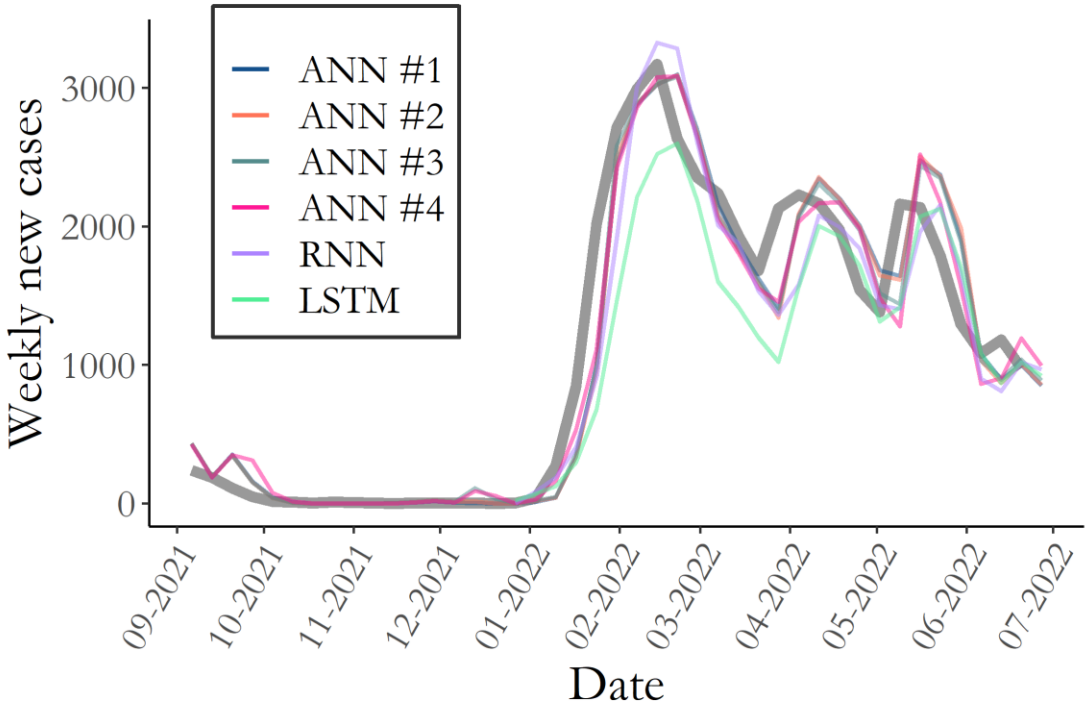

Fig. 4.12 The predictions generated by all models. The thick gray line represents the actual new case count while lines with color are predictions by different models. Note that ANN model prediction started from September 2021 while RNN and LSTM were later added to the modeling study and the predictions started from the end of 2021.

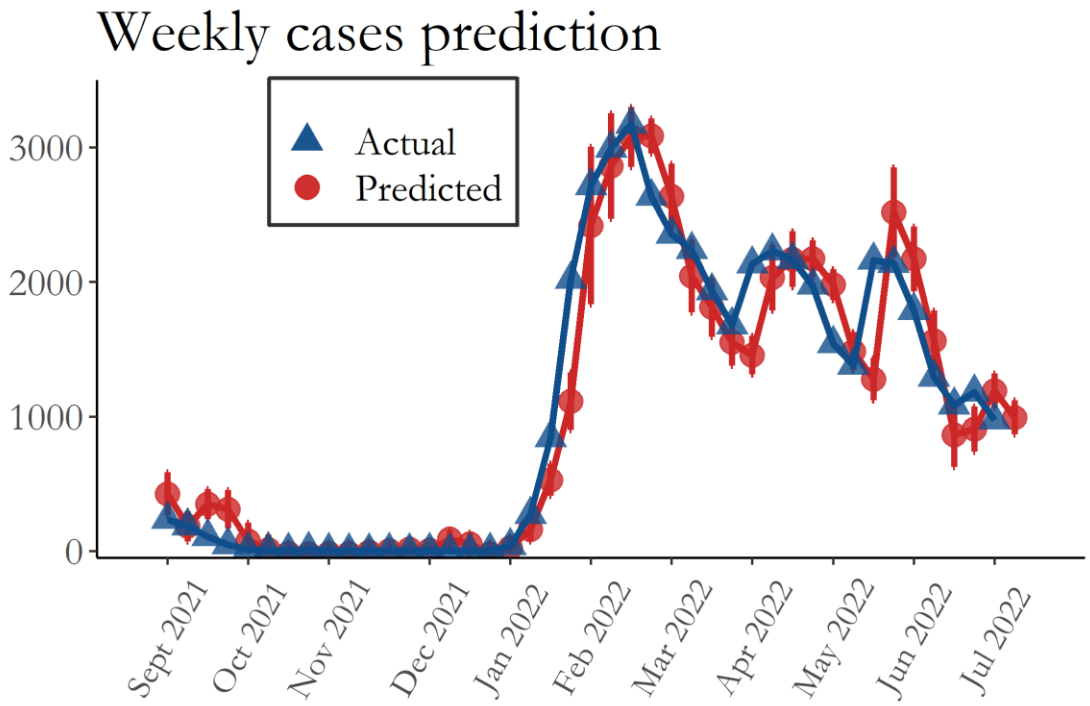

Fig. 4.13 The predictions generated by ANN model #4. The points and error bars represent the median values and standard deviations calculated from the 5,000 iterations.

Also, the models demonstrated some forward-looking capability. During the week December 27, 2021 to January 02, 2022, all but one models predicted that the weekly case count would be zero and two new cases were reported in that week. However, based on wastewater surveillance result alone, all models increased their predictions for the next week (January 03 to 09, 2022). The predictions ranged from 9 (model #1) to 87 (RNN). As it turned out, 38 new cases were reported in that week, which marked the beginning of a major outbreak event caused by the highly contagious Omicron variant.

However, a closer look into the results reveals something worrisome. Although in general a good match between prediction and actual case count was achieved and there were times when the models gave warning signals before the outbreak events began, how accurate the models can predict the way epidemic unfolds remains an open question. When there is a drastic change in new

cases, no matter upward or downward, all models showed some difficulty catching up, reflected by some extent of delay following those turning points. It typically takes two to three weeks for the model to keep up with the new epidemic progression trend and for a short-term epidemic prediction project, such delay is certainly unwanted and may mitigate its feasibility as a public health warning system. There are two possible reasons for this delay. One of them is overfitting, which refers to the situation where the model fits too closely to the training data. Despite the implementation of cross validation methods, the nature of neural network models determines that the large number of neurons inside also demand a huge dataset to be properly tuned. Although wastewater surveillance had been performed for nearly two years, the obtained data may still be inadequate. The second plausible explanation is that because the models were trained by past data, when the inputs are out-of-range, the model may lose context and cannot extrapolate well. This can be partially reflected by the fact that although the initial new case surge in January 2022 was not well captured by the models, in later months the delay became more and more insignificant.

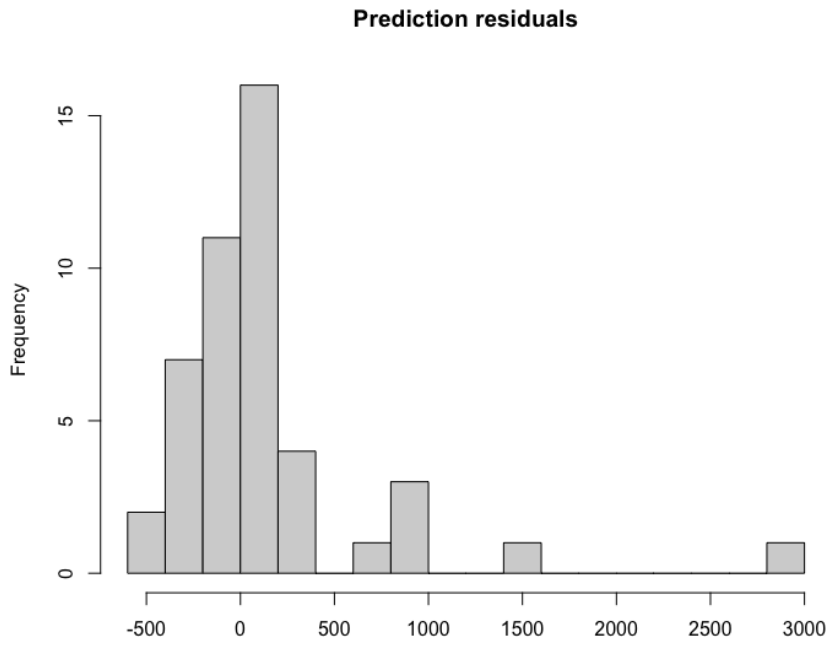

1

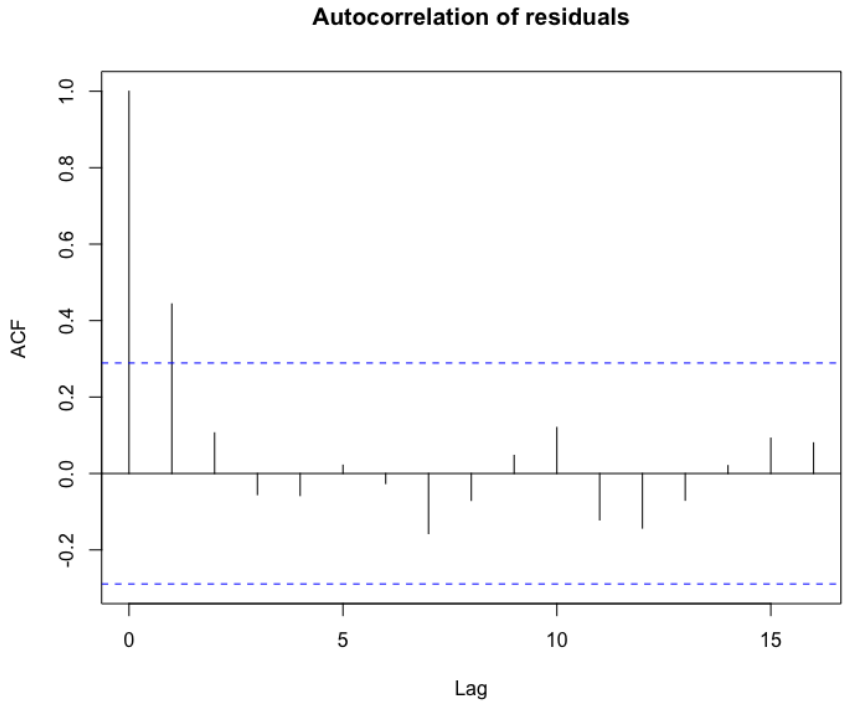

2

3 **Fig. 4.14** The residuals of the model prediction and its autocorrelation.

4

5 One potential way to mitigate the delay factor is to further introduce explanatory variables

that help reveal the epidemic progression. For instance, many recent studies have discussed the role population mobility plays in the transmission pattern of COVID-19 [316,317]. In short, population mobility reflects the degree of social contact and consequently, the infection probability. This is in line with what we observed in Fig. 4.4, although the connection between the two factors may vary over time. Due to the incubation period and delay in clinical testing/reporting, the population mobility level at a given point may have an impact on the new cases in near future. However, adding mobility data to the formula will take considerable efforts as many key questions remain unanswered including which index is the most appropriate proxy for population mobility and how to incorporate mobility data into the current wastewater surveillance-based modeling framework.

4.5 Conclusion

In this chapter, by conducting a step-by-step research project from literature review to real-world application, we explored the feasibility of wastewater surveillance, enhanced by data-driven modeling, in epidemic support. The results show that with proper experiment design, data processing, and modeling technique, wastewater surveillance can indeed complement other epidemic countermeasures in the forms of issuing warning signals and enhance preparedness. However, while the possibility is clearly shown, considering the public service nature it carries, there is still a long way to go for this relatively new approach to gain acceptance among researchers, authority, and public.

Copyright

5. Discussion and conclusion

5.1 Lessons learned from applying data-driven modeling to wastewater pathogen issues

From the projects featured in this dissertation, it is clear that data-driven modeling holds huge potential when it comes to performing regression and prediction tasks that cannot be addressed by mechanistic models yet.

One thing we learned from literature review and conducting the research in this dissertation is how little attention data-driven modeling receives. Traditionally, in both water and epidemiology sectors, mechanistic models are preferred due to a taste for a solid understanding of the underlying processes. However, establishing one may be hindered by the complexity that researchers often encounter in these two fields. With the ever-evolving computational power from personal computers and better software support, individuals can now easily process the data and apply data-driven models. Therefore, data-driven models really should come out of research labs and enter real-world application, but the acceptance will not be easy to gain until they can truly prove themselves.

5.2 Challenges, opportunities, and future works

There are some common bottlenecks faced by researchers applying data-driven modeling to practical problems. The first one is data availability. As the name suggests, data-driven models require an adequately large training set to be properly tuned. However, data availability is not always guaranteed, particularly in two scenarios: 1) the data itself is hard to get hands on. This is also a problem we occurred in this dissertation (Section 3) where the model development and verification rely on influent/effluent virus concentrations yet molecular virus quantification is both costly and time-consuming, making accumulating a large dataset challenging. Also, when the reactor reaches stable operation, there is very little variation in the operational condition, making the data collection process even harder; 2) an urgent project does not have enough time for building up a large dataset. Take epidemic prediction for example, in

our study the data collected for over one year was used for testing model structures and verification, yet when faced with new viruses or diseases, researchers may not have this luxury as the public health hangs in the balance. Therefore, models like that may be more suitable for not-so-urgent programs such as the long-term monitoring and prediction of common diseases. The second issue is the long-term feasibility. Whether it is an epidemic prediction model or a soft sensor for virus removal monitoring, routine maintenance and recalibration are needed to work properly over time. For instance, front-line operators at wastewater treatment plants may not all have the required knowledge to maintain an update the soft sensor, which in the long run may even lead to compromised microbial safety.

On the topic of wastewater pathogen surveillance, as a relatively new research field, much is needed to continue unleashing its full potential. Firstly, more statistical tools need to be adopted and applied to the analysis and interpretation. Most SARS-CoV-2 wastewater surveillance projects report the raw quantification results without further polishing, which may make it hard for the authority and public to obtain epidemic-related information. Second, as the quantification results are still subject to strong variation and fluctuation, how to handle the noise in data will have a huge impact on model robustness. Some approaches such as using wastewater flow rate and human fecal indicator to normalize the virus detection signal have been tested and implemented, although to what extent is it useful is still under debate [318,319]. Introducing statistical methods is another option to iron out some uncertainty, but information about this remains rare.

While there is still huge room for the improvement of prediction accuracy and timeliness, the possibilities opened by data-driven modeling are hard to ignore. Because the mechanistic understanding of processes is not emphasized as such, combining knowledge and data from different fields also becomes easier. Therefore, from an interdisciplinary perspective, water

researchers should work closely with other stakeholders, such as doctors, epidemiologists, and political decision makers, to find out how can this approach be improved with extra data and bring out maximum benefit to the society. We should have some relief, though, knowing a very powerful tool is at our hands when facing future public health challenges. It is worth mentioning that although the models used in this dissertation are all black-box models, there is an increasing interest in extracting information from the established models themselves, also referred to as explainable machine learning. Applying explainable machine learning may help expand the knowledge about the systems to be modelled and contribute to future research design.

Finally, it should be mentioned that this study focused on the applications in centralized wastewater collection and treatment systems. While the accessibility of such systems has greatly improved over the years with the rapid global urbanization, many rural regions, especially in developing countries where microbial safety assessment on water reclamation and affordable epidemic monitoring methods are needed the most, still only have limited access to large-scale infrastructures. Although wastewater surveillance on smaller scales (e.g., campus and building) has been proven feasible, whether the efficacy and cost efficiency will meet the demand of rural areas remains to be seen.

References

1. UN Water. The United Nations World Water Development Report 2019. *The United Nations World Water Development Report 2019* Preprint at https://doi.org/10.18356/0d8fe383-en (2019).
2. Sun, Y. *et al.* Characteristics of water quality of municipal wastewater treatment plants in China: Implications for resources utilization and management. *Journal of Cleaner Production* **131**, 1–9 (2016).
3. Wu, B. Membrane-based technology in greywater reclamation: A review. *Science of the Total Environment* **656**, 184–200 (2019).
4. Angelakis, A. N., Asano, T., Bahri, A., Jimenez, B. E. & Tchobanoglous, G. Water reuse: From ancient to modern times and the future. *Frontiers in Environmental Science* **6**, (2018).
5. Angelakis, A. N. & Snyder, S. A. Wastewater treatment and reuse: Past, present, and future. *Water (Switzerland)* **7**, 4887–4895 (2015).
6. Jaramillo, M. F. & Restrepo, I. Wastewater reuse in agriculture: A review about its limitations and benefits. *Sustainability (Switzerland)* **9**, (2017).
7. Diemer, D. M. *An Overview of Water Recycling in the United States*. *Japan-U.S. Conference on Drinking Water Quality and Wastewater Control* vol. 196 (2007).
8. Duong, K. & Saphores, J.-D. M. Obstacles to wastewater reuse: An overview. *Wiley Interdisciplinary Reviews: Water* **2**, 199–214 (2015).
9. Smith, H. M., Brouwer, S., Jeffrey, P. & Frijns, J. Public responses to water reuse – Understanding the evidence. *Journal of Environmental Management* **207**, 43–50 (2018).
10. Vuppaladadiyam, A. K. *et al.* A review on greywater reuse: Quality, risks, barriers and global scenarios. *Reviews in Environmental Science and Biotechnology* **18**, 77–99 (2019).
11. Lofrano, G. & Brown, J. Wastewater management through the ages: A history of mankind. *Science of the Total Environment* **408**, 5254–5264 (2010).
12. Chen, W., Lu, S., Jiao, W., Wang, M. & Chang, A. C. Reclaimed water : A safe irrigation water source ? *Environmental Development* **8**, 74–83 (2013).
13. Chen, W., Lu, S., Peng, C., Jiao, W. & Wang, M. Accumulation of Cd in agricultural soil under long-term reclaimed water irrigation. *Environmental Pollution* **178**, 294–299 (2013).
14. Dodgen, L. K. & Zheng, W. Effects of reclaimed water matrix on fate of pharmaceuticals and personal care products in soil. *Chemosphere* **156**, 286–293 (2016).
15. Qadir, M. *et al.* The challenges of wastewater irrigation in developing countries. *Agricultural Water Management* **97**, 561–568 (2010).
16. Qadir, M. *et al.* Agricultural use of marginal-quality water— Opportunities and challenges. *Water for Food Water for Life: A Comprehensive Assessment of Water Management in Agriculture* 425–458 (2013) doi:10.4324/9781849773799.

17. Oteng-Peprah, M., Acheampong, M. A. & DeVries, N. K. Greywater characteristics, treatment systems, reuse strategies and user perception—A review. *Water, Air, and Soil Pollution* **229**, (2018).
18. Gibson, K. E. Viral pathogens in water: Occurrence, public health impact, and available control strategies. *Current Opinion in Virology* **4**, 50–57 (2014).
19. Shakir, E., Zahraw, Z. & Al-Obaidy, A. H. M. J. Environmental and health risks associated with reuse of wastewater for irrigation. *Egyptian Journal of Petroleum* **26**, 95–102 (2017).
20. Teunis, P. F. M. *et al.* Shedding of norovirus in symptomatic and asymptomatic infections. *Epidemiology and Infection* **143**, 1710–1717 (2015).
21. Fox, R. & Stuckey, D. MS-2 and T4 phage removal in an anaerobic membrane bioreactor (AnMBR): Effect of gas sparging rate. *Journal of Chemical Technology and Biotechnology* **90**, 384–390 (2015).
22. Sano, D., Amarasiri, M., Hata, A., Watanabe, T. & Katayama, H. Risk management of viral infectious diseases in wastewater reclamation and reuse : Review. *Environment International* **91**, 220–229 (2016).
23. Moazeni, M. *et al.* Estimation of health risks caused by exposure to enteroviruses from agricultural application of wastewater effluents. *Water Research* **125**, 104–113 (2017).
24. Prado, T. *et al.* Performance of wastewater reclamation systems in enteric virus removal. *Science of the Total Environment* **678**, 33–42 (2019).
25. Qiu, Y. *et al.* Assessment of human virus removal during municipal wastewater treatment in Edmonton, Canada. *Journal of Applied Microbiology* **119**, 1729–1739 (2015).
26. Prevost, B. *et al.* Viral persistence in surface and drinking water: Suitability of PCR pre-treatment with intercalating dyes. *Water Research* **91**, 68–76 (2016).
27. Dickin, S. K., Schuster-Wallace, C. J., Qadir, M. & Pizzacalla, K. A review of health risks and pathways for exposure to wastewater use in agriculture. *Environmental Health Perspectives* **124**, 900–909 (2016).
28. Ito, T. *et al.* Target virus log 10 reduction values determined for two reclaimed wastewater irrigation scenarios in Japan based on tolerable annual disease burden. *Water Research* **125**, 438–448 (2017).
29. Okoh, A. I., Sibanda, T. & Gusha, S. S. Inadequately treated wastewater as a source of human enteric viruses in the environment. *International Journal of Environmental Research and Public Health* **7**, 2620–2637 (2010).
30. US Environmental Protection Agency. *2012 Guidelines for Water Reuse*. *Epa/600/R-12/618* (2012).
31. Jeong, H., Kim, H. & Jang, T. Irrigation water quality standards for indirect wastewater reuse in agriculture: A contribution toward sustainablewastewater reuse in South korea.

Water (Basel) **8**, (2016).

32. Hot, D. *et al.* Detection of somatic phages, infectious enteroviruses and enterovirus genomes as indicators of human enteric viral pollution in surface water. *Water Research* **37**, 4703–4710 (2003).
33. Jurzik, L., Hamza, I. A., Puchert, W., Überla, K. & Wilhelm, M. Chemical and microbiological parameters as possible indicators for human enteric viruses in surface water. *International Journal of Hygiene and Environmental Health* **213**, 210–216 (2010).
34. Pang, X. *et al.* Prevalence, levels and seasonal variations of human enteric viruses in six major rivers in Alberta, Canada. *Water Research* **153**, 349–356 (2019).
35. Das, O., Lekshmi, M., Kumar, S. & Nayak, B. B. Incidence of norovirus in tropical seafood harbouring fecal indicator bacteria. *Marine Pollution Bulletin* **150**, 110777 (2020).
36. Coudray-Meunier, C. *et al.* A comparative study of digital RT-PCR and RT-qPCR for quantification of Hepatitis A virus and Norovirus in lettuce and water samples. *International Journal of Food Microbiology* **201**, 17–26 (2015).
37. Miura, T., Okabe, S., Nakahara, Y. & Sano, D. Removal properties of human enteric viruses in a pilot-scale membrane bioreactor (MBR) process. *Water Research* **75**, 282–291 (2015).
38. Haramoto, E. *et al.* A review on recent progress in the detection methods and prevalence of human enteric viruses in water. *Water Research* **135**, 168–186 (2018).
39. Randazzo, W. *et al.* Interlaboratory comparative study to detect potentially infectious human enteric viruses in influent and effluent waters. *Food and Environmental Virology* **11**, 350–363 (2019).
40. Parsons, L. R., Sheikh, B., Holden, R. & York, D. W. Reclaimed water as an alternative water source for crop irrigation. *HortScience* **45**, 1626–1629 (2010).
41. CDPH. California Regulations Related to Drinking Water. 1–351 (2016).
42. Mbonimpa, E. G., Blatchley, E. R., Applegate, B. & Harper, W. F. Ultraviolet A and B wavelength-dependent inactivation of viruses and bacteria in the water. *Journal of Water and Health* **16**, 796–806 (2018).
43. Richardson, S. D., Plewa, M. J., Wagner, E. D., Schoeny, R. & DeMarini, D. M. Occurrence, genotoxicity, and carcinogenicity of regulated and emerging disinfection by-products in drinking water: A review and roadmap for research. *Mutation Research - Reviews in Mutation Research* **636**, 178–242 (2007).
44. Li, X. F. & Mitch, W. A. Drinking water disinfection byproducts (DBPs) and human health effects: Multidisciplinary challenges and opportunities. *Environmental Science and Technology* **52**, 1681–1689 (2018).
45. Collivignarelli, M. C., Abbà, A., Benigna, I., Sorlini, S. & Torretta, V. Overview of the main disinfection processes for wastewater and drinking water treatment plants. *Sustainability*

(Switzerland) **10**, 1–21 (2018).

46. Rizzo, L. *et al.* Urban wastewater treatment plants as hotspots for antibiotic resistant bacteria and genes spread into the environment: A review. *Science of the Total Environment* **447**, 345–360 (2013).
47. Li, D., Zeng, S., He, M. & Gu, A. Z. Water disinfection byproducts induce antibiotic resistance-role of environmental pollutants in resistance phenomena. *Environmental Science and Technology* **50**, 3193–3201 (2016).
48. Wang, K., Abdalla, A. A., Khaleel, M. A., Hilal, N. & Khraisheh, M. K. Mechanical properties of water desalination and wastewater treatment membranes. *Desalination* **401**, 190–205 (2017).
49. Santos, A., Ma, W. & Judd, S. J. Membrane bioreactors: Two decades of research and implementation. *Desalination* **273**, 148–154 (2011).
50. Lin, H. *et al.* A review on anaerobic membrane bioreactors: Applications, membrane fouling and future perspectives. *Desalination* **314**, 169–188 (2013).
51. Ma, J., Dai, R., Chen, M., Khan, S. J. & Wang, Z. Applications of membrane bioreactors for water reclamation: Micropollutant removal, mechanisms and perspectives. *Bioresource Technology* **269**, 532–543 (2018).
52. Cecconet, D., Callegari, A., Hlavínek, P. & Capodaglio, A. G. Membrane bioreactors for sustainable, fit-for-purpose greywater treatment: A critical review. *Clean Technologies and Environmental Policy* **21**, 745–762 (2019).
53. Krzeminski, P., Leverette, L., Malamis, S. & Katsou, E. Membrane bioreactors – A review on recent developments in energy reduction, fouling control, novel configurations, LCA and market prospects. *Journal of Membrane Science* **527**, 207–227 (2017).
54. Xiao, K., Liang, S., Wang, X., Chen, C. & Huang, X. Current state and challenges of full-scale membrane bioreactor applications: A critical review. *Bioresource Technology* **271**, 473–481 (2019).
55. Lei, Z. *et al.* Application of anaerobic membrane bioreactors to municipal wastewater treatment at ambient temperature: A review of achievements, challenges, and perspectives. *Bioresource Technology* **267**, 756–768 (2018).
56. Harb, M. & Hong, P. Y. Molecular-based detection of potentially pathogenic bacteria in membrane bioreactor (MBR) systems treating municipal wastewater: A case study. *Environmental Science and Pollution Research* **24**, 5370–5380 (2017).
57. Francy, D. S. *et al.* Comparative effectiveness of membrane bioreactors, conventional secondary treatment, and chlorine and UV disinfection to remove microorganisms from municipal wastewaters. *Water Research* **46**, 4164–4178 (2012).
58. Baek, S. H. & Pagilla, K. Aerobic and anaerobic membrane bioreactors for municipal

wastewater treatment. *Proceedings of the Water Environment Federation* **2003**, 356–375 (2012).

59. Judd, S. J. The status of industrial and municipal effluent treatment with membrane bioreactor technology. *Chemical Engineering Journal* **305**, 37–45 (2016).
60. Gentile, G. J., Cruz, M. C., Rajal, V. B. & Fidalgo de Cortalezzi, M. M. Electrostatic interactions in virus removal by ultrafiltration membranes. *Journal of Environmental Chemical Engineering* **6**, 1314–1321 (2018).
61. Peña, M. *et al.* Anaerobic submerged membrane bioreactor (AnSMBR) treating municipal wastewater at ambient temperature: Operation and potential use for agricultural irrigation. *Bioresource Technology* **282**, 285–293 (2019).
62. Santasmasas, C., Rovira, M., Clarens, F. & Valderrama, C. Grey water reclamation by decentralized MBR prototype. *Resources, Conservation and Recycling* **72**, 102–107 (2013).
63. Purnell, S., Ebdon, J., Buck, A., Tupper, M. & Taylor, H. Removal of phages and viral pathogens in a full-scale MBR: Implications for wastewater reuse and potable water. *Water Research* **100**, 20–27 (2016).
64. Wu, B. & Kim, J. Anaerobic membrane bioreactors for nonpotable water reuse and energy recovery. *Journal of Environmental Engineering (United States)* **146**, 1–9 (2020).
65. De Luca, G., Sacchetti, R., Leoni, E. & Zanetti, F. Removal of indicator bacteriophages from municipal wastewater by a full-scale membrane bioreactor and a conventional activated sludge process: Implications to water reuse. *Bioresource Technology* **129**, 526–531 (2013).
66. Xagoraraki, I. & O'Brien, E. Wastewater-based epidemiology for early detection of viral outbreaks. in *Women in Water Quality* 75–97 (Springer, 2020).
67. Sims, N. & Kasprzyk-Hordern, B. Future perspectives of wastewater-based epidemiology: Monitoring infectious disease spread and resistance to the community level. *Environment International* **139**, 105689 (2020).
68. Daughton, C. G. Wastewater surveillance for population-wide Covid-19: The present and future. *Science of the Total Environment* **736**, 139631 (2020).
69. Thompson, J. R. *et al.* Making waves: Wastewater surveillance of SARS-CoV-2 for population-based health management. *Water Research* **184**, (2020).
70. La Rosa, G. *et al.* First detection of SARS-CoV-2 in untreated wastewaters in Italy. *Science of the Total Environment* **736**, 139652 (2020).
71. Randazzo, W. *et al.* SARS-CoV-2 RNA in wastewater anticipated COVID-19 occurrence in a low prevalence area. *Water Research* **181**, (2020).
72. Medema, G., Heijnen, L., Elsinga, G., Italiaander, R. & Brouwer, A. Presence of SARS-Coronavirus-2 RNA in sewage and correlation with reported COVID-19 prevalence in the

early stage of the epidemic in the Netherlands. *Environmental Science & Technology Letters* (2020) doi:10.1021/acs.estlett.0c00357.

73. Ahmed, W. *et al.* First confirmed detection of SARS-CoV-2 in untreated wastewater in Australia: A proof of concept for the wastewater surveillance of COVID-19 in the community. *Science of the Total Environment* **728**, 138764 (2020).
74. D'Aoust, P. M. *et al.* Quantitative analysis of SARS-CoV-2 RNA from wastewater solids in communities with low COVID-19 incidence and prevalence. *Water Research* **188**, 116560 (2021).
75. Hata, A., Hara-Yamamura, H., Meuchi, Y., Imai, S. & Honda, R. Detection of SARS-CoV-2 in wastewater in Japan during a COVID-19 outbreak. *Science of The Total Environment* **758**, 143578 (2021).
76. Westhaus, S. *et al.* Detection of SARS-CoV-2 in raw and treated wastewater in Germany – Suitability for COVID-19 surveillance and potential transmission risks. *Science of the Total Environment* **751**, 141750 (2021).
77. Yaniv, K., Ozer, E., Lewis, Y. & Kushmaro, A. RT-qPCR assays for SARS-CoV-2 variants of concern in wastewater reveals compromised vaccination-induced immunity. *Water Research* **207**, 117808 (2021).
78. Betancourt, W. Q. *et al.* COVID-19 containment on a college campus via wastewater-based epidemiology, targeted clinical testing and an intervention. *Science of the Total Environment* **779**, 146408 (2021).
79. Gibas, C. *et al.* Implementing building-level SARS-CoV-2 wastewater surveillance on a university campus. *Science of the Total Environment* **782**, 146749 (2021).
80. Wong, T. E. *et al.* Evaluating the sensitivity of SARS-CoV-2 infection rates on college campuses to wastewater surveillance. *Infect Dis Model* **6**, 1144–1158 (2021).
81. Elhadidy, A. M., Peldszus, S. & Van Dyke, M. I. An evaluation of virus removal mechanisms by ultrafiltration membranes using MS2 and φx174 bacteriophage. *Separation and Purification Technology* **120**, 215–223 (2013).
82. Da Silva, A. K., Kavanagh, O. V., Estes, M. K. & Elimelech, M. Adsorption and aggregation properties of norovirus GI and GII virus-like particles demonstrate differing responses to solution chemistry. *Environmental Science and Technology* **45**, 520–526 (2011).
83. Samandoulgou, I., Fliss, I. & Jean, J. Zeta potential and aggregation of virus-like particle of human norovirus and feline calicivirus under different physicochemical conditions. *Food and Environmental Virology* (2015) doi:10.1007/s12560-015-9198-0.
84. Chaudhry, R. M., Nelson, K. L. & Drewes, J. E. Mechanisms of pathogenic virus removal in a full-scale membrane bioreactor. *Environmental Science and Technology* **49**, 2815–2822 (2015).

85. Hai, F. I., Riley, T., Shawkat, S., Magram, S. F. & Yamamoto, K. Removal of pathogens by membrane bioreactors: A review of the mechanisms, influencing factors and reduction in chemical disinfectant dosing. *Water (Switzerland)* **6**, 3603–3630 (2014).
86. Fox, R. & Stuckey, D. MS-2 and T4 phage removal in an anaerobic membrane bioreactor (AnMBR): Effect of gas sparging rate. *Journal of Chemical Technology and Biotechnology* **90**, 384–390 (2015).
87. Zhang, J. *et al.* Virus removal during sewage treatment by anaerobic membrane bioreactor (AnMBR): The role of membrane fouling. *Water Research* **211**, 118055 (2022).
88. Wu, B. *et al.* Interface behavior and removal mechanisms of human pathogenic viruses in anaerobic membrane bioreactor (AnMBR). **219**, (2022).
89. Wong, K. *et al.* Removal of Viruses and Indicators by Anaerobic Membrane Bioreactor Treating Animal Waste. *Journal of Environment Quality* **38**, 1694 (2009).
90. Chaudhry, R. M., Holloway, R. W., Cath, T. Y. & Nelson, K. L. Impact of virus surface characteristics on removal mechanisms within membrane bioreactors. *Water Research* **84**, 144–152 (2015).
91. Casabuena, A. L., Shi, H., Yin, Z., Xagoraraki, I. & Tarabara, V. V. Human adenovirus 40 removal in sidestream membrane bioreactor. *Journal of Environmental Engineering* **145**, 1–6 (2019).
92. Gurung, K., Ncibi, M. C. & Sillanpää, M. Assessing membrane fouling and the performance of pilot-scale membrane bioreactor (MBR) to treat real municipal wastewater during winter season in Nordic regions. *Science of the Total Environment* **579**, 1289–1297 (2017).
93. Miura, T., Schaeffer, J., le Saux, J. C., le Mehaute, P. & le Guyader, F. S. Virus type-specific removal in a full-scale membrane bioreactor treatment process. *Food and Environmental Virology* **10**, 176–186 (2018).
94. Francy, D. S. *et al.* Comparative effectiveness of membrane bioreactors, conventional secondary treatment, and chlorine and UV disinfection to remove microorganisms from municipal wastewaters. *Water Research* **46**, 4164–4178 (2012).
95. Simmons, F. J., Kuo, D. H. W. & Xagoraraki, I. Removal of human enteric viruses by a full-scale membrane bioreactor during municipal wastewater processing. *Water Research* **45**, 2739–2750 (2011).
96. Tufenkji, N. Modeling microbial transport in porous media: Traditional approaches and recent developments. *Advances in Water Resources* **30**, 1455–1469 (2007).
97. Matsushita, T., Suzuki, H., Shirasaki, N., Matsui, Y. & Ohno, K. Adsorptive virus removal with super-powdered activated carbon. *Separation and Purification Technology* **107**, 79–84 (2013).
98. Madaeni, S. S. Mechanism of virus removal using membranes. *Filtration & Separation* **34**,

61–65 (1997).

99. Tanneru, C. T. & Chellam, S. Mechanisms of virus control during iron electrocoagulation - Microfiltration of surface water. *Water Research* **46**, 2111–2120 (2012).
100. Kosiol, P., Kahrs, C., Thom, V., Ulbricht, M. & Hansmann, B. Investigation of virus retention by size exclusion membranes under different flow regimes. *Biotechnology Progress* **35**, (2019).
101. Sidhu, J. P. S. *et al. Development of Validation Protocol for Activated Sludge Process in Water Recycling Project Leader Partners About the Australian Water Recycling Centre of Excellence*. (2015).
102. Jeong, Y., Hermanowicz, S. W. & Park, C. Treatment of food waste recycling wastewater using anaerobic ceramic membrane bioreactor for biogas production in mainstream treatment process of domestic wastewater. *Water Research* **123**, 86–95 (2017).
103. Van Voorthuizen, E. M., Ashbolt, N. J. & Schäfer, A. I. Role of hydrophobic and electrostatic interactions for initial enteric virus retention by MF membranes. *Journal of Membrane Science* **194**, 69–79 (2001).
104. Armanious, A. *et al.* Viruses at solid-water interfaces: A systematic assessment of interactions driving adsorption. *Environmental Science and Technology* **50**, 732–743 (2016).
105. Xagoraraki, I., Yin, Z. & Svambayev, Z. Fate of viruses in water systems. *Journal of Environmental Engineering (United States)* **140**, 1–18 (2014).
106. Hirani, Z. M., DeCarolis, J. F., Adham, S. S. & Jacangelo, J. G. Peak flux performance and microbial removal by selected membrane bioreactor systems. *Water Research* **44**, 2431–2440 (2010).
107. Fane, A. G., Wang, R. & Hu, M. X. Synthetic membranes for water purification: Status and future. *Angewandte Chemie - International Edition* **54**, 3368–3386 (2015).
108. Zydney, A. L., Aimar, P., Meireles, M., Pimbley, J. M. & Belfort, G. Use of the log-normal probability density function to analyze membrane pore size distributions: Functional forms and discrepancies. *Journal of Membrane Science* (1994) doi:10.1016/0376-7388(94)80090-1.
109. Giglia, S., Bohonak, D., Greenhalgh, P. & Leahy, A. Measurement of pore size distribution and prediction of membrane filter virus retention using liquid-liquid porometry. *Journal of Membrane Science* **476**, 399–409 (2015).
110. Duek, A., Arkhangelsky, E., Krush, R., Brenner, A. & Gitis, V. New and conventional pore size tests in virus-removing membranes. *Water Research* **46**, 2505–2514 (2012).
111. Kosiol, P., Hansmann, B., Ulbricht, M. & Thom, V. Determination of pore size distributions of virus filtration membranes using gold nanoparticles and their correlation with virus retention. *Journal of Membrane Science* **533**, 289–301 (2017).

112. Madaeni, S. S., Fane, A. G. & Grohmann, G. S. Virus removal from water and wastewater using membranes. *Journal of Membrane Science* (1995) doi:10.1016/0376-7388(94)00252-T.
113. Wu, J., Li, H. & Huang, X. Indigenous somatic coliphage removal from a real municipal wastewater by a submerged membrane bioreactor. *Water Research* **44**, 1853–1862 (2010).
114. Huang, H., Young, T. A., Schwab, K. J. & Jacangelo, J. G. Mechanisms of virus removal from secondary wastewater effluent by low pressure membrane filtration. *Journal of Membrane Science* **409–410**, 1–8 (2012).
115. Yin, Z., Tarabara, V. V. & Xagoraraki, I. Effect of pressure relaxation and membrane backwash on adenovirus removal in a membrane bioreactor. *Water Research* **88**, 750–757 (2016).
116. Zheng, X. & Liu, J. X. Mechanism investigation of virus removal in a membrane bioreactor. *Water Science and Technology: Water Supply* **6**, 51–59 (2006).
117. Lu, R., Mosiman, D. & Nguyen, T. H. Mechanisms of MS2 bacteriophage removal by fouled ultrafiltration membrane subjected to different cleaning methods. *Environmental Science and Technology* **47**, 13422–13429 (2013).
118. Shang, C., Hiu, M. W. & Chen, G. Bacteriophage MS-2 removal by submerged membrane bioreactor. *Water Research* **39**, 4211–4219 (2005).
119. Noshadi, I., Salahi, A., Hemmati, M., Rekabdar, F. & Mohammadi, T. Experimental and ANFIS modeling for fouling analysis of oily wastewater treatment using ultrafiltration. *Asia-Pacific Journal of Chemical Engineering* (2013) doi:10.1002/apj.1691.
120. Sutherland, I. W., Hughes, K. A., Skillman, L. C. & Tait, K. The interaction of phage and biofilms. *FEMS Microbiology Letters* **232**, 1–6 (2004).
121. Sheng, G. P., Yu, H. Q. & Li, X. Y. Extracellular polymeric substances (EPS) of microbial aggregates in biological wastewater treatment systems: A review. *Biotechnology Advances* **28**, 882–894 (2010).
122. Ueda, T. & Horan, N. J. Fate of indigenous bacteriophage in a membrane bioreactor. *Water Research* **34**, 2151–2159 (2000).
123. Nguyen, T., Roddick, F. A. & Fan, L. Biofouling of water treatment membranes: A review of the underlying causes, monitoring techniques and control measures. *Membranes (Basel)* **2**, 804–840 (2012).
124. Bagheri, M., Akbari, A. & Mirbagheri, S. A. Advanced control of membrane fouling in filtration systems using artificial intelligence and machine learning techniques: A critical review. *Process Safety and Environmental Protection* **123**, 229–252 (2019).
125. Melin, T. *et al.* Membrane bioreactor technology for wastewater treatment and reuse. *Desalination* **187**, 271–282 (2006).

126. Iorhemen, O. T., Hamza, R. A. & Tay, J. H. Membrane bioreactor (Mbr) technology for wastewater treatment and reclamation: Membrane fouling. *Membranes (Basel)* **6**, 13–16 (2016).
127. Yang, S. *et al.* Comparing powdered and granular activated carbon addition on membrane fouling control through evaluating the impacts on mixed liquor and cake layer properties in anaerobic membrane bioreactors. *Bioresource Technology* **294**, 122137 (2019).
128. Cui, Z. F., Chang, S. & Fane, A. G. The use of gas bubbling to enhance membrane processes. *Journal of Membrane Science* Preprint at https://doi.org/10.1016/S0376-7388(03)00246-1 (2003).
129. Madaeni, S. S., Fane, A. G. & Grohmann, G. S. Virus removal from water and wastewater using membranes. *Journal of Membrane Science* (1995) doi:10.1016/0376-7388(94)00252-T.
130. Shirasaki, N., Matsushita, T., Matsui, Y. & Ohno, K. Effects of reversible and irreversible membrane fouling on virus removal by a coagulation-microfiltration system. *Journal of Water Supply: Research and Technology - AQUA* (2008) doi:10.2166/aqua.2008.048.
131. Hao, X. Di, Wang, Q. L., Zhu, J. Y. & Van Loosdrecht, M. C. M. Microbiological endogenous processes in biological wastewater treatment systems. *Critical Reviews in Environmental Science and Technology* vol. 40 239–265 Preprint at https://doi.org/10.1080/10643380802278901 (2010).
132. Farahbakhsh, K. & Smith, D. W. Removal of coliphages in secondary effluent by microfiltration - Mechanisms of removal and impact of operating parameters. *Water Research* **38**, 585–592 (2004).
133. Langlet, J. *et al.* Efficiency of MS2 phage and Qβ phage removal by membrane filtration in water treatment: Applicability of real-time RT-PCR method. *Journal of Membrane Science* **326**, 111–116 (2009).
134. Ng, A. N. L. & Kim, A. S. A mini-review of modeling studies on membrane bioreactor (MBR) treatment for municipal wastewaters. *Desalination* **212**, 261–281 (2007).
135. Robles, Á. *et al.* A review on anaerobic membrane bioreactors (AnMBRs) focused on modelling and control aspects. *Bioresource Technology* **270**, 612–626 (2018).
136. Henze, M., Gujer, W., Mino, T. & van Loosedrecht, M. *Activated Sludge Models ASM1, ASM2, ASM2d and ASM3*. *Water Intelligence Online* vol. 5 (2015).
137. McKinney, R. Mathematics of complete-mixing activated sludge. *Transactions of the American Society of Civil …* **88**, 87–113 (1962).
138. Naessens, W., Maere, T. & Nopens, I. Critical review of membrane bioreactor models - Part 1: Biokinetic and filtration models. *Bioresource Technology* **122**, 95–106 (2012).
139. Wintgens, T. *et al.* Modelling of a membrane bioreactor system for municipal wastewater

treatment. *Journal of Membrane Science* **216**, 55–65 (2003).

140. Fenu, A. *et al.* Activated sludge model (ASM) based modelling of membrane bioreactor (MBR) processes: A critical review with special regard to MBR specificities. *Water Research* **44**, 4272–4294 (2010).
141. Henze, M., Gujer, W., Mino, T. & van Loosdrecht, M. C. M. *Activated sludge models ASM1, ASM2, ASM2d and ASM3*. (IWA publishing, 2000).
142. Mannina, G., Cosenza, A., Viviani, G. & Ekama, G. A. Sensitivity and uncertainty analysis of an integrated ASM2d MBR model for wastewater treatment. *Chemical Engineering Journal* **351**, 579–588 (2018).
143. Bis, M., Montusiewicz, A., Piotrowicz, A. & Łagód, G. Modeling of wastewater treatment processes in membrane bioreactors compared to conventional activated sludge systems. *Processes* **7**, (2019).
144. Batstone, D. J. *et al.* The IWA Anaerobic Digestion Model No 1 (ADM1). *Water Sci Technol* **45**, 65–73 (2002).
145. Batstone, D. J., Puyol, D., Flores-Alsina, X. & Rodríguez, J. Mathematical modelling of anaerobic digestion processes: Applications and future needs. *Reviews in Environmental Science and Biotechnology* **14**, 595–613 (2015).
146. Sulaiman, A., Nikbakht, A. M., Tabatabaei, M., Khatamifar, M. & Hassan, M. A. Modeling anaerobic process for wastewater treatment: New trends and methodologies. *International Conference on Biology, Environment and Chemistry: ICBEC. Hong Kong* **1**, 28–30 (2010).
147. Turkdogan-Aydinol, F. I. & Yetilmezsoy, K. A fuzzy-logic-based model to predict biogas and methane production rates in a pilot-scale mesophilic UASB reactor treating molasses wastewater. *Journal of Hazardous Materials* **182**, 460–471 (2010).
148. Chan, C. W. & Huang, G. H. Artificial intelligence for management and control of pollution minimization and mitigation processes. *Engineering Applications of Artificial Intelligence* **16**, 75–90 (2003).
149. Mannina, G., Di Bella, G. & Viviani, G. An integrated model for biological and physical process simulation in membrane bioreactors (MBRs). *Journal of Membrane Science* **376**, 56–69 (2011).
150. Charfi, A. *et al.* A modelling approach to study the fouling of an anaerobic membrane bioreactor for industrial wastewater treatment. *Bioresource Technology* **245**, 207–215 (2017).
151. Ferrero, G., Rodríguez-Roda, I. & Comas, J. Automatic control systems for submerged membrane bioreactors: A state-of-the-art review. *Water Research* **46**, 3421–3433 (2012).
152. Kim, T. D., Shiragami, N. & Unno, H. Development of a model describing virus removal process in an activated sludge basin. *Journal of Chemical Engineering of Japan* vol. 28

257–262 Preprint at https://doi.org/10.1252/jcej.28.257 (1995).

153. Xing, Y., Ellis, A., Magnuson, M. & Harper, W. F. Adsorption of bacteriophage MS2 to colloids: Kinetics and particle interactions. *Colloids and Surfaces A: Physicochemical and Engineering Aspects* **585**, 124099 (2019).
154. Grant, S. B., List, E. J. & Lidstrom, M. E. Kinetic analysis of virus adsorption and inactivation in batch experiments. *Water Resources Research* **29**, 2067–2085 (1993).
155. Sigstam, T. *et al.* Subtle differences in virus composition affect disinfection kinetics and mechanisms. *Applied and Environmental Microbiology* **79**, 3455–3467 (2013).
156. Yates, M. V., Yates, S. R., Wagner, J. & Gerba, C. P. Modeling virus survival and transport in the subsurface. *Journal of Contaminant Hydrology* **1**, 329–345 (1987).
157. Zydney, A. L., Aimar, P., Meireles, M., Pimbley, J. M. & Belfort, G. Use of the log-normal probability density function to analyze membrane pore size distributions: Functional forms and discrepancies. *Journal of Membrane Science* (1994) doi:10.1016/0376-7388(94)80090-1.
158. Bungay, P. M. & Brenner, H. The motion of a closely-fitting sphere in a fluid-filled tube. *International Journal of Multiphase Flow* (1973) doi:10.1016/0301-9322(73)90003-7.
159. Rathore, A. S. *et al.* Mechanistic modeling of viral filtration. *Journal of Membrane Science* **458**, 96–103 (2014).
160. Le-Clech, P., Chen, V. & Fane, T. A. G. Fouling in membrane bioreactors used in wastewater treatment. *Journal of Membrane Science* **284**, 17–53 (2006).
161. Haimi, H., Mulas, M., Corona, F. & Vahala, R. Data-derived soft-sensors for biological wastewater treatment plants: An overview. *Environmental Modelling and Software* **47**, 88–107 (2013).
162. Madaeni, S. S. & Kurdian, A. R. Fuzzy modeling and hybrid genetic algorithm optimization of virus removal from water using microfiltration membrane. *Chemical Engineering Research and Design* **89**, 456–470 (2011).
163. Li, X. yan & Wang, X. mao. Modelling of membrane fouling in a submerged membrane bioreactor. *Journal of Membrane Science* **278**, 151–161 (2006).
164. Hwang, T. M. *et al.* Development of a statistical and mathematical hybrid model to predict membrane fouling and performance. *Desalination* **247**, 210–221 (2009).
165. Yin, S., Ding, S. X., Xie, X. & Luo, H. A review on basic data-driven approaches for industrial process monitoring. *IEEE Transactions on Industrial Electronics* **61**, 6414–6428 (2014).
166. Han, H., Zhu, S., Qiao, J. & Guo, M. Data-driven intelligent monitoring system for key variables in wastewater treatment process. *Chinese Journal of Chemical Engineering* **26**, 2093–2101 (2018).

167. Dürrenmatt, D. J. Ô. & Gujer, W. Data-driven modeling approaches to support wastewater treatment plant operation. *Environmental Modelling and Software* **30**, 47–56 (2012).
168. Nadiri, A. A., Shokri, S., Tsai, F. T. C. & Asghari Moghaddam, A. Prediction of effluent quality parameters of a wastewater treatment plant using a supervised committee fuzzy logic model. *Journal of Cleaner Production* **180**, 539–549 (2018).
169. Yusuf, Z., Wahab, N. A. & Sudin, S. Soft computing techniques in modelling of membrane filtration system: A review. *Desalination and Water Treatment* **161**, 144–155 (2019).
170. Wan, J. *et al.* Prediction of effluent quality of a paper mill wastewater treatment using an adaptive network-based fuzzy inference system. *Applied Soft Computing Journal* **11**, 3238–3246 (2011).
171. Liu, Q. F. & Kim, S. H. Evaluation of membrane fouling models based on bench-scale experiments: A comparison between constant flowrate blocking laws and artificial neural network (ANNs) model. *Journal of Membrane Science* **310**, 393–401 (2008).
172. Baker, R. E., Peña, J. M., Jayamohan, J. & Jérusalem, A. Mechanistic models versus machine learning, a fight worth fighting for the biological community? *Biology Letters* **14**, 1–4 (2018).
173. Thürlimann, C. M., Dürrenmatt, D. J. & Villez, K. Soft-sensing with qualitative trend analysis for wastewater treatment plant control. *Control Engineering Practice* **70**, 121–133 (2018).
174. Chew, C. M., Aroua, M. K. & Hussain, M. A. A practical hybrid modelling approach for the prediction of potential fouling parameters in ultrafiltration membrane water treatment plant. *Journal of Industrial and Engineering Chemistry* **45**, 145–155 (2017).
175. WHO. WHO Coronavirus Disease (COVID-19) Dashboard. https://covid19.who.int/ (2021).
176. Medema, G., Been, F., Heijnen, L. & Petterson, S. Implementation of environmental surveillance for SARS-CoV-2 virus to support public health decisions: Opportunities and challenges. *Current Opinion in Environmental Science and Health* **17**, 49–71 (2020).
177. Krantz, S. G. & Rao, A. S. R. S. Level of underreporting including underdiagnosis before the first peak of COVID-19 in various countries: Preliminary retrospective results based on wavelets and deterministic modeling. *Infection Control and Hospital Epidemiology* **41**, 857–859 (2020).
178. Bivins, A. *et al.* Wastewater-based epidemiology: Global collaborative to maximize contributions in the fight against COVID-19. *Environmental Science & Technology* (2020) doi:10.1021/acs.est.0c02388.
179. Venugopal, A. *et al.* Novel wastewater surveillance strategy for early detection of coronavirus disease 2019 hotspots. *Current Opinion in Environmental Science and Health*

17, 8–13 (2020).

180. Hata, A., Hara-Yamamura, H., Meuchi, Y., Imai, S. & Honda, R. Detection of SARS-CoV-2 in wastewater in Japan during a COVID-19 outbreak. *Science of the Total Environment* **758**, 143578 (2021).
181. Wurtzer, S. *et al.* Evaluation of lockdown impact on SARS-CoV-2 dynamics through viral genome quantification in Paris wastewaters. *Eurosurveillance* **25**, (2020).
182. Gandhi, M., Yokoe, D. S. & Havlir, D. V. Asymptomatic transmission, the achilles' heel of current strategies to control Covid-19. *New England Journal of Medicine* **382**, 2158–2160 (2020).
183. Arons, M. M. *et al.* Presymptomatic SARS-CoV-2 infections and transmission in a skilled nursing facility. *New England Journal of Medicine* **382**, 2081–2090 (2020).
184. He, X. *et al.* Temporal dynamics in viral shedding and transmissibility of COVID-19. *Nature Medicine* **26**, 672–675 (2020).
185. Jones, D. L. *et al.* Shedding of SARS-CoV-2 in feces and urine and its potential role in person-to-person transmission and the environment-based spread of COVID-19. *Science of the Total Environment* **749**, 141364 (2020).
186. Jaclyn Peiser. University of Arizona used wastewater testing to detect cases of coronavirus in a dorm. *The Washington Post* https://www.washingtonpost.com/nation/2020/08/28/arizona-coronavirus-wastewater-testing/ (2020).
187. Nemudryi, A. *et al.* Temporal detection and phylogenetic assessment of SARS-CoV-2 in municipal wastewater. *Cell Reports Medicine* **1**, 100098 (2020).
188. Peccia, J. *et al.* Measurement of SARS-CoV-2 RNA in wastewater tracks community infection dynamics. *Nature Biotechnology* **38**, 1164–1167 (2020).
189. Hart, O. E. & Halden, R. U. Computational analysis of SARS-CoV-2/COVID-19 surveillance by wastewater-based epidemiology locally and globally: Feasibility, economy, opportunities and challenges. *Science of the Total Environment* **730**, 138875 (2020).
190. Lauer, S. A. *et al.* The incubation period of coronavirus disease 2019 (CoVID-19) from publicly reported confirmed cases: Estimation and application. *Annals of Internal Medicine* **172**, 577–582 (2020).
191. Li, T. Z. *et al.* Duration of SARS-CoV-2 RNA shedding and factors associated with prolonged viral shedding in patients with COVID-19. *Journal of Medical Virology* 1–7 (2020) doi:10.1002/jmv.26280.
192. McAloon, C. *et al.* Incubation period of COVID-19: A rapid systematic review and meta-analysis of observational research. *BMJ Open* **10**, 1–9 (2020).
193. Walsh, K. A. *et al.* SARS-CoV-2 detection, viral load and infectivity over the course of an

infection. *Journal of Infection* **81**, 357–371 (2020).

194. Wölfel, R. *et al.* Virological assessment of hospitalized patients with COVID-2019. *Nature* **581**, 465–469 (2020).
195. Parasa, S. *et al.* Prevalence of gastrointestinal symptoms and fecal viral shedding in patients with coronavirus disease 2019: A systematic review and meta-analysis. *JAMA Netw Open* **3**, e2011335 (2020).
196. Gupta, S., Parker, J., Smits, S., Underwood, J. & Dolwani, S. Persistent viral shedding of SARS-CoV-2 in faeces – a rapid review. *Colorectal Disease* **22**, 611–620 (2020).
197. Xu, Y. *et al.* Characteristics of pediatric SARS-CoV-2 infection and potential evidence for persistent fecal viral shedding. *Nature Medicine* **26**, 502–505 (2020).
198. Wang, X. *et al.* Fecal viral shedding in COVID-19 patients: Clinical significance, viral load dynamics and survival analysis. *Virus Research* **289**, 198147 (2020).
199. Xiao, F. *et al.* Evidence for gastrointestinal infection of SARS-CoV-2. *Gastroenterology* **158**, 1831-1833.e3 (2020).
200. Wu, Y. *et al.* Prolonged presence of SARS-CoV-2 viral RNA in faecal samples. *The Lancet Gastroenterology and Hepatology* **5**, 434–435 (2020).
201. Miura, F., Kitajima, M. & Omori, R. Duration of SARS-CoV-2 viral shedding in faeces as a parameter for wastewater-based epidemiology: Re-analysis of patient data using a shedding dynamics model. *Science of The Total Environment* 144549 (2020) doi:10.1016/j.scitotenv.2020.144549.
202. Huynh, G. T. & Rong, L. Modeling the dynamics of virus shedding into the saliva of Epstein-Barr virus positive individuals. *Journal of Theoretical Biology* **310**, 105–114 (2012).
203. Osuna, C. E. *et al.* Zika viral dynamics and shedding in rhesus and cynomolgus macaques. *Nature Medicine* **22**, 1448–1455 (2016).
204. La Rosa, G., Bonadonna, L., Lucentini, L., Kenmoe, S. & Suffredini, E. Coronavirus in water environments: Occurrence, persistence and concentration methods - A scoping review. *Water Research* **179**, 115899 (2020).
205. Ahmed, W. *et al.* Comparison of virus concentration methods for the RT-qPCR-based recovery of murine hepatitis virus, a surrogate for SARS-CoV-2 from untreated wastewater. *Science of the Total Environment* **739**, 139960 (2020).
206. Torii, S., Furumai, H. & Katayama, H. Applicability of polyethylene glycol precipitation followed by acid guanidinium thiocyanate-phenol-chloroform extraction for the detection of SARS-CoV-2 RNA from municipal wastewater. *Science of the Total Environment* **756**, 143067 (2021).
207. Rusiñol, M. *et al.* Concentration methods for the quantification of coronavirus and other potentially pandemic enveloped virus from wastewater. *Current Opinion in Environmental*

Science and Health **17**, 21–28 (2020).

208. Ye, Y., Ellenberg, R. M., Graham, K. E. & Wigginton, K. R. Survivability, Partitioning, and Recovery of Enveloped Viruses in Untreated Municipal Wastewater. *Environmental Science and Technology* **50**, 5077–5085 (2016).
209. Kaplan, E. H. *et al.* Aligning SARS-CoV-2 indicators via an epidemic model: application to hospital admissions and RNA detection in sewage sludge. *Health Care Management Science* (2020) doi:10.1007/s10729-020-09525-1.
210. Kitamura, K., Sadamasu, K., Muramatsu, M. & Yoshida, H. Efficient detection of SARS-CoV-2 RNA in the solid fraction ofwastewater. *Science of the Total Environment* **763**, 144587 (2021).
211. Westhaus, S. *et al.* Detection of SARS-CoV-2 in raw and treated wastewater in Germany – Suitability for COVID-19 surveillance and potential transmission risks. *Science of the Total Environment* **751**, 141750 (2021).
212. Schwab, K. J., Estes, M. K., Neill, F. H. & Atmar, R. L. Use of heat release and an internal RNA standard control in reverse transcription-PCR detection of Norwalk virus from stool samples. *Journal of Clinical Microbiology* **35**, 511–514 (1997).
213. Corpuz, M. V. A. *et al.* Viruses in wastewater: occurrence, abundance and detection methods. *Science of the Total Environment* **745**, 140910 (2020).
214. Kitajima, M. *et al.* SARS-CoV-2 in wastewater: State of the knowledge and research needs. *Science of the Total Environment* **739**, 139076 (2020).
215. Hamouda, M., Mustafa, F., Maraqa, M., Rizvi, T. & Aly Hassan, A. Wastewater surveillance for SARS-CoV-2: Lessons learnt from recent studies to define future applications. *Science of the Total Environment* **759**, 143493 (2020).
216. Sidhu, J. P. S., Ahmed, W. & Toze, S. Sensitive detection of human adenovirus from small volume of primary wastewater samples by quantitative PCR. *Journal of Virological Methods* **187**, 395–400 (2013).
217. Dang, Y. *et al.* Comparison of qualitative and quantitative analyses of COVID-19 clinical samples. *Clinica Chimica Acta* **510**, 613–616 (2020).
218. Suo, T. *et al.* ddPCR: a more accurate tool for SARS-CoV-2 detection in low viral load specimens. *Emerging Microbes and Infections* **9**, 1259–1268 (2020).
219. Yu, F. *et al.* Quantitative detection and viral load analysis of SARS-CoV-2 in infected patients. *Clinical Infectious Diseases* **71**, 793–798 (2020).
220. Falzone, L. *et al.* Sensitivity assessment of droplet digital PCR for SARS-CoV-2 detection. *International Journal of Molecular Medicine* **46**, 957–964 (2020).
221. Michael-Kordatou, I., Karaolia, P. & Fatta-Kassinos, D. Sewage analysis as a tool for the COVID-19 pandemic response and management: the urgent need for optimised protocols

for SARS-CoV-2 detection and quantification. *Journal of Environmental Chemical Engineering* **8**, 104306 (2020).

222. Heaton, K. W. *et al.* Defecation frequency and timing, and stool form in the general population: A prospective study. *Gut* **33**, 818–824 (1992).
223. Campisano, A. & Modica, C. Appropriate resolution timescale to evaluate water saving and retention potential of rainwater harvesting for toilet flushing in single houses. *Journal of Hydroinformatics* **17**, 331–346 (2015).
224. Kumar, M. *et al.* First proof of the capability of wastewater surveillance for COVID-19 in India through detection of genetic material of SARS-CoV-2. *Science of the Total Environment* **746**, 141326 (2020).
225. Kitajima, M., Iker, B. C., Pepper, I. L. & Gerba, C. P. Relative abundance and treatment reduction of viruses during wastewater treatment processes - Identification of potential viral indicators. *Science of the Total Environment* **488–489**, 290–296 (2014).
226. Symonds, E. M., Nguyen, K. H., Harwood, V. J. & Breitbart, M. Pepper mild mottle virus: A plant pathogen with a greater purpose in (waste)water treatment development and public health management. *Water Research* **144**, 1–12 (2018).
227. Ballesté, E. *et al.* Dynamics of crAssphage as a human source tracking marker in potentially faecally polluted environments. *Water Research* **155**, 233–244 (2019).
228. Bofill-Mas, S. *et al.* Quantification and stability of human adenoviruses and polyomavirus JCPyV in wastewater matrices. *Applied and Environmental Microbiology* **72**, 7894–7896 (2006).
229. Thai, P. K. *et al.* Effects of sewer conditions on the degradation of selected illicit drug residues in wastewater. *Water Research* **48**, 538–547 (2014).
230. Kapo, K. E., Paschka, M., Vamshi, R., Sebasky, M. & McDonough, K. Estimation of U.S. sewer residence time distributions for national-scale risk assessment of down-the-drain chemicals. *Science of the Total Environment* **603–604**, 445–452 (2017).
231. D'Ascenzo, G. *et al.* Fate of natural estrogen conjugates in municipal sewage transport and treatment facilities. *Science of the Total Environment* **302**, 199–209 (2003).
232. Holt, M. S., Fox, K. K., Burford, M., Daniel, M. & Buckland, H. UK monitoring study on the removal of linear alkylbenzene sulphonate in trickling filter type sewage treatment plants. Contribution to GREAT-ER project 2. *Science of the Total Environment* vols. 210–211 255–269 Preprint at https://doi.org/10.1016/S0048-9697(98)00016-3 (1998).
233. Ahmed, W. *et al.* Decay of SARS-CoV-2 and surrogate murine hepatitis virus RNA in untreated wastewater to inform application in wastewater-based epidemiology. *Environmental Research* **191**, 110092 (2020).
234. Mandal, P., Gupta, A. K. & Dubey, B. K. A review on presence, survival,

disinfection/removal methods of coronavirus in wastewater and progress of wastewater-based epidemiology. *Journal of Environmental Chemical Engineering* **8**, 104317 (2020).

235. Bivins, A. *et al.* Persistence of SARS-CoV-2 in water and wastewater. *Environmental Science and Technology Letters* (2020) doi:10.1021/acs.estlett.0c00730.
236. Ahmed, W. *et al.* Decay of SARS-CoV-2 and surrogate murine hepatitis virus RNA in untreated wastewater to inform application in wastewater-based epidemiology. 1–27.
237. Mao, K., Zhang, H. & Yang, Z. Can a paper-based device trace COVID-19 sources with wastewater-based epidemiology? *Environmental Science and Technology* **54**, 3733–3735 (2020).
238. Bhalla, N., Pan, Y., Yang, Z. & Payam, A. F. Opportunities and challenges for biosensors and nanoscale analytical tools for pandemics: COVID-19. *ACS Nano* **14**, 7783–7807 (2020).
239. Yang, Z., Xu, G., Reboud, J., Kasprzyk-Hordern, B. & Cooper, J. M. Monitoring genetic population biomarkers for wastewater-based epidemiology. *Analytical Chemistry* **89**, 9941–9945 (2017).
240. Nguyen, T., Bang, D. D. & Wolff, A. 2019 Novel coronavirus disease (COVID-19): Paving the road for rapid detection and point-of-care diagnostics. *Micromachines (Basel)* **11**, 1–7 (2020).
241. Gracia-Lor, E. *et al.* Estimation of caffeine intake from analysis of caffeine metabolites in wastewater. *Science of the Total Environment* **609**, 1582–1588 (2017).
242. Feng, L., Zhang, W. & Li, X. Monitoring of regional drug abuse through wastewater-based epidemiology—A critical review. *Science China Earth Sciences* **61**, 239–255 (2018).
243. Lai, F. Y. *et al.* Refining the estimation of illicit drug consumptions from wastewater analysis: Co-analysis of prescription pharmaceuticals and uncertainty assessment. *Water Research* **45**, 4437–4448 (2011).
244. Choi, P. M. *et al.* Wastewater-based epidemiology biomarkers: Past, present and future. *TrAC - Trends in Analytical Chemistry* **105**, 453–469 (2018).
245. O'Brien, J. W. *et al.* A model to estimate the population contributing to the wastewater using samples collected on census day. *Environmental Science and Technology* **48**, 517–525 (2014).
246. Ahmed, W. *et al.* Detection of SARS-CoV-2 RNA in commercial passenger aircraft and cruise ship wastewater: a surveillance tool for assessing the presence of COVID-19 infected travellers. *J Travel Med* **27**, 1–11 (2020).
247. Rong, C. *et al.* Chemical oxygen demand and nitrogen transformation in a large pilot-scale plant with a combined submerged anaerobic membrane bioreactor and one-stage partial nitritation-anammox for treating mainstream wastewater at 25 °C. *Bioresource Technology* **341**, 125840 (2021).

248. Rong, C. *et al.* Seasonal temperatures impact on the mass flows in the innovative integrated process of anaerobic membrane bioreactor and one-stage partial nitritation-anammox for the treatment of municipal wastewater. *Bioresource Technology* **349**, 126864 (2022).
249. Haramoto, E., Katayama, H. & Ohgaki, S. Detection of noroviruses in tap water in Japan by means of a new method for concentrating enteric viruses in large volumes of freshwater. *Applied and Environmental Microbiology* **70**, 2154–2160 (2004).
250. Kuroda, K. *et al.* Pepper mild mottle virus as an indicator and a tracer of fecal pollution in water environments: Comparative evaluation with wastewater-tracer pharmaceuticals in Hanoi, Vietnam. *Science of the Total Environment* **506–507**, 287–298 (2015).
251. Prieto, A. L., Futselaar, H., Lens, P. N. L., Bair, R. & Yeh, D. H. Development and start up of a gas-lift anaerobic membrane bioreactor (Gl-AnMBR) for conversion of sewage to energy, water and nutrients. *Journal of Membrane Science* **441**, 158–167 (2013).
252. Scarascia, G. *et al.* UV and bacteriophages as a chemical-free approach for cleaning membranes from anaerobic bioreactors. *Proc Natl Acad Sci U S A* **118**, 1–9 (2021).
253. Nordgren, J., Matussek, A., Mattsson, A., Svensson, L. & Lindgren, P. E. Prevalence of norovirus and factors influencing virus concentrations during one year in a full-scale wastewater treatment plant. *Water Research* **43**, 1117–1125 (2009).
254. Prevost, B. *et al.* Large scale survey of enteric viruses in river and waste water underlines the health status of the local population. *Environment International* **79**, 42–50 (2015).
255. Katayama, H. *et al.* One-year monthly quantitative survey of noroviruses, enteroviruses, and adenoviruses in wastewater collected from six plants in Japan. *Water Research* **42**, 1441–1448 (2008).
256. Ahmed, S. M., Lopman, B. A. & Levy, K. A systematic review and meta-analysis of the global seasonality of norovirus. *PLoS ONE* **8**, 1–7 (2013).
257. Aydin, S., Can, K., Çalışkan, M. & Balcazar, J. L. Bacteriophage cocktail as a promising bio-enhancer for methanogenic activities in anaerobic membrane bioreactors. *Science of The Total Environment* **832**, 154716 (2022).
258. Li, X., Zhang, S., Shi, J., Luby, S. P. & Jiang, G. Uncertainties in estimating SARS-CoV-2 prevalence by wastewater-based epidemiology. *Chemical Engineering Journal* **415**, 129039 (2021).
259. Devaux, C. A., Lagier, J. C. & Raoult, D. New insights into the physiopathology of COVID-19: SARS-CoV-2-associated gastrointestinal illness. *Frontiers in Medicine* **8**, 3–8 (2021).
260. Li, B., Di, D. Y. W., Saingam, P., Jeon, M. K. & Yan, T. Fine-scale temporal dynamics of SARS-CoV-2 RNA abundance in wastewater during a COVID-19 lockdown. *Water Research* **197**, (2021).
261. Fernandez-Cassi, X. *et al.* Wastewater monitoring outperforms case numbers as a tool to

track COVID-19 incidence dynamics when test positivity rates are high. *Water Research* **200**, 117252 (2021).

262. Kirby, A. E. *et al.* Using wastewater surveillance data to support the COVID-19 response — United States, 2020-2021. *MMWR Recommendations and Reports* **70**, 1242–1244 (2021).
263. Ahmed, W. *et al.* Wastewater surveillance demonstrates high predictive value for COVID-19 infection on board repatriation flights to Australia. *Environment International* **158**, 106938 (2022).
264. Crits-Christoph, A. *et al.* Genome sequencing of sewage detects regionally prevalent SARS-CoV-2 variants. *mBio* **12**, 1–9 (2021).
265. BIMSB Bioinformatics Platform. SARS-CoV-2 Wastewater Sampling Reports. https://bimsbstatic.mdc-berlin.de/akalin/AAkalin_pathogenomics/sarscov2_ww_reports/210528_wastewaterall_pigxsarscov2ww_default/index.html (2021).
266. Melvin, R. G. *et al.* A novel wastewater-based epidemiology indexing method predicts SARS-CoV-2 disease prevalence across treatment facilities in metropolitan and regional populations. *Scientific Reports* **11**, 1–9 (2021).
267. Coffman, M. M. *et al.* Preventing scientific and ethical misuse of wastewater surveillance data. *Environmental Science and Technology* **55**, 11473–11475 (2021).
268. Bibby, K., Bivins, A., Wu, Z. & North, D. Making waves: Plausible lead time for wastewater based epidemiology as an early warning system for COVID-19. *Water Research* **202**, 117438 (2021).
269. Gnanvi, J. E., Salako, K. V., Kotanmi, G. B. & Glèlè Kakaï, R. On the reliability of predictions on Covid-19 dynamics: A systematic and critical review of modelling techniques. *Infect Dis Model* **6**, 258–272 (2021).
270. Leung, K., Wu, J. T. & Leung, G. M. Effects of adjusting public health, travel, and social measures during the roll-out of COVID-19 vaccination: A modelling study. *The Lancet Public Health* **6**, e674–e682 (2021).
271. Huang, R., Ma, C., Ma, J., Huangfu, X. & He, Q. Machine learning in natural and engineered water systems. *Water Research* **205**, 117666 (2021).
272. Russo, S. *et al.* The value of human data annotation for machine learning based anomaly detection in environmental systems. *Water Research* **206**, 117695 (2021).
273. Li, X. *et al.* Data-driven estimation of COVID-19 community prevalence through wastewater-based epidemiology. *Science of The Total Environment* **789**, 147947 (2021).
274. Rallapalli, S., Aggarwal, S. & Singh, A. P. Detecting SARS-CoV-2 RNA prone clusters in a municipal wastewater network using fuzzy-Bayesian optimization model to facilitate wastewater-based epidemiology. *Science of the Total Environment* **778**, 146294 (2021).

275. Miura, F., Kitajima, M. & Omori, R. Duration of SARS-CoV-2 viral shedding in faeces as a parameter for wastewater-based epidemiology: Re-analysis of patient data using a shedding dynamics model. *Science of the Total Environment* **769**, 2020.11.22.20236323 (2020).
276. Rose, C., Parker, A., Jefferson, B. & Cartmell, E. The characterization of feces and urine: A review of the literature to inform advanced treatment technology. *Critical Reviews in Environmental Science and Technology* **45**, 1827–1879 (2015).
277. Chen, Y. *et al.* The presence of SARS-CoV-2 RNA in the feces of COVID-19 patients. *Journal of Medical Virology* **92**, 833–840 (2020).
278. Morone, G. *et al.* Incidence and persistence of viral shedding in COVID-19 post-acute patients with negativized pharyngeal swab: A systematic review. *Frontiers in Medicine* **7**, 1–9 (2020).
279. Mesoraca, A. *et al.* Evaluation of SARS-CoV-2 viral RNA in fecal samples. *Virology Journal* **17**, 1–3 (2020).
280. Sun, K. *et al.* Transmission heterogeneities, kinetics, and controllability of SARS-CoV-2. *Science (1979)* **371**, (2021).
281. Cevik, M. *et al.* SARS-CoV-2, SARS-CoV, and MERS-CoV viral load dynamics, duration of viral shedding, and infectiousness: a systematic review and meta-analysis. *The Lancet Microbe* **5247**, 1–10 (2020).
282. Néant, N. *et al.* Modeling SARS-CoV-2 viral kinetics and association with mortality in hospitalized patients from the French COVID cohort. *Proceedings of the National Academy of Sciences* **118**, e2017962118 (2021).
283. Widders, A., Broom, A. & Broom, J. SARS-CoV-2: The viral shedding vs infectivity dilemma. *Infection, Disease and Health* **25**, 210–215 (2020).
284. Nishiura, H., Linton, N. M. & Akhmetzhanov, A. R. Serial interval of novel coronavirus (COVID-19) infections. *International Journal of Infectious Diseases* **93**, 284–286 (2020).
285. Gonzalez, R. *et al.* COVID-19 surveillance in Southeastern Virginia using wastewater-based epidemiology. *Water Research* **186**, 116296 (2020).
286. Hasan, S. W. *et al.* Detection and quantification of SARS-CoV-2 RNA in wastewater and treated effluents: Surveillance of COVID-19 epidemic in the United Arab Emirates. *Science of the Total Environment* **764**, 142929 (2021).
287. Pecson, B. M. *et al.* Reproducibility and sensitivity of 36 methods to quantify the SARS-CoV-2 genetic signal in raw wastewater: findings from an interlaboratory methods evaluation in the U.S. *Environmental Science: Water Research & Technology* (2021) doi:10.1039/d0ew00946f.
288. Zhu, Y. *et al.* Early warning of COVID-19 via wastewater-based epidemiology : potential

and bottlenecks. *Science of the Total Environment* **767**, 145124 (2021).

289. Ahmed, W. *et al.* Intraday variability of indicator and pathogenic viruses in 1-h and 24-h composite wastewater samples: Implications for wastewater-based epidemiology. *Environmental Research* **193**, 110531 (2021).
290. Butler, D., Friedler, E. & Gatt, K. Characterising the quantity and quality of domestic wastewater inflows. *Water Science and Technology* **31**, 13–24 (1995).
291. Canales, R. A., Wilson, A. M., Pearce-Walker, J. I., Vorhougstraete, M. P. & Reynolds, K. A. Methods for handling left-censored data in quantitative microbial risk assessment. *Applied and Enviromental Microbiology* **84**, 1–10 (2018).
292. Marcel, S. *et al.* COVID-19 epidemic in Switzerland: On the importance of testing, contact tracing and isolation. *Swiss Medical Weekly* **150**, 4–6 (2020).
293. Lau, H. *et al.* Internationally lost COVID-19 cases. *Journal of Microbiology, Immunology and Infection* **53**, 454–458 (2020).
294. Kronbichler, A. *et al.* Asymptomatic patients as a source of COVID-19 infections: A systematic review and meta-analysis. *International Journal of Infectious Diseases* **98**, 180–186 (2020).
295. Lau, H. *et al.* Evaluating the massive underreporting and undertesting of COVID-19 cases in multiple global epicenters. *Pulmonology* **27**, 110–115 (2020).
296. Murhekar, M. V *et al.* SARS-CoV-2 antibody seroprevalence in India, August–September, 2020: findings from the second nationwide household serosurvey. *The Lancet Global Health* 257–266 (2021) doi:10.1016/s2214-109x(20)30544-1.
297. Lau, L. T. *et al.* A real-time PCR for SARS-coronavirus incorporating target gene pre-amplification. *Biochemical and Biophysical Research Communications* **312**, 1290–1296 (2003).
298. Arimura, M., Ha, T. V., Okumura, K. & Asada, T. Changes in urban mobility in Sapporo city, Japan due to the Covid-19 emergency declarations. *Transportation Research Interdisciplinary Perspectives* **7**, 100212 (2020).
299. Yabe, T. *et al.* Non-compulsory measures sufficiently reduced human mobility in Tokyo during the COVID-19 epidemic. *Scientific Reports* **10**, 1–9 (2020).
300. Katafuchi, Y., Kurita, K. & Managi, S. COVID-19 with stigma: Theory and evidence from mobility data. *Economics of Disasters and Climate Change* (2020) doi:10.1007/s41885-020-00077-w.
301. Shigemura, J. & Kurosawa, M. Mental health impact of the COVID-19 pandemic in Japan. *Psychological Trauma: Theory, Research, Practice, and Policy* **12**, 478–479 (2020).
302. Sasaki, N., Kuroda, R., Tsuno, K. & Kawakami, N. Workplace responses to COVID-19 associated with mental health and work performance of employees in Japan. *Journal of*

Occupational Health **62**, 1–6 (2020).

303. Machida, M. *et al.* Adoption of personal protective measures by ordinary citizens during the COVID-19 outbreak in Japan. *International Journal of Infectious Diseases* **94**, 139–144 (2020).
304. CDC. Real-time RT-PCR Primers and Probes for COVID-19 | CDC. https://www.cdc.gov/coronavirus/2019-ncov/lab/rt-pcr-panel-primer-probes.html (2021).
305. Bustin, S. A. *et al.* The MIQE Guidelines: Minimum information for publication of quantitative real-time PCR experiments. Preprint at (2009).
306. Hokajärvi, A. M. *et al.* The detection and stability of the SARS-CoV-2 RNA biomarkers in wastewater influent in Helsinki, Finland. *Science of the Total Environment* **770**, 145274 (2021).
307. Ahmed, W., Kitajima, M., Tandukar, S. & Haramoto, E. Recycled water safety: Current status of traditional and emerging viral indicators. *Current Opinion in Environmental Science and Health* **16**, 62–72 (2020).
308. Haramoto, E., Malla, B., Thakali, O. & Kitajima, M. First environmental surveillance for the presence of SARS-CoV-2 RNA in wastewater and river water in Japan. *Science of the Total Environment* **737**, 140405 (2020).
309. Torii, S. *et al.* Comparison of five polyethylene glycol precipitation procedures for the RT-qPCR based recovery of murine hepatitis virus, bacteriophage phi6, and pepper mild mottle virus as a surrogate for SARS-CoV-2 from wastewater. *Science of the Total Environment* **807**, 150722 (2022).
310. Bibby, K. & Peccia, J. Identification of viral pathogen diversity in sewage sludge by metagenome analysis. *Environmental Science and Technology* **47**, 1945–1951 (2013).
311. Bibby, K., Viau, E. & Peccia, J. Viral metagenome analysis to guide human pathogen monitoring in environmental samples. *Letters in Applied Microbiology* **52**, 386–392 (2011).
312. Gibson, K. E., Schwab, K. J., Spencer, S. K. & Borchardt, M. A. Measuring and mitigating inhibition during quantitative real time PCR analysis of viral nucleic acid extracts from large-volume environmental water samples. *Water Research* **46**, 4281–4291 (2012).
313. Hong, P. Y. *et al.* Estimating the minimum number of SARS-CoV-2 infected cases needed to detect viral RNA in wastewater: To what extent of the outbreak can surveillance of wastewater tell us? *Environmental Research* **195**, 110748 (2021).
314. Weidhaas, J. *et al.* Correlation of SARS-CoV-2 RNA in wastewater with COVID-19 disease burden in sewersheds. *Science of the Total Environment* **775**, 145790 (2021).
315. Huang, C. *et al.* Clinical features of patients infected with 2019 novel coronavirus in Wuhan, China. *The Lancet* **395**, 497–506 (2020).
316. Badr, H. S. *et al.* Association between mobility patterns and COVID-19 transmission in the

USA: a mathematical modelling study. *The Lancet Infectious Diseases* **20**, 1247–1254 (2020).

317. Nouvellet, P. *et al.* Reduction in mobility and COVID-19 transmission. *Nature Communications* 1–9 (2021) doi:10.1038/s41467-021-21358-2.
318. Ai, Y. *et al.* Wastewater SARS-CoV-2 monitoring as a community-level COVID-19 trend tracker and variants in Ohio, United States. *Science of the Total Environment* **801**, (2021).
319. Isaksson, F., Lundy, L., Hedström, A., Székely, A. J. & Mohamed, N. Evaluating the Use of Alternative Normalization Approaches on SARS-CoV-2 Concentrations in Wastewater: Experiences from Two Catchments in Northern Sweden. *Environments - MDPI* **9**, (2022).

Appendix

Table S1 The operational variables of the AnMBR.

Variable name	Unit	Abbreviation in the text
Air temperature	°C	Temperature
HRT	h	HRT
TMP	kPa	TMP
Gas cleaning frequency	Hz	GasClean_freq
Gas cleaning flux	m^3/min	GasClean_flux
MLSS temperature	°C	MLSS_temp
Influent pH	/	Inf_ph
MLSS pH	/	MLSS_ph
Biogas production rate	L/day	Gas_prod
CH_4 ratio in biogas	%	CH4
N_2 ratio in biogas	%	N2
CO_2 ratio in biogas	%	CO2
H_2S ratio in biogas	%	H2S
MLSS concentration	mg/L	MLSS
MLVSS concentration	mg/L	MLVSS
Influent total COD	mg/L	Inf_TCOD
Influent soluble COD	mg/L	Inf_SCOD
MLSS total COD	mg/L	MLSS_TCOD
MLSS soluble COD	mg/L	MLSS_SCOD
Effluent COD	mg/L	Eff_COD

Table S1 (continued)

Variable name	Unit	Abbreviation in the text
Influent total protein	mg/L	Inf_TPROT
Influent soluble protein	mg/L	Inf_SPROT
MLSS total protein	mg/L	MLSS_TPROT
Effluent protein	mg/L	Eff_PROT
EPS1 protein	mg/L	EPS1_PROT
EPS2 protein	mg/L	EPS2_PROT
SMP1 protein	mg/L	SMP1_PROT
SMP2 protein	mg/L	SMP2_PROT
Influent total polysaccharide	mg/L	Inf_TPS
Influent soluble polysaccharide	mg/L	Inf_SPS
MLSS total polysaccharide	mg/L	MLSS_TPS
Effluent polysaccharide	mg/L	Eff_PS
EPS1 polysaccharide	mg/L	EPS1_PS
EPS2 polysaccharide	mg/L	EPS2_ PS
SMP1 polysaccharide	mg/L	SMP1_ PS
SMP2 polysaccharide	mg/L	SMP2_ PS

Table S2 Sequences of primers and probe sets, PCR mix formula, and RT-qPCR conditions in experiments mentioned in Section 3 and 4.

Sequences

PMMoV	Sequence (from 5’ to 3’)
Forward primer	GAG TGG TTT GAC CTT AAC GTT TGA
Reverse primer	TTG TCG GTT GCA ATG CAA GT
Probe	[FAM] CCT ACC GAA GCA AAT G [MGBEQ]

PCR condition

NoV GII	Temperature	Time
Hot start	95 ℃	30 sec
Denaturing	95 ℃	30 sec
Annealing	53 ℃	60 sec
Extension	72℃	60 sec

PCR mix formula

Reagent	Volume
Forward primer	0.8 μL
Reverse primer	0.8 μL
Probe	0.25 μL
PCR water	3.15 μL
Sample	5 μL
SsoAdvanced Universal Probes Supermix	10 μL

Sequences

NoV GII	Sequence (from 5’ to 3’)
Forward primer	CAR GAR BCN ATG TTY AGR TGG ATG AG
Reverse primer	TCG ACG CCA TCT TCA TTC ACA
Probe	[FAM] TGG GAG GGS GAT CGC RAT CT [TAMRA]

PCR condition

NoV GII	Temperature	Time
Hot start	95 ℃	30 sec
Denaturing	95 ℃	15 sec
Annealing	56 ℃	60 sec
Extension	72℃	30 sec

Table S1 (continued)

PCR mix formula

Reagent	Volume
Forward primer	0.8 μL
Reverse primer	0.8 μL
Probe	0.2 μL
PCR water	3.2 μL
Sample	5 μL
SsoAdvanced Universal Probes Supermix	10 μL

Sequences

MNV	Sequence (from 5’ to 3’)
Forward primer	CGG TGA AGT GCT TCT GAG GTT
Reverse primer	GCA GCG TCA GTG CTG TCA A
Probe	[FAM] CGA ACC TAC ATG CGT CAG [TAMRA]

PCR condition

NoV GII	Temperature	Time
Hot start	95 ℃	30 sec
Denaturing	95 ℃	5 sec
Annealing	56 ℃	20 sec
Extension	72℃	30 sec

PCR mix formula

Reagent	Volume
Forward primer	0.8 μL
Reverse primer	0.8 μL
Probe	0.6 μL
PCR water	2.8 μL
Sample	5 μL
SsoAdvanced Universal Probes Supermix	10 μL

Table S3 Prediction performance evaluated by median MSR with different number of inputs and different models.

Four-week cumulative cases, GLM					
	Number of inputs				
		2	3	4	5
Quantile	0%	587.47	80.16	423.23	710.50
	25%	6088.65	6193.52	7405.19	9349.07
	50%	9038.60	10374.27	12033.00	15036.48
	75%	14437.37	15715.59	16849.10	20298.70
	100%	41871.27	41552.90	47591.32	53204.23

Four-week cumulative cases, ANN					
	Number of inputs				
		2	3	4	5
Quantile	0%	406.91	492.49	468.77	237.73
	25%	4768.64	4999.76	5650.15	5472.55
	50%	7520.22	8557.63	9000.55	9085.33
	75%	14043.80	13395.98	12812.55	13274.65
	100%	126209.56	109870.22	107596.08	108124.93

Four-week cumulative cases, RF					
	Number of inputs				
		2	3	4	5
Quantile	0%	380.10	996.05	159.88	144.04
	25%	7121.26	9568.18	10705.46	12470.59
	50%	12021.26	14334.22	15800.09	17389.67
	75%	16344.77	21266.71	23260.93	24967.54
	100%	49902.10	59457.74	70565.83	85994.01

R code for configuring the GLM, ANN, and RF models in Section 4.3

```
library(neuralnet) # For ANN
library(randomForest) # For RF
library(MLmetrics) # For MSE calculation

# GLM
# Set the size of training set
samp_size <- floor(0.8*nrow(data)) # 80% data used for model training
# Create a dataframe to store 5,000 predictions
glm.loop <- as.data.frame(matrix(NA, ncol = 5001, nrow = nrow(data)))
# Actual value of output was introduced
colnames(glm.loop)[1] <- 'Actual'
glm.loop$Actual <- data$output
# Run the simulation
for (i in 1:5000){
   set.seed(i)
   train.ind <- sample(seq_len(nrow(data)), size = samp_size)
# Separate the training data and test data
   train.data <- data[train.ind, ]
   test.data <- data[-train.ind, ]
   glm.model <- glm(output~input1+input2+input3, data= train.data, family="gaussian")
# Prediction is made using only the inputs of test data
   glm.predict <- predict.glm(glm.model, newdata = test.data[,-4)
   glm.loop[-train.ind,i+1] <- glm.predict$fit
}


# ANN
samp_size <- floor(0.8*nrow(data))
ann.loop <- as.data.frame(matrix(NA, ncol = 5001, nrow = nrow(data)))
colnames(ann.loop)[1] <- 'Actual'
ann.loop $Actual <- data$output
for (i in 1:5000){
   set.seed(i)
   train.ind <- sample(seq_len(nrow(data)), size = samp_size)
```

```
    train.data <- data[train.ind, ]
    test.data <- data[-train.ind, ]
    ann.model <- neuralnet(output~input1+input2+input3, data = train.data, hidden=c(5,5,5),
linear.output=T)
    ann.predict <- compute(ann.model, test.data[,-4])
    ann.loop[-train.ind,i+1] <- ann.predict$net.result
}


# RF
samp_size <- floor(0.8*nrow(data))
rf.loop <- as.data.frame(matrix(NA, ncol = 5001, nrow = nrow(data)))
colnames(rf.loop)[1] <- 'Actual'
rf.loop$Actual <- data$output
for (i in 1:5000){
    set.seed(i)
    train.ind <- sample(seq_len(nrow(data)), size = samp_size)
    train.data <- data[train.ind, ]
    test.data <- data[-train.ind, ]
    rf.model <- randomForest(output~input1+input2+input3, data=train.data, ntree = 500)
    rf.loop[-train.ind,i+1] <- predict(rf.model, newdata = test.data[,-4])
}


# MSE calculation
# Insert a new row into the loop to store MSE value
glm/ann/rf.loop[(nrow(data)+1),] <- 0
for (i in 1:5000){
# Keep the actual output value and the predicted value from one step
    temp <- glm/ann/rf.loop[which(is.na(glm/ann/rf.loop[,i+1]) == FALSE) ,c(1,i+1)]
    temp <- temp [-nrow(temp),]
# Calculate MSE
    glm/ann/rf.loop[(nrow(data)+1),i+1] <- MSE(glm/ann/rf.loop[,1], glm/ann/rf.loop[,2])
}

```